AN AI APPROACH TO TASKING AND CONTROL OF AN INDUSTRIAL LASER SYSTEM

A Thesis Submitted to the

Faculty of Engineering,

University of Glasgow for the

Degree of Doctor of Philosophy

By

See Yew Lim - BEng(HONS)

ProQuest LLC.
789 East Eisenhower Parkway
P.O. Box 1346
Ann Arbor, MI 48106 – 1346

TO MY PARENTS,
MY BROTHER, MY SISTERS AND VICTORIA
WITH ALL MY LOVE

Acknowledgements

I would like to express my gratitude to my supervisor, Dr. Chris R. Chatwin, for his guidance, patience and encouragement throughout this work.

I would also like to thank the University of Glasgow for the graduate research scholarship and the department of Mechanical Engineering for the provision of the research facilities.

Additionally, I am grateful to Mrs Irene Tait for critically reading the manuscript.

Thanks is also given for the valuable discussions with Dr. Hussein Ali Abdullah, Dr. Mohamand Zerrokat, Mr Rupert Young and Mr Azeddin Shaeb.

I would like to thank all those who have assisted this work as well as provide many happy moments during my stay in the Department of Mechanical Engineering. These include Mr George Faulkner, Mr Victor Mclaughin, Mr Ian Peden, Mr Cameron Miller, Mr Jimmy Wilson, my colleagues in the Laser and Optical System Engineering Group and all the technical and secretarial staff.

Finally, special thanks are due to my family and Miss Victoria L.C. Lei for their patience and moral support.

Synopsis

Effective use of lasers for materials processing applications requires a thorough knowledge of the fundamental mechanisms governing the interaction of radiation with matter. A discussion of the highly non-linear laser-material interaction is thus presented. The research then focusses on alternative approaches to the non-linear analysis of laser material processing through the application of genetic algorithms and chaos theory. A genetic algorithm is developed which predicts the laser cutting rate with good accuracy. The theory of deterministic chaos was exploited to investigate laser cutting of stainless steel; a new fundamental understanding of the interaction via the energy phase portrait was established. The construction of the phase portrait is illustrated.

The work then focusses on the actual design and implementation of a hybrid intelligent system for the tasking and control of a gas laser for materials processing. Existing artificial intelligence (AI) methodologies are reviewed. A new AI topological technique is developed to facilitate the design of a Proportional-Integral-Differential Knowledge Based Management System (PID-KBMS). The final intelligent system comprises of the PID-KBMS and a Cone Decision Support System (CDSS). The CDSS provides on-line image acquisition and analysis of the laser cutting process. The architecture of the hybrid intelligent system is illustrated.

The intelligent system source code was implemented in a Microsoft Windows and UNIX XWindows environment using Borland C. The intelligent system is hosted by a Viglen 486 PC and a SUN-SPARC 4.

A virtual graphical user interface is presented on the Viglen 486 via the network.

A final evaluation of the investigations into : the non-linear characteristics of laser-material interactions and prediction schemes, the AI topological technique for the design of AI control engines, the design and implementation of the PID-KBMS and CDSS are presented in the concluding chapter.

The algorithms and methods applied herein have general applicability to any non-linear control problem. Finally, recommendations for future research are given.

LIST OF CONTENTS

LIST OF FIGURES

LIST OF TABLES

LIST OF GRAPHS

1 INTRODUCTION

1.1 Historial Review of Lasers

Prior to the development of the laser, a similar device which produces radio-microwaves was developed. This device was called the maser. The first maser was built by C.H. Townes and his associates at Columbia University between 1951 and 1954. In 1958, A.H. Schawlow and C.H. Townes [1] extended the principles of the maser to the possibilities of producing shorter wavelengths. In the summer of 1960, the first maser that produced visible light waves was developed by T.H. Maiman [2] of the Hughes Aircraft Company Laboratories. Maiman then coined the term, "Laser" an acronym for light amplification by stimulated emission of radiation. Maiman's optical maser or laser used a single crystal of ruby as its

resonating cavity and hence was a solid state laser. In 1961, the first successful gas laser using Helium Neon was put into operation by Javan, Bernette and Harriott [3]. Extensive research on laser development has been carried on since that time, which resulted in development of many lasers such as the Neodymium glass and Neodymium (YAG) laser [4], the semi-conductor laser and the carbon dioxide laser [5]. The dominant industrial materials processing devices are Nd^{3+} YAG and carbon dioxide lasers. The research herein concentrates on the optimisation and control of a CO_2 laser for materials processing applications.

1.2 Nomenclature

α_R = Rate of evaporation (kg/m^3sec)

A = Projected groove surface area (m^2)

A_1 = Projected groove surface area in the x-y plane (m^2)

A2 = Projected groove surface area on the plane of symmetry (m^2)

b_m = Total melt width (m)

b_w = Depth of striations (m)

C = Specific heat capacity of the solid (kJ/kgK)

CO_2 = Carbon dioxide

δ = Absorption coefficient of material (1/m)

δ_s = Density of the melt (kg/m^3)

d_{sp} = Spot size diametre (m)

D = Diametre of beam (m)

ε_R = Average energy removed through evaporation (J)

ε_{th} = Average energy removed from the melt through the reactive gas (J)

E = Energy (J)

E_0 = Maximum energy (J)

f = Fraction of material melted which is subsequently evaporated

f'(t) = Hole depth as a function of time (m/sec)

F = Focal length (m)

η_R = Dynamic viscousity of the reactive gas ($Nsecm^{-2}$)

I = Intensity (W/m^2)

I_0 = Maximum intensity (W/m^2)

k = $K/\rho C$ = Thermal diffusivity (m^2/sec)

k_0 = Bessel function of the first kind and zero order

k_0' = Differential of k_0 with respect to Ur

k_R = Reaction rate (kg/sec)

k_w = Kerf width (m)

K = Thermal conductivity (W/mK)

λ = Wavelength (μm)

λ_L = Beam divergence (m)

λ_s = Striations frequency (Hz)

L_f = Latent heat of vaporization (kJ/kg)

L_m = Latent heat of fusion (kJ/kg)

n = Iteration step size

n_A = Partial solid material density (kg/m^3)

n_0 = Solid workpiece density (kg/m^3)

norm= A coordinate normal to the surface pointing into the workpiece

n_R = Reaction gas density (kg/m^3)

N_2 = Nitrogen

P = Power (W)

P_v = Heat Production rate (W/m^3)

q = Heat source per unit thickness (J/m)

q_R = Heat of reaction (J)

q_o = Absorbed radiation power per unit volume at the surface of the irradiated body (W/m^3)

q_v = Absorbed radiation power per unit volume at distance z from the surface of the irradiated body (W/m^3)

Q = Heat source (J)

ρ = Density (kg/m^3)

r = Radian position (m)

r_B = Molten layer reflectivity

R_b = Radius in 3 dimension = $\sqrt{x^2 + y^2 + z^2}$ (m)

R = Reflectivity of material (1/m)

s = Melt thickness (m)

S = Conduction integral $\int_0^T K \partial T$ (W/m)

t = Time (sec)

t_z = Thickness of material (m)

T = Temperature (K)

U = Normalised velocity per unit length (1/m)

v_s = Velocity at the lower surface of cut (m/sec)

v_R = Reaction speed (m/sec)

V = Velocity of cut (m/sec)

w = Oscillations frequency of the kerf width (Hz)

W_2 = Beam waist diameter at $1/e^2$ intensity value of a Gaussian beam (m)

X = Normalised isothermal power (P/zS)

Y = Normalised isothermal width (Vb_m/κ)

z = Depth of cut (m)

ZnSe = Zinc Selenide

1.3 Carbon Dioxide (CO_2) Laser - an outline

The laser system used in this research is the Ferranti MFKP, slow flow, longitudinal discharge CO_2 laser. The laser can be operated in either the continous wave mode or pulsed mode. The peak power of the laser is 1.2 kW. The addition of nitrogen gas (N_2) to the laser cavity results in the selective raising of the CO_2 to the desired laser levels [6]. The high efficiency of the CO_2 is largely attributed to the fact that low lying vibrational and rotational states require little energy for excitation and a substantial percentage of this energy is coupled out as laser radiation, i.e. the system has a high quantum efficiency. The laser cuts a workpiece using a CNC flying optics beam delivery system. The ZnSe lens has a diameter of 30mm and a focal length of 110mm. The nozzle outlet diameter is 1.5mm. Assuming a Gaussian beam (Figure 1.1), the spot size or the diameter of the beam at $1/e^2$ of the beam intensity can be calculated.

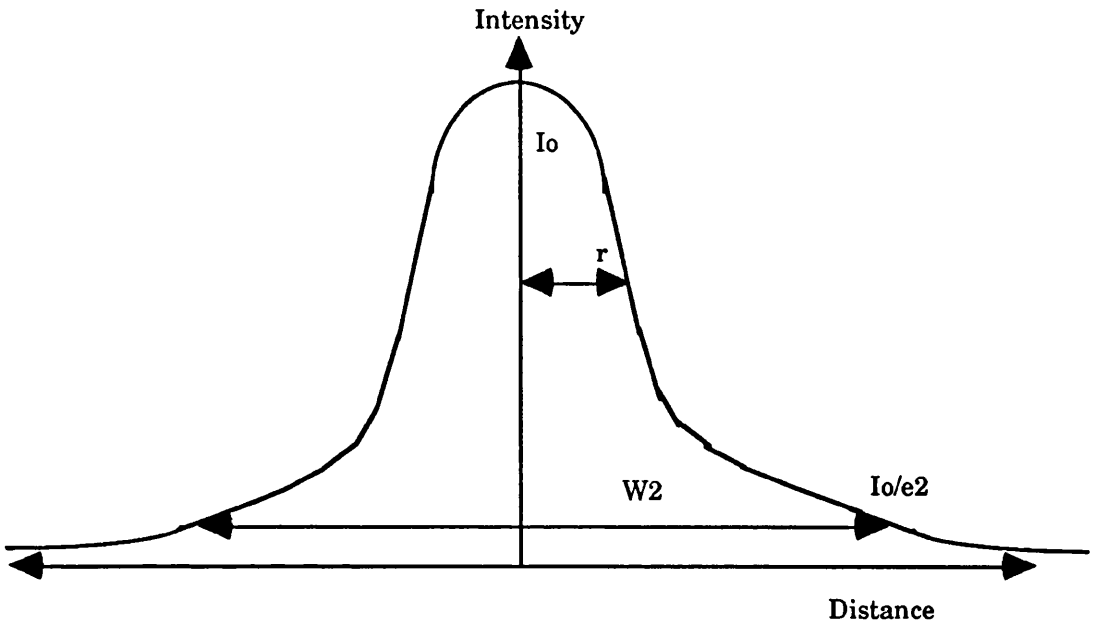

Fig 1.1 Spatial intensity distribution for TEM_{00} laser beam

at W_2,

$$E = E_0 \exp^{-\left[\frac{2r^2}{w_2^2}\right]} \tag{1.1}$$

The spot size, W_2 is given by the formula (Fig 1.2) [7],

$$W2 = \frac{8 \lambda F}{\pi D} \tag{1.2}$$

$$= \frac{8 * 10.6 * 10^{-6} * 110 * 0.001}{\pi * 0.012}$$

$$= \underline{0.247} \text{ mm}$$

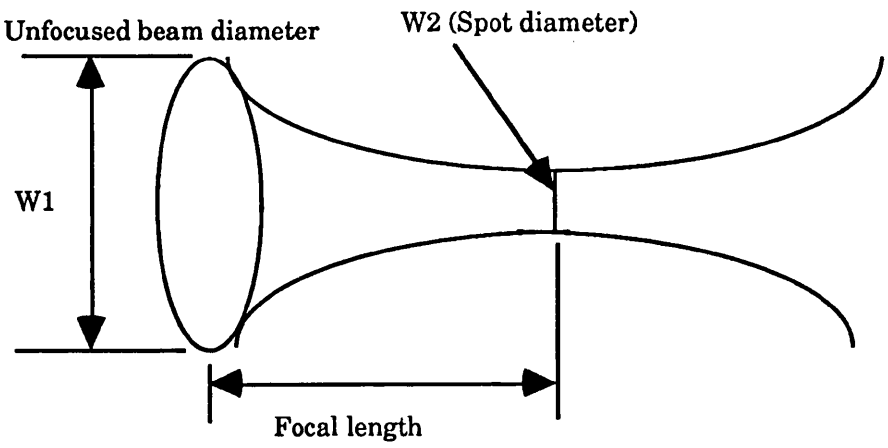

Fig 1.2 Calculation of the laser Spot size diameter

1.4 Laser - material interaction

Since the 1960s, there have been many developments in the area of laser technology [7]. Due to its high intensity and monochromaticity, the laser has become one of the most powerful tool in physics and chemistry. In industry, the laser is used mainly for materials processing [8][9][10]. The unique advantages of laser material processing such as a highly localised heat affected zone, the ability to weld dissimilar materials and cope with complex geometries has led to extensive international research and many industrial applications [11][12]. The main material processing applications are laser drilling, cutting, micromachining, welding and laser surface modification such as laser annealing, laser transformation hardening, laser surface melting (laser glazing), laser surface alloying and laser-induced chemistry. The main laser

processing parametres are wavelength, mode configuration, power density, focal spot diameter, pulse duration, divergence, polarization [13], pointing stability and feedrate. The main material properties are : reflectivity, absorption, thermal conductivity and diffusivity, melting and boiling temperature, vapour pressure, heat of transition (fusion and vaporization), and chemical properties, especially during reactive gas cutting [14]. In this thesis, the use of the laser as a cutting tool is investigated.

1.4.1 Laser cutting

In the majority of industrial laser cutting applications [15], a gas stream is used to purge the melt, evaporated, or sublimated material from the kerf (Figure 1.3). One of the best known examples of laser processing is the cutting of steel. Here, high power lasers are used to produce energy densities that bring about melting and vaporization of the material. When oxygen is used instead of air, cutting and drilling velocities can be increased due to the exothermic reaction. This technique is widely used and has been extensively reviewed [16][17][18]. The lateral dimensions of the cuts are typically between 0.5 to 2 millimetres. The following sections will concentrate on the different techniques of laser cutting. There are basically three main cutting processes:

(a) Vaporized cutting

(b) Inert-gas assisted cutting.

(c) Reactive-gas assisted cutting.

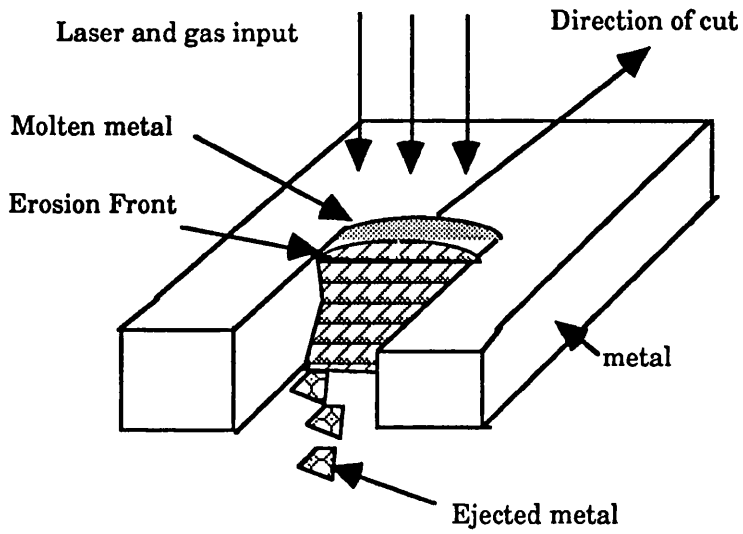

Fig 1.3 Physical Mechanism of Laser processing

1.4.1.1 Vaporized cutting

In vaporized cutting, the beam energy heats the workpiece to above its boiling point and material leaves as vapour and ejecta. The cutting mechanism can be viewed as the increase in temperature in the material resulting in a phase transition. Vaporization cutting is normally used to cut thin sheet, since a gas jet would lead to the inadmissable deformation of the workpiece.

1.4.1.2 Inert-gas assisted cutting

The inert gas assisted cutting process is used to avoid burning damage of flammable materials and surface oxidisation. The

physical mechanism of this process is to cut into the material and set up a temperature gradient to initiate the melting of the material. The gas acts as a removal mechanism to remove the molten material as well as the vapour. The result is a clean cut with around one tenth of the power density required for vapourization cutting.

1.4.1.3 Reactive-gas assisted cutting

The reactive gas jet assisted laser cutting process takes advantage of the energy supplied by the exothermic chemical reaction of the gas jet with the material being removed. The material burns in the reactive gas jet when its surface temperature reaches the material ignition temperature threshold. The jet also blows the melt out of the cut region. The rate of cut depends on the rate of mass transfer to the molten dross and diffusion through the dross to the ignition front. The higher the gas jet velocity, the faster the chemical reaction and removal of the material. Since the burning process provides additional energy, the laser energy per unit cut volume is decreased.

1.5 Characteristics of the laser beam

Laser radiation has a number of unique properties - high intensity (power) of electromagnetic energy flux, high monochromaticity and high spatial and temporal coherence. In order to understand the effects of laser material interaction, it is imperative that the

characteristics are reviewed. The six major characteristics of the laser beam which are critical when using the laser are :

(a) Beam power

(b) Beam Polarisation/cut direction

(c) Wavelength

(d) Transverse mode - Beam Divergence

(e) Focal spot size

(f) Pointing stability

1.5.1. Beam power

The beam power is the most fundamental characteristic of a laser. Laser material processing is usually carried out with continuously radiating (CW) high power lasers [19][20] or with pulsed radiation (see Figure 1.4). In recent years, pulsed lasers [21][22] have been used for producing a series of holes, it has been used for cutting contours with sharp edges and bends, and for cutting special material such as stainless steel and copper [23]. In general, the highest CW power is obtained from CO_2 lasers, whilst Nd-YAG lasers provide the highest peak power for pulsed operation. The power coupled into the material is largely influenced by the optical properties of the material. The material absorptivity determines

the fraction of the impinging radiation energy that is actually absorbed by the material. In most cases, the absorbed radiation power density varies in the bulk of a solid according to Bouguer's Law [24]:

$$q_v(z) = q_o(1-R)\exp(-\delta z) \qquad (1.3)$$

Absorption of light and subsequent energy transfers in the bulk material occur via a different process in metals, insulators and semi-conductors. Power that is not absorbed by the material is reflected back into the environment, hence, adjustment of the laser power is required to ensure that the power threshold required for material removal is exceeded. The absorptivity value is a variable, highly dependent on factors such as surface roughness, laser wavelength, phase and temperature of the material [25].

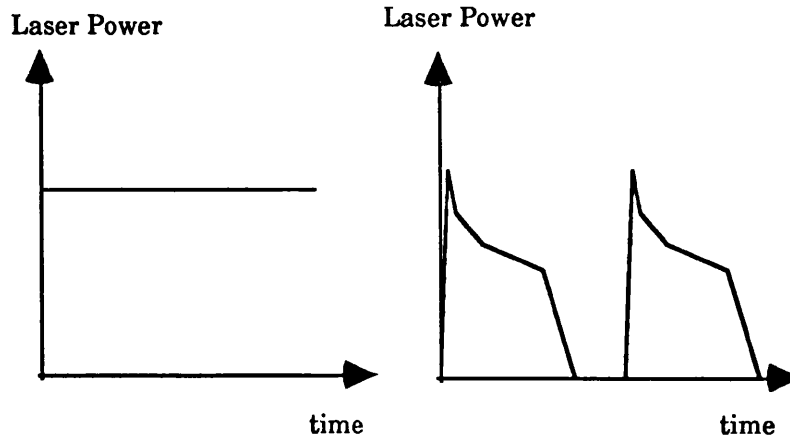

(a) Continuous Wave (b) Pulsed beam

Fig 1.4 Laser Beam temporal modes

1.5.1.1 Beam polarization

Light consists of transverse waves, in which the oscillating electric and magnetic fields oscillate sinusoidally. If the electric vector oscillates in a single plane, then the light is plane polarized. A laser beam can be polarized into either : linear, circular or elliptical orientation [26]. The direction of polarization is an important factor not usually taken into account during materials processing. By orientating the polarization direction parallel to the cut direction in a plane polarized beam, more energy is absorbed by the front of the cut kerf. If the angle between the direction of cut and the polarization plane increases, there would be a corresponding decrease in the power absorbed by the material.

1.5.2 Wavelength

The wavelength is the characteristic spatial length associated with one cycle of vibration of the electro-magnetic wave. The wavelength of a laser is a factor used in deciding the design of the laser optical equipment such as the optical resonator, lenses, mirrors, polarizers and windows. Absorption coefficient for a particular material is wavelength dependent. For the CO_2 laser wavelength of 10.6μm, metals that are highly reflective; gold, silver, copper and aluminium reflect most of the radiation.

1.5.3 Transverse mode

The angular divergence can be related to the beam profile characteristed by the Transverse Electromagnetic Mode TEM [27]. TEM modes can be written in the form TEM_{nm}. The subscript n and m denote the number of nodes in directions orthogonal to the beam propagation (Figure 1.5) The smallest angular divergence is the Gaussian spatial distribution or TEM_{00} mode, this is the best mode for laser cutting as it provides the greatest irradiance.

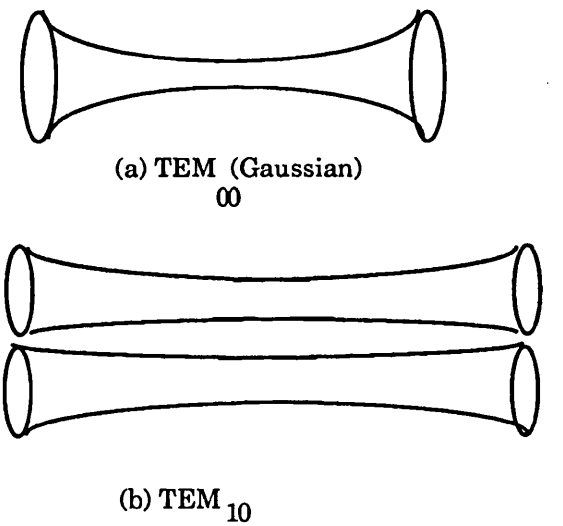

Fig 1.5 TEM modes

1.5.4 Focal Spot size

When a beam is focussed accurately on the workpiece surface, the maximum power density is obtained on the surface. The focal spot size is hence an important factor in relation to the efficiency of

laser power coupling into the workpiece. The focal spot size is influenced by factors such as :

(a) Transverse mode

(b) Diffraction

When focussing a diffraction - limited laser beam with a lens, a longer focal length or higher f number corresponds to a larger focussed spot diametre.

(c) Divergence

The beam divergence angle is proportional to the spot diametre ie. a large divergence implies a larger spot diametre.

(d) Focussing beam diameter [28]

The focal spot diameter, d_{sp}, and the focussing beam diameter, D, for a Gaussian beam, are related by;

$$d_{sp} = \frac{4F\lambda}{\pi D} = 1.2F\lambda \qquad (1.4)$$

1.6 Fundamentals of Laser Machining

Laser material processing [29] is a process that is dependent on many variables. For example, laser power, the formation of molten layers, process feedrate, etc. It is hence desirable that methods of modelling the laser interaction process be developed to make it

possible to calculate approximate data and plot relationships which before could only be obtained directly by a large number of time consuming and costly experiments. Approaches so far can be classified into two classes:

(a) Analytical solutions

The basic analytical solution governing the thermodynamic kinematics of the laser heating process is:

$$\rho C \frac{\partial T}{\partial t} = \frac{\partial}{\partial x}(K\frac{\partial T}{\partial x})+\frac{\partial}{\partial y}(K\frac{\partial T}{\partial y})+ \frac{\partial}{\partial z}(K\frac{\partial T}{\partial z}) + P_v(x,y,z,t) \quad (1.5)$$

For a solid assumed to be homogenous and isotopic, equation (1.5) reduces to

$$\nabla^2 T - \frac{1}{k}\frac{\partial T}{\partial t} = - \frac{P_v(x,y,zt)}{K} \quad (1.6)$$

Many analytical solutions for the laser-material interaction exist [30][31].

(i) Overall heat balance

$$P(1-R) = V k_w t_z \rho(C \Delta T + L_m + f L_f) \quad (1.7)$$

(ii) Point heat source [32]

$$T = \frac{Q(x',y',z')}{8(\pi kt)^{\frac{3}{2}}} \exp(-\frac{(x-x')^2 - (y-y')^2 + (z-z')^2}{4kt} \quad (1.8)$$

where the superscipt ' denotes instantaneous point source location.

(iii) Disc heat source [32]

$$T(r,z,t) = \frac{E_o\left(\frac{W_2}{2}\right)^2}{\rho C(\pi K t)^{\frac{1}{2}}(4kt+\left(\frac{W_2}{2}\right)^2} \exp(-\frac{z^2}{4kt} - \frac{r^2}{4kt+\left(\frac{W_2}{2}\right)^2}) \quad (1.9)$$

(iv) Line source

Swifthook and Gick [33] established for a line source that a particular isothermal is described by :

$$Y = 4Ur\left\{1-\left[\frac{k_o^2(Ur)}{(k_o'^2)(Ur)}\right]\right\}^{\frac{1}{2}} \quad (1.10)$$

$$X = 2\pi \exp \frac{\left\{\frac{Urk_o(Ur)}{k_o'(Ur)}\right\}}{k_o(Ur)}$$

(b) Numerical solutions

There are numerous finite difference and finite element models [34][35][36][37], which are based on differential equations derived from the conservation of energy. The finite difference method treats the effect of the laser-material interaction parametres as time and temperature dependent. This allows non-linearity to be considered during a simulation. The only disadvantage of this approach is that the method is very computationaly intensive.

Process models have been developed that will simulate laser machining in one, two and three dimensions, see Figure (1.6).

(a) Drilling (1 - Dimensional analysis)

(b) Cutting/Welding (2 - Dimensional analysis)

(c) Turning/Milling (3 - Dimensional analysis)

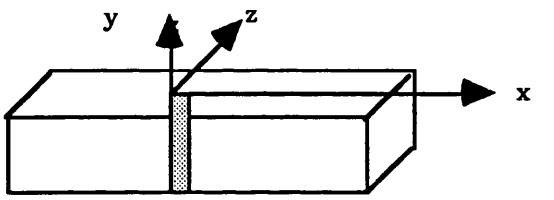

a. 1 -Dimension(drilling)

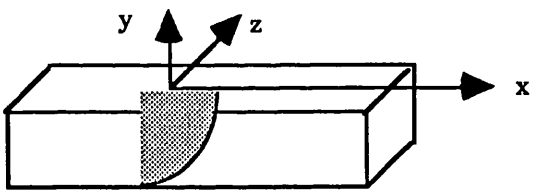

b. 2 - Dimension(cutting)

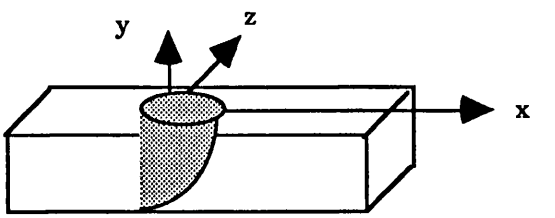

c. 3 - Dimension(milling)

Fig 1.6 A schematic of 1,2 and 3 dimension machining

1.6.1 One dimensional approach (Drilling)

Laser drilling is a process in which the beam intensity is sufficiently intense to overcome the material damage threshold and hence induce boiling and vaporization of the material [38]. For drilling, the lasers are often operated in a pulsed mode. This is usually selected due to the fact that the reflectivity of the material is high at room temperature. A greater fraction of the power would be reflected if a CW laser were used. Using pulsed operation, the initially high reflectivity can be overcome more rapidly, i.e. when the temperature rises in the material, the reflectivity of the material decrease [39]. Many models for laser drilling exist [40]. Using the method of images [41], the temperature distribution for a workpiece of infinite thickness can be calculated as:

$$T(r,z,t)=\int_0^{W_2}\int_0^{t}\frac{P(r',t')}{4\rho C\sqrt{\pi}\,\{(k(t-t'))\}^{\frac{3}{2}}}\exp\left(-\frac{r^2+r'^2}{4k(t-t')}\right) \qquad (1.11)$$

$$I_o\left(\frac{rr'}{2k(t-t')}\right)r'\left(\exp\left(-\frac{(z-f(t'))^2}{4k(t-t')}\right)+\right.$$

$$\left.\exp\left(-\frac{(z+f(t'))^2}{4k(t-t')}\right)\right)\partial t'\,\partial r'$$

For a finite workpiece thickness, the temperature distribution is :

$$T(r,z,t) = \int_0^{W_2} \int_0^{t} \frac{P((r',t'))}{2\rho Ck(t-t')t_z} \exp\left(-\frac{r^2 + r'^2}{4k(t-t')}\right) \qquad (1.12)$$

$$I_o\left(\frac{rr'}{2k(t-t')}\right)\left(1 + \sum_{n=1}^{n=\infty} \cos\frac{n\pi(z+f(t'))}{t_z}\right)$$

$$\exp\left(-\frac{kn^2\pi^2(t-t')}{t_z^2}\right) + \sum_{n=1}^{n=\infty} \cos\frac{n\pi(z-f(t'))}{t_z}\Bigg)$$

$$\exp\left(-\frac{kn^2\pi^2(t-t')}{t_z}\right)\Bigg) r'\,\partial t'\,\partial r'$$

1.6.2 Two dimensional laser machining (Cutting and welding)

Laser cutting is the most widely used of all laser machining processes. Extensive research work into the cutting process has been completed to date [42][43][44][45][46]. There are two main modelling approaches : sublimation and fusion cutting. In modelling the two cutting processes, the sublimation model emphazies the effect of vaporisation whilst the fusion cutting model is based on the effect of melting, In laser cutting, a reactive or non-reactive gas jet is used to increase the rate of metal removal. A model proposed by Prof D. Schuocker based on the conservation of mass and energy flux [47] provides a relatively accurate model. From the mass equation for the reactive gas particles on the melt (equation 1.13) and the mass equation for the pure melted metal (equation 1.14), an energy balance can be derived (equation 1.15).

$$k_w t_z q_R = s k_w t_z k_R n_R n_R + s k_V n_R v_s + k_w t_z \alpha_R n_R \qquad (1.13)$$

$$k_w t_z V n_0 = s k_w t_z k_R n_R n_A + s k_w n_A v_s + k_w t_z \alpha_A n_A \qquad (1.14)$$

The net energy gain of the molten layer due to the reactive gas flow is :

$$(\frac{\partial E}{\partial t})net_R = \frac{\varepsilon_R k_w t_z V n_o q_R}{q_R + s k_R (\frac{v_s}{t_z} + \frac{\alpha_A}{s})(\frac{v_s}{t_z} + \frac{\alpha_R}{s})} - \varepsilon_{th}(\frac{1-r_B}{r_B})q_R \qquad (1.15)$$

maximizing equation (1.15);

$$(\frac{\partial E}{\partial t})net_R = \varepsilon_R k_w t_z V n_o \qquad (1.16)$$

The velocity (equation 1.17) of the ejected molten metal and the thickness (equation 1.18) of the erosion front were also derived;

$$v_s = \sqrt{\frac{\eta_R t_z}{\delta_s s k_w}} v_R \qquad (1.17)$$

$$s = \frac{2k}{V}(1 - \frac{T_s}{T})\frac{k_o\left(\frac{Vk_w}{4k}\right)}{K\left(\frac{Vk_w}{4k}\right)} \qquad (1.18)$$

The quality of cut is a function of the roughness of the cut kerf. This roughness is due to the presence of striations, which is the result of the periodic oscillation of the molten material, this is controlled by complex boundary layer interactions. In order to have a good quality cut, these periodic striations must be kept to a very close interspacing. A physical way to do this is to use a

continuous high Pulse Repetition Frequency (PRF) laser. Equations (1.19) and (1.20) derived by Prof. D. Schuocker determine the depth of striations and the frequency of the striations respectively. From the equations, it can be concluded that the velocity of the cut and the power of the laser beam are the two main parametres to be considered in the cutting or welding process.

$$b_w = \frac{1}{K_o} T \tag{1.19}$$

$$\lambda_s = \frac{2\pi V}{w} \tag{1.20}$$

Two dimensional analysis of laser welding [48][49][50] is usually performed using the heat transfer approach similar to that of laser cutting.

The heat required for melting a metal plate of thickness t_z, at speed V [51]:

$$q = 8KT(\frac{1}{5} + \frac{Vt_z}{4k}) \tag{1.21}$$

1.6.3 Three dimensional laser machining (Milling)

Three dimension laser machining is used mainly for bulk material removal with two or more laser beams. The relative angular position of the beams provides the shape axis during the milling action. Three-dimensional modelling is based on the approach of

laser grooving. A model proposed by George Chryssolouris [52] is as follows (Figure 1.7)

$$E(x,y,z)A_1 = -k\left(\frac{\partial T}{\partial norm}\right) A + \rho L_v A_2 \qquad (1.22)$$

Assuming a Gaussian laser beam intensity;

$$P(x,y,z) = \frac{(1-R)\,P}{\pi r(z)^2}\exp(-\frac{x^2+y^2}{r(z)^2}) \qquad (1.23)$$

$$r(z) = R_b\,(\,1+(\,\frac{\lambda_L\, z}{\pi\, R_b^{\,2}})^2\,)^{\frac{1}{2}} \qquad (1.24)$$

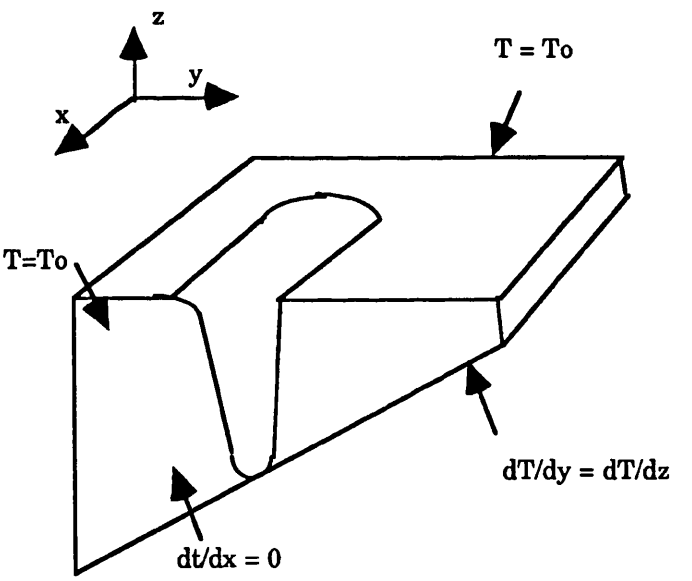

Fig 1.7 Control volume for three dimension analysis

1.7 Laser-material interaction analysis and control

Due to the high capital and operating costs of laser systems, economic viability in installing a laser as a machine tool must be

justified in terms of : good degree of repeatability, high metal removal rates, high dimensional accuracy and good quality surface finish. The laser-material interaction is a highly non-linear process; hence, optimal operating parametres i.e. power, feedrate, focal position ... are established by *ad hoc* experience based techniques. Slight changes in either the laser focal height, gas pressure, feed rate may result in transient and unpredictable behaviour of the cutting process. The current practice in the prediction of laser machining control parametres has significant disadvantages. The most prominent being the time spent in calibrating the laser-material interaction characteristics. Not only must there be calibration experiments conducted for all thicknesses of a specific material, a different set of calibrations must be conducted for each different material. The *ad hoc* trial and error approach, which at times produces acceptable cut quality, often results in non-optimal machining conditions. Power fluctuations and local changes in material composition can lead to inconsistencies in the cut kerf width and cut quality; hence, to date, a lot of work has been conducted to try to control the laser-material machining process. The objective of the research described in the following chapters is to establish models and methods with which to overcome the afore-mentioned disadvantages of laser-materials processing. The research has been conducted in three stages:

(a) Prediction of optimal operation parametres for pulsed laser cutting.

An evolutionary prediction scheme has been

developed so that a set of optimum machining parametres can be predicted by a method that is not obstructed by the non-linearities that defeat a more conventional mathematical model.

(b) Investigation into the non-linear characteristics of laser-material interactions.

Although many models exists, i.e. analytical and numerical, that describe the laser-material inter-action over limited regions of operation, they cannot follow the trajectory of control parametres over any extended operational envelope. These prediction schemes always lead to regimes of unstable transient behaviour where the model is invalid. The theory of chaos has been used to investigate these transient phenomena. The energy phase portrait of the laser-material interaction process is produced and used for the prediction of the laser operating conditions.

(c) Development of an intelligent control, tasking and forecasting system for the laser manufacturing system.

This treatise aims to produce a solution to the design, development and implementation of an intelligent system for the control and tasking of an existing carbon dioxide laser at the University

of Glasgow. A new topological technique for designing both process and knowledge control has been developed for the design stage of the intelligent system. The intelligent system provides direct computer control facilities for the manufacturing system pulser and work handling units. Furthermore, it predicts the required operating conditions for specific material processing tasks. Closed-loop control is also incorporated into the intelligent system to compensate for any process disturbances. A computer vision discriminator system has been built to provide a vision judgement facility for the analysis of the exit spark cone during laser processing.

The final hybrid intelligent system provides control, tasking and forecasting functions for the laser manufacturing system in addition to providing a consultation-teaching facility to train new users in laser material processing. Finally, the research demonstrates methods that are extremely powerful in dealing with a highly non-linear control problem. These methods are therefore generally applicable for the control of all other non-linear systems.

REFERENCES.

[1] A.H. Schawlow and C.H. Townes, "Infrared and Optical Masers", Phys. Review, 112,pp 40(1958).

[2] T.H. Maiman, "Stimulated optical radiation in ruby maser", Phys. Review,187,pp 493(1960).

[3] A. Javan, *et al*, "Population inversion and continuous optic maser oscillation in a gas discharge containing a He-Ne mixture", Phys. Review, 6, pp 106(1961).

[4] P.P Sorokin and M.J. Stevenson,"Stimulated infrared emission of trivalent uranium", Phys. Review, 5, pp 557(1960).

[5] C. K. N Patel,*et al*, "CW laser action on rotational transition of the $\Sigma u+ = \Sigma g+$ vibrational band of CO_2", Bull. Am. Phys. Soc. , 9, pp 500 (1964).

[6] W.M Steen, "Laser material processing",Springer-Verlag, London, pp 7 - 38(1991).

[7] W.W. Duley,"CO_2, Effects and Applications", NY(1976).

[8] G. Chryssolouris, "Laser Machining - Theory and Practice", Springer-Verlag, NY, pp 43 - 46(1991).

[9] D.Belfore and M. Levitt (eds), "The Industrial Laser Annual Handbook", Penn Well books, Laser Focus, Tulsa, Okhoma(1986).

[10] J.F. Ready, "Industrial Applications of Laser", Academic Press, NY(1978).

[11] SS. Charschan, "Laser in Industry", Van Nostrand Reinhold Comp, NY(1972).

[12] L. Garifo and A. Sona, "High Power lasers and their industrial applications", SPIE, 650, pp 47(1986).

[13] F.O. Olsen, "Cutting with polarized laser beams", DVS Berichte, 63, pp 197(1980).

[14] D. Schuocker and B. Walter, "Theoretical model of oxygen assisted laser cutting", Inst. Phys. Conf. Ser. No. 72, Adam Hilger Ltd, pp 111(1985).

[15] B.Steverding, "Thermomechanical change by pulsed laser", J. Physics: Applied Phys., 4, pp 787(1971).

[16] G.Herziger and E.W. Kreutz, "Laser Processing and Diagnositc", Phys. Vol 39, Springer, Berlin, pp 90(1984).

[17] D.Schuoker,"Industrial applications of high power lasers", SPIE, Vol 455(1983).

[18] W.M. Steen and J.N. Kamalu, "Laser cutting", M. Bass (ed.), Laser material processing, North - Holland, Amsterdam, pp 15 - 113(1987).

[19] Yoshiaki Arata, Hiroshi Maruo,"Dynamic Behaviour in laser gas cutting of mild steel", Trans of JWRI,Vol 8, No 2, pp 15 - 26(1979).

[20] M.J.Adams,"Gas jet laser cutting", Proc. of Conf. on Advance of welding process, The British Weld. Inst., pp 140 - 146(1970).

[21] N. Forbes, "The application of pulsed lasers to the welding and machining of mirocircuit components", IEEE Conf. on lasers and their applications, pp 11(1964).

[22] H.H.Martien and Van Dijk ,"Pulsed Nd-YAG laser cutting", Industrial Laser Handbook, Penn well Books, pp 52 - 65(1987).

[23] Ancel Thompson,"CO_2 laser cutting of highly reflective material", The Industrial Laser Handbook, Penn well books, pp 149 - 153(1986).

[24] N. Rykalin, A. Uglov and A. Kokora, "Laser machining and welding", translated by O. Glebov, Pergamon Press, pp 9 - 26(1978).

[25] A.M. Prokhorov, V.I. Konov, "Laser heating of metals", Adam Hilger, NY, pp 1 - 19(1990).

[26] F.A. Jenkins, "Fundamentals of Optics", McGraw-Hill International, pp 497-520(1981)

[27] Coherent, Inc. staff, " Lasers: Operations, Equipment, Applications, and Design", McGraw-Hill, NY(1980).

[28] W.M. Steen, "Laser material processing", Springer - Verlag, London, pp 58(1991).

[29] D. Belforte and M. Levitt(eds), "The industrial laser", The laser annual handbook, Penwell Books(1987).

[30] D. Schuocker, "The physical mechanism and theory of laser cutting", The Industrial Handbook, pp 65 - 80(1987).

[31] W.M. Steen and J.N. Kamalu, "Laser cutting", "Laser material processing", edited by M.Bass, North-Holland, pp 17 - 111(1983).

[32] H.S. Carslaw and J.C. Jaeger, Conduction of heat in solids, Oxford University Press, NY(1959).

[33] Swifthook and Gick, Welding Institute, Res. Suppl., pp 492S(1973).

[34] J. Mazumder, "Overview of melt dynamics in laser processing", Optical Engineering, Vol 30 No.8., pp 1208 - 1219(1991).

[35] M. Lax, "Temperature rise induced by a laser beam", Journal of Appl. Physics, Vol 48, No. 9, pp 3919 - 3924(1977).

[36] J. Mazumder and W.M. Steen," Heat transfer for CW laser material processing", Journal of App. Physics, Vol 51, No. 2, pp 941 - 947(1980).

[37] W.W. Duley,"CO_2 Effects and Applications", Academic Press,NY pp 177 - 189(1976).

[38] C.R. Chatwin,"Thermodynamics of pulsed carbon dioxide laser for machining metals", PhD Thesis, University of Birminghan(1979).

[39] Von Allmen, M.,"Laser drillng velocity in metals", Journal of Appl. Phys., Vol 47, No. 12, pp 5460 - 5463(1976).

[40] U.C. Pock and F.P. Gagliano, "Thermal analysis of laser drilling processes", IEEE Journal of Quantum Electrons, Vol QE-8, No. 2, pp 112 - 119(1972).

[41] G. Chryssolouris, "Laser machining - Theory and Practice", Springer-Verlag, NY, pp 162 - 169(1991).

[42] Erich H. Berloffa, J. Witzmann,"Laser cuttings of metallic and non-metallic minerals with medium powered(1.2kW) CW lasers", Proc SPIE 398, Geneva, pp 354 - 361(1983).

[43] D. Schuocker, "Dynamic Phenomena in laser cutting and cut quality", Journal of Appl. Phys., Vol 40, pp 9 - 14(1986).

[44] N.Rajendran and M.B. Pate, "The thermal response of a material during a laser cutting process", Proc of 6th International Conference in Application of Lasers,ICALEO'87, pp 129 - 135(1987).

[45] K.A. Bunting and G. Cornfield, "Towards a General Theory of cutting: A relationship between the incident power and the cut speed", Journal of Heat Transfer, pp 116 - 122(1975).

[46] P.Henry, T. Chande, K. Lipscombe, J. Mazumder and W.M. Steen, "Modelling laser heating effects", LIA, ICALEO, Vol(3), pp 25 - 31(1982).

[47] D. Schuocker and W. Abel, "Material removal mechanism of laser cutting", Proc. of SPIE, pp 88 - 95(1983).

[48] E.A. Metzbower,"Heat flow in laser beam welding", 6th International Conf. on Applications of Lasers, ICALEO ' 87, pp 37 - 47(1987).

[49] J. Mazumder, "Laser Welding", Laser for laser material processing, North-Holland, Michael Bass(ed.), pp 113 - 201(1983).

[50] R.F. Duhamel, "Laser welding of X-65 oil and gas transmission pipe", ICALEO '86, pp 161 - 169(1986).

[51] A.A. Wells," Heat flow on welding", Welding Journal, Vol 31, pp 263 - 266(1952).

[52] George Chryssolourus,"Laser machining - Theory and Practice", Springer-Verlag,Mechanical Engineering Science, pp 186 - 189(1991).

2 EVOLUTIONARY PROCESS PREDICTION AND OPTIMIZATION FOR LASER MATERIAL INTERACTION

2.1. Introduction

Producing complex [1], high quality components often made from exotic refractory materials is an ongoing problem in manufacturing. These problems are usually solved utilising specialised machines which often reduce the flexibility of the machining process. It is possible for the output of a laser of sufficient power to raise the temperature of any material in excess of its phase transformation limit resulting in melting and evaporation; hence, a laser may be used as a machine tool [2][3][4][5]. Existing applications software provides operators with an interactive method of part programming. The integration of the laser system, CAD/CAM and automated workpiece handling equipment serves to further automate the system. The interaction of laser light with matter is a

relatively complex phenomenon. An understanding of the laser/material interaction process, is hence crucial; a great amount of research has been conducted in this area which has resulted in a substantial body of literature [6][7][8]. Numerous models defining the conditions and variables affecting the laser/material interaction have been developed and applied to physical applications with remarkable success [9][10]. For the industrial applications of laser materials processing, it is important to optimise all the process parameters. This leads to the maximum processing speed and normally the lowest production costs. The quality criteria may be different for different applications. A method is hence required to perform this optimal selection for this highly non-linear process. Recently, genetic algorithms (GA) [11][12] have been studied to solve many combinatorial problems. Genetic algorithm systems start with a fixed population of data structures which are used to perform specified tasks. After multiple attempts at executing the tasks also known as evolution, each of the participating structures is tagged and rated with a specific utility value quantifying its performance.

2.2 Nomenclature

a = Thickness of the material (m)

b = Kerf width (m)

CW = Continuous wave

$\delta(T)$ = Absorption coefficient as a function of temperature (1/m)

GA = Genetic algorithm

I = Intensity of the laser beam (W/m^2)

HAZ = Heat affected zone (m)

λ_f = Pulse separation (Hz)

λ_p = Pulse length (sec)

L_v = Latent heat of fusion (kJ/kg)

m = Mass of material removal (kg)

p.r.f = Pulse repetitive frequency (Hz)

P = Power of laser (W)

P_p = Pulse power (W)

P_{total} = Total power absorbed by the material (W)

ρ = Density of material (kg/m^3)

r = Reflectivity of the material

t = Time (sec)

T = Temperature (K)

T_a = Ambient temperature (K)

T_m = Material melt temperatuer (K)

V_{cut} = Velocity of the cut (m/sec)

x = Direction of radiation propagation (m)

2.3 Outline of the industrial laser and the cutting process

The characteristics of laser radiation have been studied extensively as they represent both singly and collectively a completely new type of energy source with properties not previously achievable (i.e. wavelength, coherence, power output, etc.). It is due to these characteristics that lasers are now used in numerous commercial applications. In this paper, we are interested in the use of the laser (a MFKP CO_2 laser) in manufacturing, particularly in the cutting of materials. The cutting process is essentially one of material removal from the cut or kerf, except in the case of thermal fracture. For continuous cutting, using a pulsed laser, a series of overlapping holes results in a continuous cut. Although the absorption of most metals [13] is low at the output wavelength of the CO_2 laser, the cutting effectiveness of a CO_2 laser is quite high for ferrous metals, titanium and other metals which react exothermically with the cutting gas; absorption also increases rapidly as the surface temperature rises. High cutting rates are achieved in this way at moderate values of laser power which would otherwise be insufficient to remove the volume of material contained in the kerf. The most controlling factors for a good cut quality is the pulse and mean beam power, pulse repetition frequency, pulse length and feedrate for a particular material[14]. Both an initial threshold level of power and feedrate are required to initiate the cut which is dependent on the workpiece reflectivity and rate of thermal diffusion from the cut region of the material. These threshold levels are also dependent on surface finish and the presence of

oxide films. For a good manufacturing process, production costs - which are related to manufacturing time - should be minimized. For cutting, operation at an optimum value of power and feedrate is essential. To obtain an optimum or maximum velocity, optimum values of pulse power, pulse length and pulse repetition frequency must be determined.

2.4 Continuous wave and pulse mode

Typically laser cutting is performed utilising either a solid state or gas laser. Solid state lasers are usually pulsed and used for low power material processing due to their low energy transfer efficiency, For high mean power material processing, gas lasers are usually operated in continuous wave (CW) mode. CW lasers are capable of cutting rates of several meters per minute for thicknesses up to 10mm. Material processing [19] is enhanced when the laser beam is coupled with the addition of a reactive gas (O_2) jet or electric arcs for ferrous materials [20]. Absorption of laser radiation in a homogenous material and its transformation into heat follows the Beer Lambert law.

$$dI = - \delta(T)\ I\ dx \qquad (2.1)$$

The absorption of most material increases as the temperature of the material increases. In the cutting of highly reflective materials such as aluminium or stainless steel, which have high initial reflectivities, the pulsed mode of operation is more effective than CW. The reason is that in CW mode, most of the input power is

reflected by the high reflectivity material. In pulsed mode there is an initial power spike and higher instantaneous power which raises the surface temperature rapidly, lowering the reflectivity which results in enhanced absorption. The properties of a pulsed gas laser [15][16] are intermediate between those of pulsed solid state and CW gas lasers, in that the beam properties are better than those of CW lasers, whilst their mean output powers are much higher that those of pulsed solid state lasers. Cutting material with a pulsed laser is very useful when cutting contours with rapid changes in direction [17]. In pulse laser cutting, the time scale for heating, melting and vaporization are much faster than in the CW mode. Due to the enhanced power density at the surface of the workpiece, the molten layer formed during laser cutting reaches a higher temperature than with CW laser cutting and thus the liquid has a lower viscosity. As a result, the ejection of molten material, including slag, is facilitated and the formation of dross is reduced. Due to the ON/OFF ratio available, a reduced average power acts on the workpiece, and therefore the cutting speed is also reduced. Thus cutting with the laser in pulse mode produces a better cut quality but with reduced cutting speed.

2.5 Optimal problem

For laser and material-interaction processes, due to the different absorptivity and reflectivity of the materials, there is a certain power threshold below which melting/evaporation of the material will not occur. The optimal mean power requirements are a function of a tuple of attributes comprising the pulse power, pulse

frequency and pulse length [18]. The pulse length has to be long enough to heat up a significant material volume for cutting. For this study, when the pulse length is increased, the pulse frequency has to be decreased since the average power is selected to be constant. At a certain value of the pulse length, the energy flux of the laser beam is sufficient to sustain a constantly evaporating or melt phase, this results in a constant temperature at the cut front. When this threshold value of the pulse length is exceeded, two adverse metal cutting defects occurs.

(a) The long pulse length allows the cut temperature gradient to decay at the end of the pulse, resulting in a rapid cooling of the cut kerf and the formation of dross.

(b) The high pulse repetition frequency results in the overlapping of the heat affected zone between the end of a pulse and the start of the next pulse. The total material surface temperature rise can induce the formation of a plasma plume which reduces the energy transfer efficiency from the laser beam to the material surface.

In principle, there are an infinite number of combinations of pulse power, pulse length and pulse frequency which lead to the same value of the average power. From equation (2.2), it can be seen that this average power can be represented as a three dimensional surface in the pulse power (P_p), pulse length (λ_p) and pulse frequency (λ_f) (Figure 2.1) .

Average Power = $P_p * \lambda_p * \lambda_f$ (2.2)

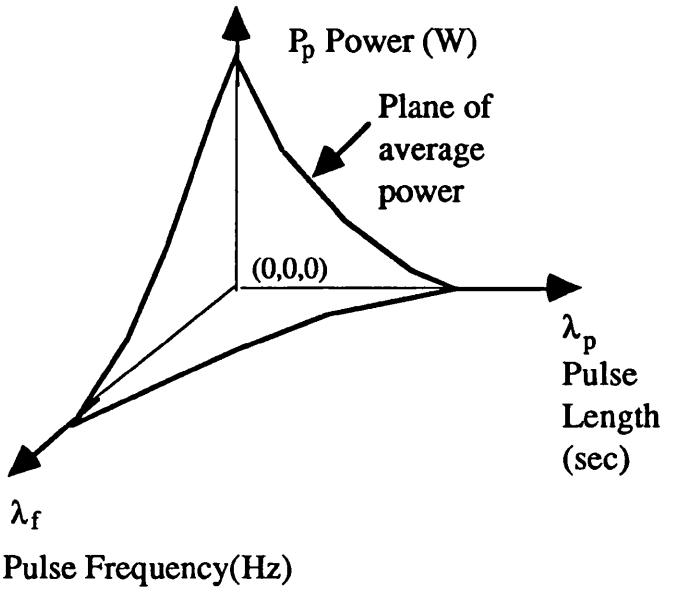

Fig 2.1 The surface of average power defined by Pp, λ1 and λf.

2.6 Outline of genetic algorithm

In the area of autonomous learning, there are several approaches [21].

(i) One approach exploits a small network of neurons

(ii) A second approach utilises adaptive parameter adjustment

(iii) A third, is in the use of self adapting stochastic automata models

(iv) A fourth approach utilises survival of the fittest through population genetics (GA)

This work exploits the GA approach (iv) for an optimisation search. At the initialisation stage the genetic system receives a valid tuple from the environment, it then searches for all population pairs which have a first member matching the input first member. From those that match, the first one found having the highest utility value is selected and the second input member is returned as the new search criteria. If no match is found, a randomly selected member is used to generate the next new state. This fitness mode carries on until all the members of the environment have a utility value. The new generation is created from the old population by first selecting a random block of the members having the highest utility value. From these, offsprings are obtained by the application of both:

(a) Crossover

(b) Inversion or mutation operators

Each offspring inherits a utility value from one of the parents and the resultant parent population with the lowest utility value are discarded. The whole system evolves until it has learnt all the optimal moves (Figure 2.2)

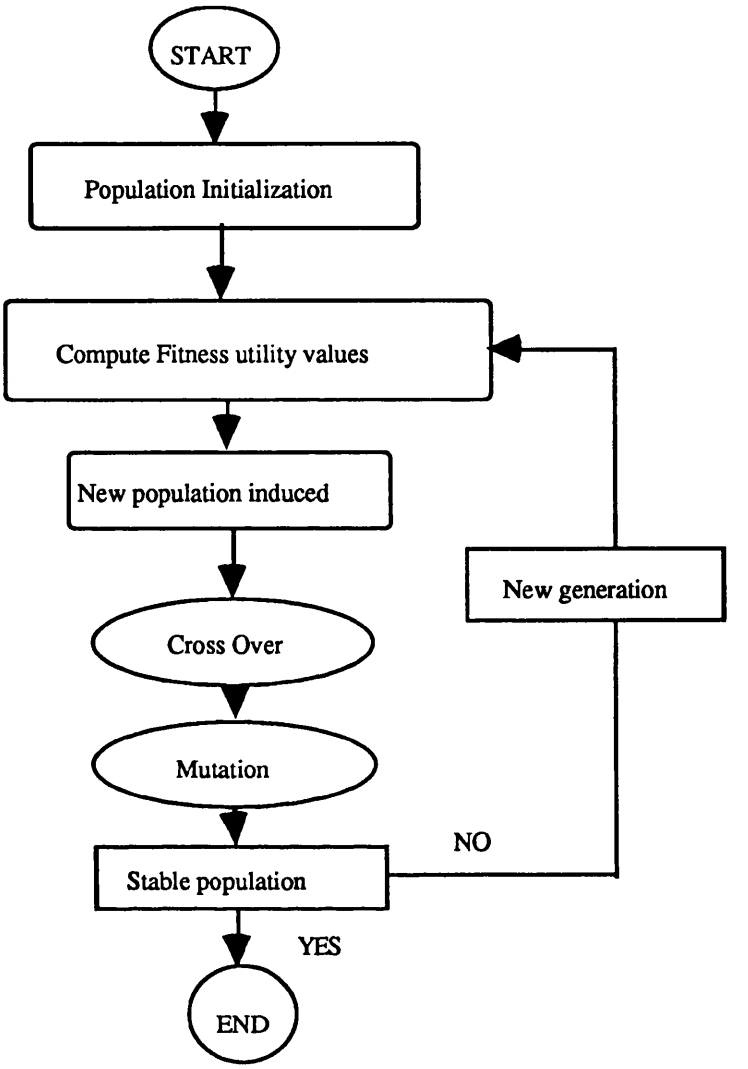

Fig 2.2 Genetic algorithm

2.7 Model/Cost function

Successful models describing the interaction kinetics between a laser and the workpiece are available as finite-element models [20][21] or analytical models [22][23]. The model derived here acts as a cost function to provide the selective survival utility value for the individual population generated by the GA. Assuming a quasi-stationary state, the approach to the analytical derivation of the

basic model is to assume that cutting of the material occurs only at melting. A reactive gas jet provides forced convection to remove the liquid metal. This serves as an important criteria during the experimental stages in identifying the validity of the model and the predicted pulsed power parameters. Based on the geometry in Figure 2.3, the physics governing the cutting mechanism can be described by an energy flux balance equation. Taking a time, t, the power absorbed by the material, (1-r)P (where r is the reflectivity of the material), heats up a cylindrical volume of a depth equal to the material skin penetration depth just below the focus of the beam. The total power is then transferred into the material to heat and melt it. Hence, in analytical power balance form;

$$(1-r)P = P_{total} \tag{2.3}$$

Rewriting (2.3) in energy form:

$$t\,[(1-r)P] = mC(Tmelt - Tambient) + mLv \tag{2.4}$$

From (2.4),

$$t = \frac{mC(Tmelt - Tambient) + mLv}{(1-r)P} \tag{2.5}$$

Referring to Figure 2.3, assuming that the time for a point source to move from an origin point to the e^{-2} value of the laser intensity is equal to the time required for a good cut.

$$t = \frac{R}{V_{cut}} \tag{2.6}$$

equating (2.5) with (2.6);

$$\frac{mC(Tmelt-Tambient)+mLv}{(1-r)P} = \frac{R}{V_{cut}} \qquad (2.7)$$

but m = abRρ, therefore, for continuous wave laser cutting :

$$V_{cut} = \frac{(1-r)P}{ab\rho[C(Tmelt-Tambient)+Lv]} \qquad (2.8)$$

and for pulsed laser cutting, the velocity of cut is :

$$V_{cut} = \frac{(1-r)P_p * \lambda_p * \lambda_f}{ab\rho[C(Tmelt-Tambient)+Lv]} \qquad (2.9)$$

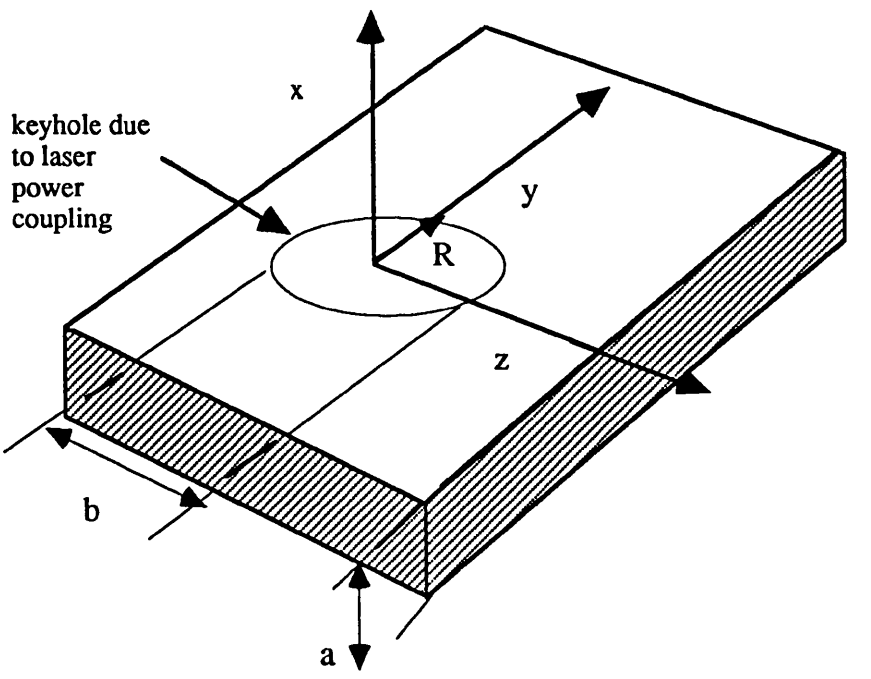

Fig 2.3 A simplified geometry of laser cutting

Although equation (2.8) is a relatively simple model, it elucidates the most important features of laser cutting and provides a model which is easy to use for real applications (see results section). The

model identifies salient control criteria for an effective cut and estimates the energy input from the reactive gas jet.

2.8 Experimental Procedures

The experiment was carried out on a Ferranti, MFKP, co-axial gas-assisted 1.2 kW CO_2 laser (see Figure C-1). The laser is able to run either in a continuous mode or pulsed mode. The focal length of the zinc selenide lens, focusing the beam onto the workpiece, is 110mm (Figure 2.4) In order to maintain a standard controlled environment, certain parameters have to be pre-set and remain constant throughout the experiment. The cutting experiment was carried out by offsetting the nozzle height to 0.6mm from the surface of the workpiece. The reactive gas used is oxygen at a pressure of 2bar. The workpiece used is commercial mild steel, BS 1449-CR4 (K = 71 W/mK, C = 0.46J/gK, Tmelt = 1490C, Lv = $0.272*10^6$ J/kg). The beam is delivered through a 1.3mm diameter nozzle.

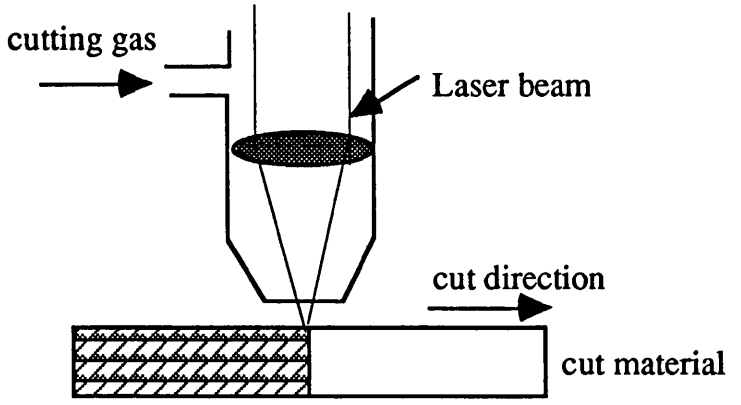

Fig 2.4 A schematic diagram of the laser arrangement

The beam operates in the TEM_{00} Gaussian mode, the spot size is calculated to be approximately 0.247 mm. This value was validated by measuring the kerf width from a cut workpiece under a preset cutting environment. Mild steel samples of thickness 1mm to 6mm were initially cut in continuous wave mode at high power (addition of nitrogen, P = 1.2 kW) and then low power (absence of nitrogen, P = 600W), the feedrate was based on the theoretically predicted cut velocity. These experiments were conducted to validate the physics represented in the model when predicting cut performance. The genetic algorithm was then run on a SUNSPARC workstation to generate a range of pulse lengths and pulse separations for different values of laser mean power. The predicted pulse values and velocity were then used to cut the corresponding workpiece. Experimental results of the cut obtained show a favourable accuracy in relation to the predicted values.

2.9 Experimental results

2.9.1 Continuous mode

The analytical model provides a range of cut velocities for the different workpiece thicknesses (1mm - 6mm) of the workpiece. Experimental velocity values for the cut at high and low power were obtained and tabulated against the theoretical velocity values (see table 2.1). The graphs (see graph 2.1, graph 2.2) obtained show an average deviation of approximately 30% between the derived model's velocities and the actual cut velocities (see graph 2.3, graph 2.4). Hence this justifies the use of the analytical model

as the fundamental equation to govern the characteristics of the laser/material interaction kinetics.

Thickness (mm)	CW Power (W)	Vtheory (mm/min)	Vactual (mm/min)	Velocity error(%)
1	1000	8110	5300	34.6
2	1000	4059	2700	33.48
3	1000	2706	2000	26.09
4	1000	2029	1420	30
5	1000	1623	1200	26
6	1000	1353	800	38
1	400	3247.3	2320	28.5
2	400	1623.6	1460	10
3	400	1082.4	840	22.4
4	400	811.83	600	24.5
5	400	649.4	480	26

Table 2.1 Tabulated values of theoretical cut velocity against actual cut velocity

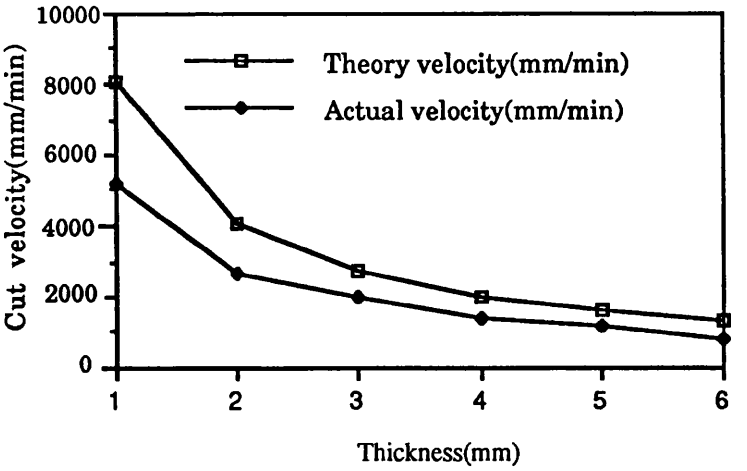

Graph 2.1 Graph of theoretical and actual cut velocities against workpiece thickness at high CW power (1 kW)

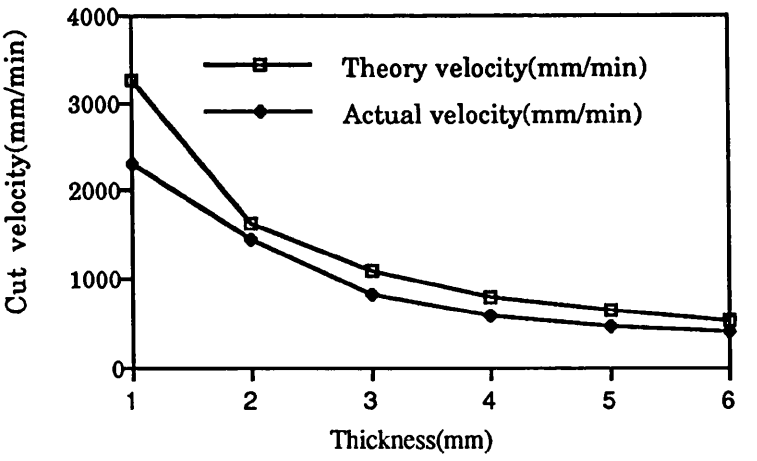

Graph 2.2 Graph of theoretical and actual cut velocities against workpiece thickness at low CW power (400 W)

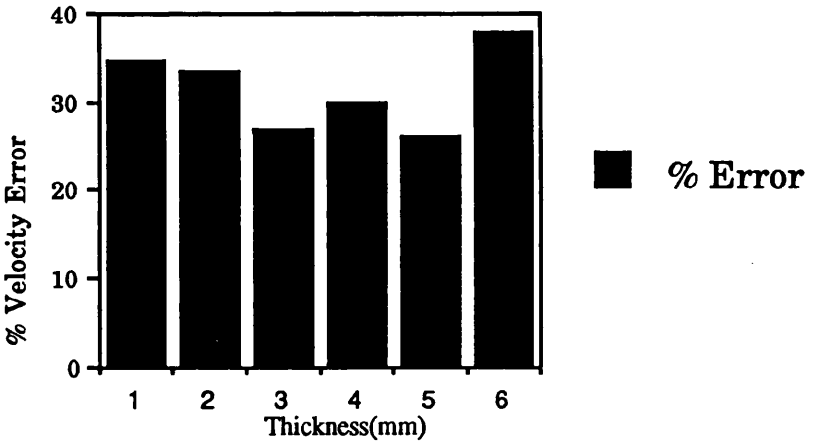

Graph 2.3 Graph of cut error deviation between predicted and actual velocities against workpiece thickness at high power (1 kW)

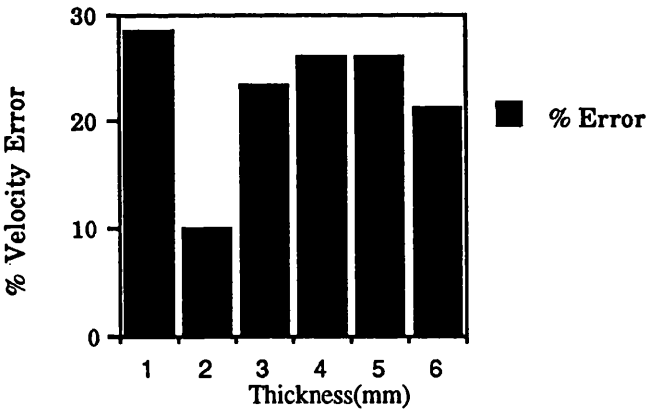

Graph 2.4 Graph of cut error deviation between predicted and actual velocities against workpiece thickness at low power (400 W)

2.9.2 Pulsed mode

In the oxygen assisted cutting of mild steel, BS 1449-CR4, the quality of the cut and kerf width in the workpiece is significantly affected by the cutting speed. Broadly, the quality of the cross section can be classified into (1) self-burning, (2) dross clinging, (3) gouging and (4) dross free (see Figure 2.5). Photographs of the mild steel cut surface using the GA for the prediction scheme can be seen in Figure 2.5(v) and Figure 2.5(vi). The criteria for a good cut accepted for the tabulated results is in the attainment of a dross free cut.

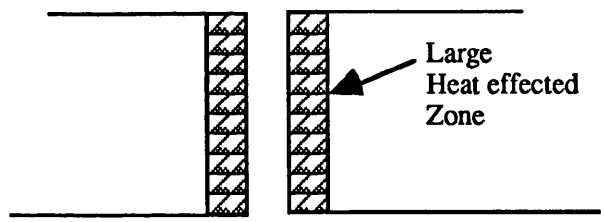

Fig 2.5(i) Self-burning

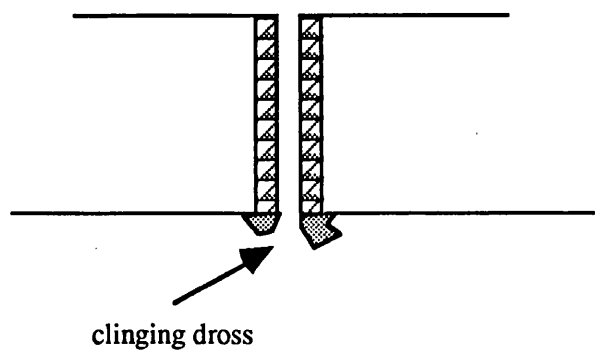

Fig 2.5(ii) Dross clinging

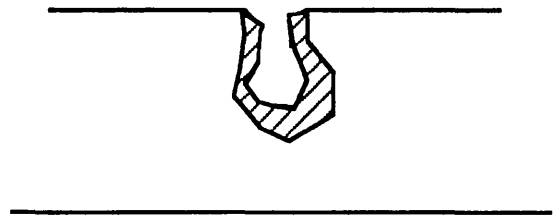

Fig 2.5(iii) **Gouging**

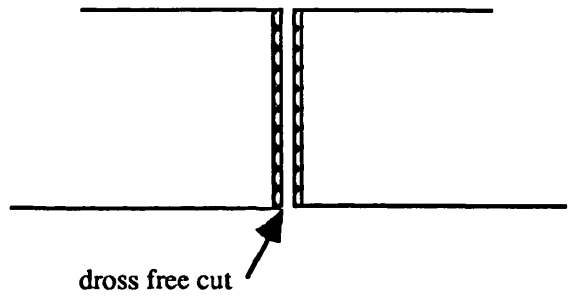

Fig 2.5(iv) **Dross free cut**

Fig 2.5(v) Photographs of laser cut 2mm thick mild steel

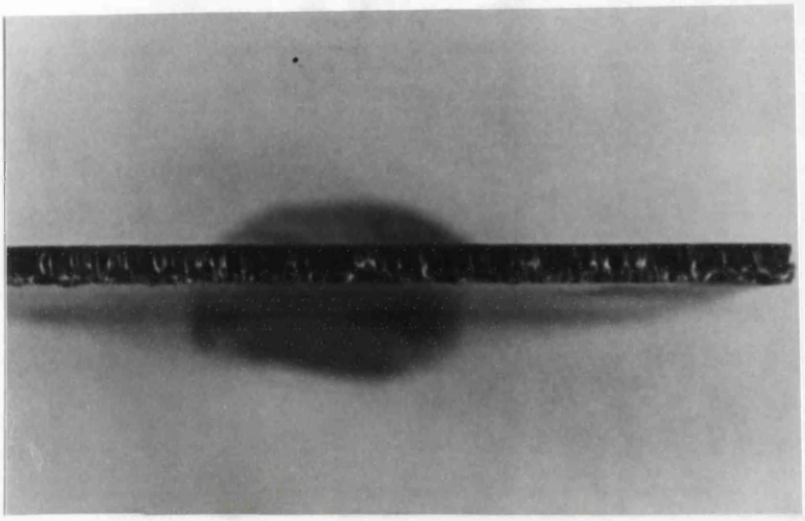

(a) GA Predicted laser parameters

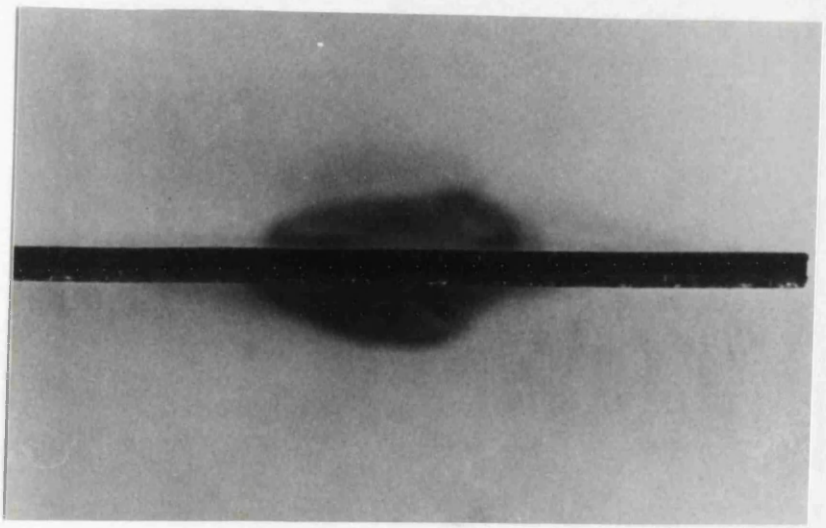

(b) Tuned laser parameters

Fig 2.5(vi) Photographs of laser cut 3mm thick mild steel

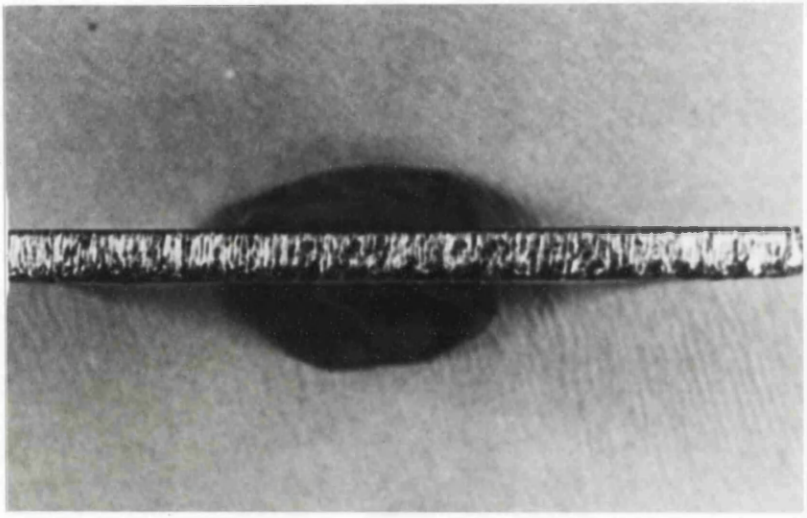

(a) GA Predicted laser parameters

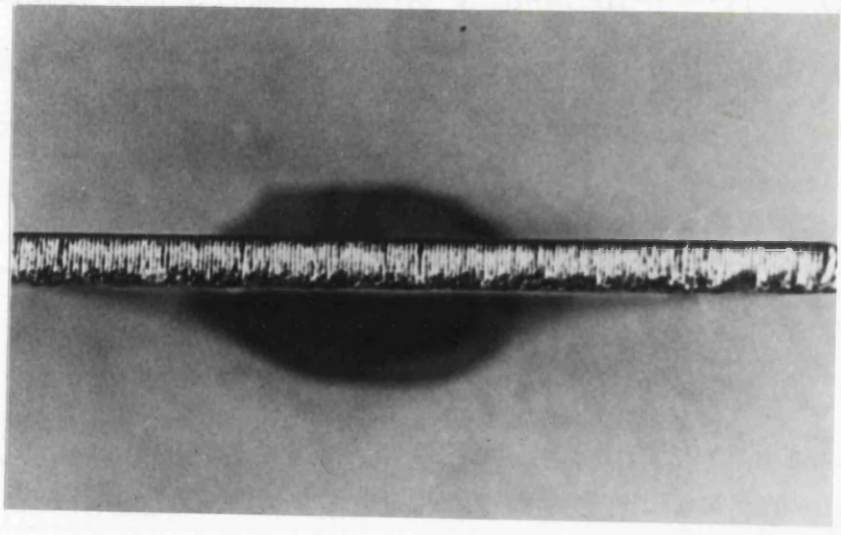

(b) Tuned laser parameters

2.9.2.1 Prediction of optimal pulse length and pulse separation for high power cut.

The populations of the pulse-length and pulse-separation generated from GA were found to converge upon a set of optimal values at the 1024th iteration. However, due to the physically available range of pulse repetition frequency, pulse separation and feedrate of the MFKP CO_2 laser, the GA optimum predictions have to be fine tuned to stop at a generation of 10. Setting the population size at 30, chromosome length at 10, cross over probability at 0.98 and mutation probability at 0.04.

At each 10th generation of the GA in predicting the optimum pulse length and pulse separation, it can be seen that the values obtained show a close accuracy to the experimental results (table 2.2, graph 2.5). It should be noted that at each optimal value of the pulse length predicted, a schema of the coding "01*****111" was noted to be present. This implies that there exists a window of pulse control parameters that will produce a good, dross free cut for any range of the thickness of the workpiece.

String	Pulselength (10^{-1}Sec)	Parents	Cross-site	New String	New Pulse-length (10^{-1} Sec)
1100101101	0.016060	27,18	6	0111101101	0.016656
0101101101	0.014208	27,18	6	0110001010	0.019516

Table 2.2 Table of the 10th GA generation for 1mm thickness

String	Pulselength (10^{-1}Sec)	Parents	Cross-site	New String	New Pulse-length (10^{-1} Sec)
0100111100	0.011264	3,19	1	0010111001	0.017256
0001001000	0.012468	3,19	1	0110111000	0.010352
0100101111	0.011072	9,12	5	1101101001	0.019548
0010101011	0.019264	9,12	5	1001101101	0.020268
0010111011	0.017452	3,18	4	0100101101	0.018272
0010101110	0.013640	3,18	4	1100111100	0.014004
1101101101	0.015284	30,23	6	0100110101	0.014172
0101110111	0.018232	30,23	6	1011101011	0.01544
0010011111	0.014616	11,10	8	0010101111	0.020040
1001101001	0.012216	11,10	8	0101110111	0.018216
0010111011	0.017096	30,17	3	0111101001	0.012368
0101101101	0.014872	30,17	3	0100101011	0.014944
0101101001	0.011336	27,15	1	0101101001	0.016572
0101100111	0.013216	27,15	1	0111101010	0.017564
0101101001	0.015784	18,13	1	1010111011	0.013520
0100101101	0.014940	18,13	1	0100101111	0.016944
0010111001	0.015992	21,4	6	0101001000	0.014092
0101111011	0.011544	21,4	6	0001001111	0.016880
0101001111	0.013672	25,11	6	0100101111	0.017220
0000111100	0.010144	25,11	6	0010010111	0.015940
1011100101	0.016260	20,26	5	0101100111	0.019744
1101101101	0.013200	20,28	5	0111011011	0.020816

Table 2.2 Table of the 10th GA generation for 1mm thickness (Continued)

String	Pulselength (10^{-1}Sec)	Parents	Cross-site	New String	New Pulse-length (10^{-1} Sec)
0100100101	0.013108	20,28	2	1100101001	0.011836
0011000110	0.016136	20,28	2	0001111011	0.013672
0111101011	0.015448	3,15	1	0101101101	0.014264
0001101101	0.016596	3,15	1	0100111100	0.018364
0101001100	0.009932	3,14	9	010001111	0.017464
0100101011	0.014624	3,14	9	0001101100	0.013108

Table 2.2 Table of the 10th GA generation for 1mm thickness (Continued)

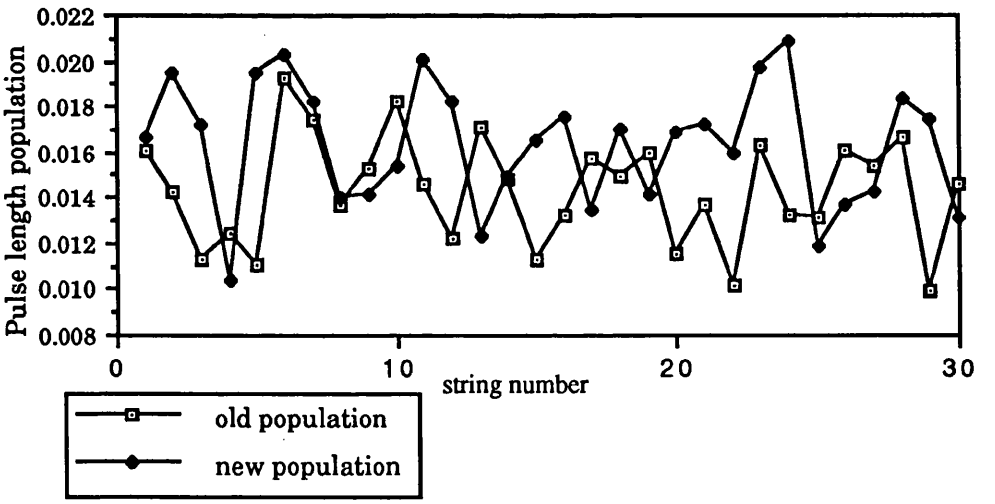

Graph 2.5 Graph of GA generated pulse length for laser cutting of a 1mm thickness workpiece at mean power = 800 W.

2.9.2.2 Prediction of optimum pulse length and pulse separation for a range of power

A 3mm thick workpiece was cut under the same laser controlled environment. The average power was then set at 100 W, 200 W, 300 W, 400 W and 600 W. The GA was run up to 20 generations with the same genetic settings. A range of pulse lengths and pulse separations were obtained and experimental justification was carried out. Tabulated results can be seen in table 2.3 and table 2.4. Graphs (graph 2.6, graph 2.7, graph 2.8) plotted for the theoretical velocity against experimental velocity and the predicted pulse parameters show that on average, the accuracy of the predictions is about 5%. Graphs 2.9.1 to 2.9.5 show the results of applying the GA algorithm to the prediction of the optimium laser pulse parameters for a particular laser mean power. Several local maximas were found during the generation of the populations of pulse length and pulse separation for a specific mean power. However, due to the physical working limitations of the laser, only the set of optimal pulse lengths and pulse separations which lies within the working range can be accepted for the material cutting process.

Mean Power(W) 3mm thick mild steel	Vtheoretical (mm/min)	Vactual (mm/min)	%velocity error	Pulselength (*10^{-5} sec)
100	270.61	255	6	10
200	540.223	500	7.6	21.55
300	811.33	605	6	36.99
400	1082.44	1145	-5.46	57
600	1623.669	1675	-3.16	129

Table 2.3 Table of optimal cut velocity for different mean powers

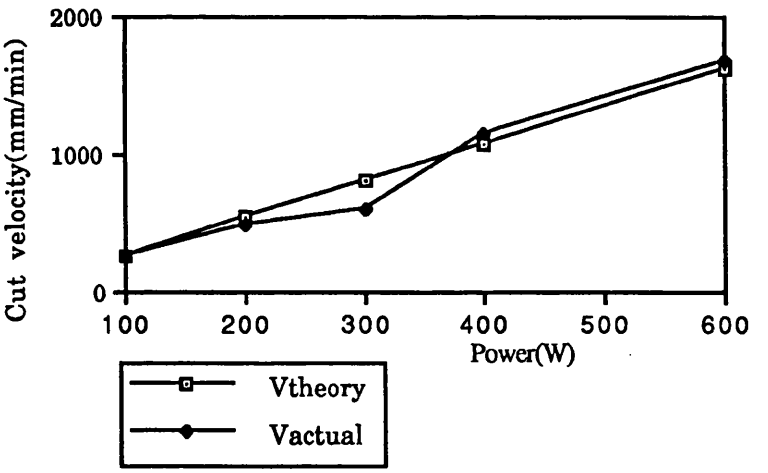

Graph 2.6 Graph of cut velocities against power variations for 3mm thickness workpiece.

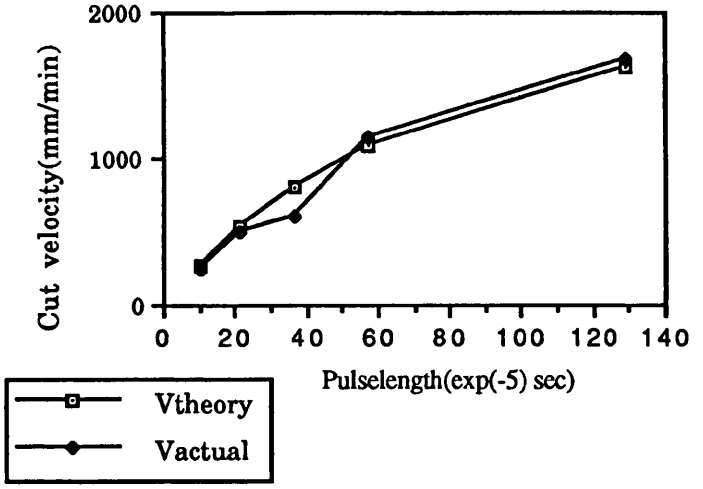

Graph 2.7 Graph of cut velocities against predicted pulse length for 3mm thickness workpiece.

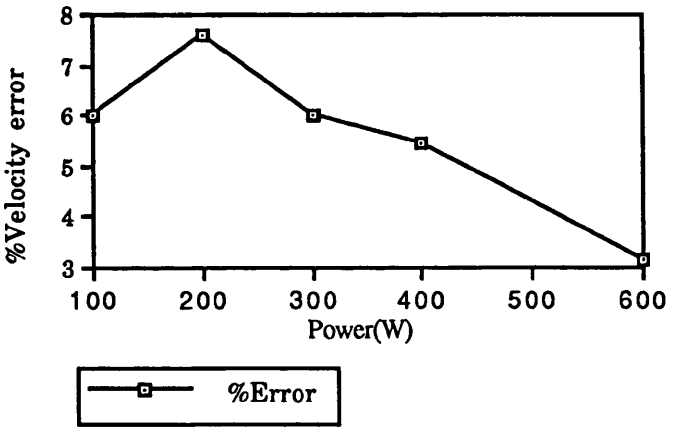

Graph 2.8 Graph of cut velocity errors against power variations for 3mm thickness workpiece.

From graph 2.6, an interesting point to note is that at a mean power input of 400 W and 600 W, the actual cut velocity becomes greater

than the predicted velocity for the same set of pulse lengths and pulse separations. The reason for this change is that from 100 W to 300 W, the pulse length predicted was too short to cut through the workpiece; hence, the actual feedrate has to be slow, but for the higher laser power, the pulse length predicted was sufficiently long to cut through the 3mm material, resulting in a higher cut velocity.

Total CrossOver	Total Mutations	Pulse_length (sec)	Pulse_Separation (sec)
14	49	0.0000435	0.0001016
29	99	0.0000857	0.0002
44	152	0.0000857	0.0002
59	201	0.0001266	0.0002954
74	245	0.0001283	0.0002994
89	290	0.0001570	0.0003664
102	352	0.0001699	0.0003964
117	403	0.0001951	0.0004553
132	445	0.000223	0.0005416
147	500	0.0002230	0.0005204
161	554	0.0002321	0.0005416
175	599	0.0002490	0.0005809
189	650	0.0002676	0.0006244
204	689	0.0002906	0.0006780
219	729	0.0002974	0.0006939
234	770	0.0003327	0.0007764
249	827	0.0003327	0.0007764
264	876	0.0003383	0.0007894
279	914	0.0003579	0.0008351
294	966	0.0003699	0.0008632

Table 2.4 Table of predicted pulse length for mean power (300 W) for 3mm thickness workpiece

Graph 2.9 Graph of pulse separation versus pulse length for 3mm thickness workpiece

2.9.1 Power = 100 W

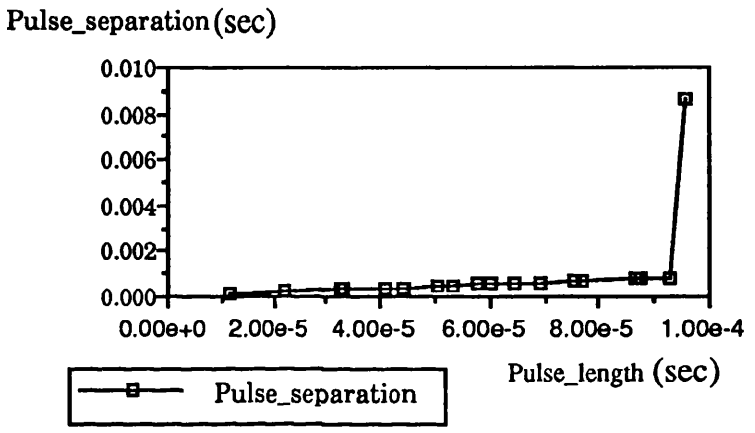

2.9.2 Power = 200 W

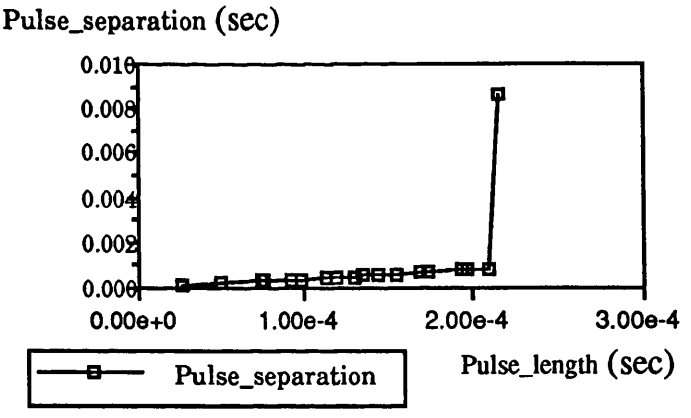

2.9.3 Power = 300 W

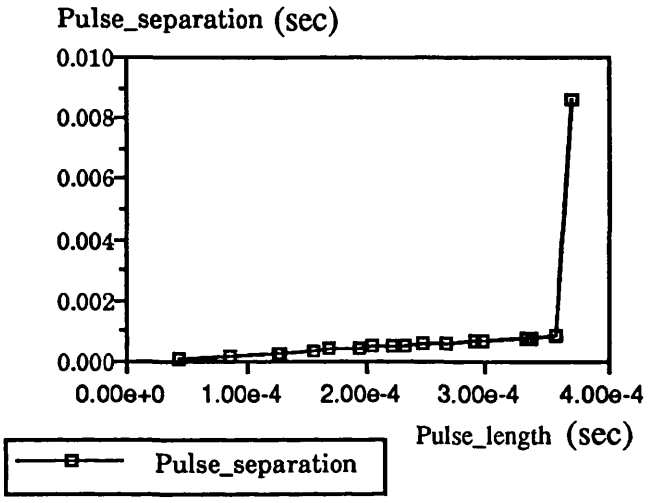

2.9.4 Power = 400 W

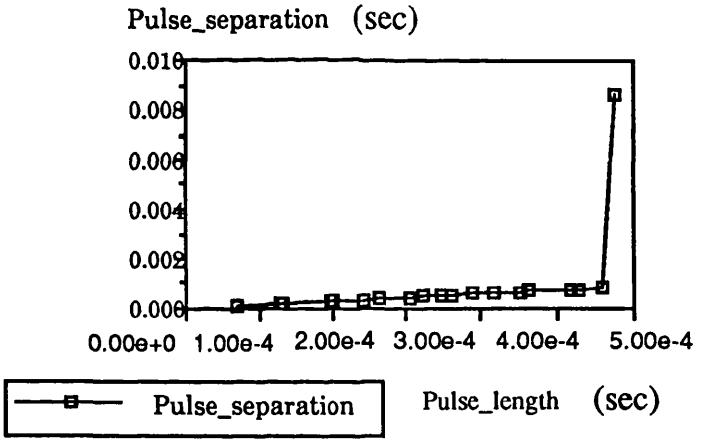

2.9.5 Power = 600 W

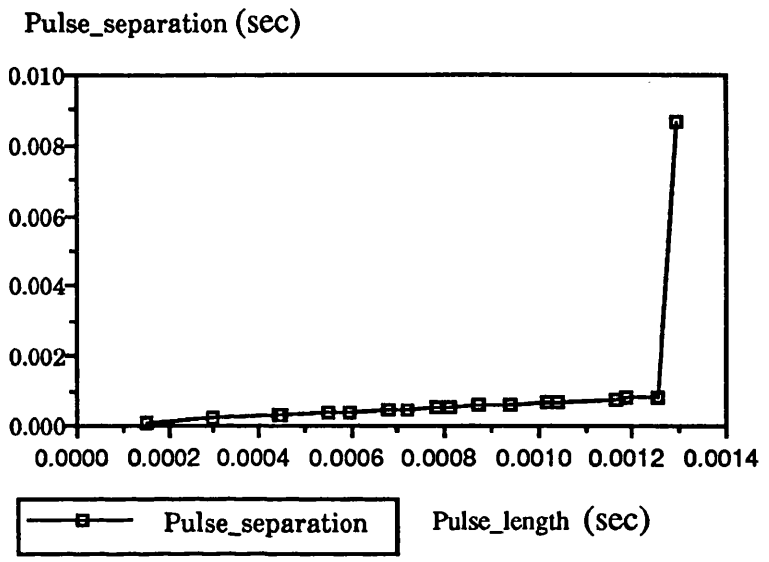

3.0. Conclusion

The analytical model derived gives a good approximation to the actual cut mechanism as seen from the results tabulated from the high and low power operations. Usage of this model as the cost function for the genetic algorithm hence is validated. The GA predicted the optimal pulse length and pulse separation, together with the theoretical feed rate for laser cutting mild steel, BS1449-CR4. Promising results were obtained in comparison with the actual cutting process. The criteria for identifying a good quality cut is a smooth finish, narrow cut kerf, small heat affected zone (HAZ) and dross free cut cross section. A model which takes no account of vapor or plasma formation was derived and used as the cost function for the GA. During experimentation, only the cross section of cut material which shows no dross, no self-burning and a small kerf width were recorded. A rapid and relatively accurate

prediction mechanism is presented by "tuning" the GA to the number of generations required to produce a reasonably optimum pulse length, pulse separation and cut velocity for a good cut. The generation was set at 10 due to limitations imposed by the particular laser design on maximum p.r.f (2kHz). The findings of a greater cut efficiency with a high pulse repetitive frequency using the GA predictions is in agreement with the findings of another LOSEG (Laser and Optics System Engineering Group) research programme into laser material/interactions. This approach to pulsed laser/material interaction prediction can be used for cutting other materials if their thermodynamic properties are known. By using this mechanism, *a priori* prediction can be utilised as a first step and then fine-tuned by introducing correction factors to the GA in respect of the actual experimental results. This results in reduced process development lead times and considerably reduces costs, making the laser far more acceptable as a machine tool.

REFERENCES

[1] Mikell P Groover, Emory W. Zimmers, Jr,"CAD/CAM Computer-aided design and manufacturing", Prentice Hall International(1984).

[2] D.L.Williams, "The laser as a machine tool", Proc Nat. Electron. Conf., Chicago, pp 574(1963).

[3] T.E. Scrose, "N.C. drilling with the laser", Metal Prod., Vol 114, pp 60(1970).

[4] Nie Bao Cheng and Li Hai Cang, "Industrial lasers and their applications in China", "The Industrial Laser Annual Handbook", pp 149 - 155(1987).

[5] Roland Ronx, "Industrial CO_2 and YAG laser systems in France", "The Industrial laser annual Handbook", pp 155 - 169(1987).

[6] W.W. Duley, "CO_2 lasers - Effects and Applications", Academic Press, NY(1976).

[7] C.M. Adam and A.G.Hardway, "Fundementals of laser beam machining and drilling", IEEE Trans. on Indust. and Gen. Applications, pp 90 - 96(1965).

[8] T. Johnson, "Flexible laser manufacturing systems", Laserobotics I, Ann Arbor, University of Michigan Press (1985).

[9] K.A. Bunting and G. Cornfield, "Towards a General Theory of cutting: A relationship between the incident power density and the cut speed", Journal of heat transfer, ASME, pp 116 - 121, Feb(1975).

[10] P.S. Myers, O.A. Uyshara and G.L. Borman, "Fundamentals of heat flow in welding", U.K. Welding Research Council Bulletin, July No 123(1967).

[11] J.H. Holland, "Adaptation in Natural and Artificial systems", Ann Arbor, University of Michigan Press(1975).

[12] D.Golberg, "Genetic Algorithms in Search, Optimisation, and Machine Learning", Addision-Wesley(1989).

[13] A.M. Prokhorov, V.I. Konov, "Laser Heating of metals", Adam Hilger, pp 1 - 29(1990).

[14] D. Schuocker and W. Abel, "Material Removal Mechanism of laser cutting", "Industrial Applications of High power laser", Proc SPIE, 455, pp 88(1984).

[15] P.A. Forrester, "High Repetition rate pulsed laser operation", IEEE Conf. on lasers and their applications, USA, pp 27(1964).

[16]. N.Forbes, "The application of pulsed gas lasers to the welding and machining of mircocircuit components", IEEE Conf. on lasers and their applications, USA, pp 11(1964).

[17] M.Moriyasu, S.Hiramoro, S.Hoshinouchi and M.Ohmine, "Adaptive control for high speed and high quality laser cutting", Laser welding and material processing, ICALEO'85, USA, pp 129(1985).

[18] B.A. Bakwell, "Performance of pulsed laser systems in relation to machining mechanisms", PhD thesis,Dept of Mechanical Engineering, University of Birmingham(1973).

[19] C.R.Chatwin, D.W. McDonald and B.F. Scott,"Design of a high PRF Carbon Dioxide laser for processing high damage threshold materials", Selected Papers on laser design, (Hugo Weichel ed.), SPIE Milestone Series, Vol MS29(1991).

[20] Ball, W.C., Bonnas, C.M.,"Welding with high power CO_2 lasers", Soc. Auto. Eng. Inc., Report No. 740863(1974).

[21] Richard Forsyth,"Machine Learning - Principles and techniques", Chapman and Hall Computing, pp 65 - 154, NY(1989).

[22] W.W. Duley and J.N. Gonsalves,Opt. laser technol., 6, pp 78 (1974).

[23] D.Rosenthal, "The theory of moving sources of heat and its applications to metal treatments", Trans of the ASME, pp 849-866, Nov(1946).

[24] Joyti Mazumder, "Mathematical modelling of laser surface treatments", LTM 86, USA, pp 186 - 197(1986).

[25] D. Chan, J.Mazumder, and M.M. Chen, "Applications of lasers in material processing", Journal of Heat Transfer, ASME, pp 150 (1983).

3 CHAOS IN LASER-MATERIAL INTERACTION

3.1 Introduction

Since the early contribution to chaos by the Russian mathematician Sophia Kovalevskaya in the 19th century, many other mathematicians such as S. Smale [1], Andreli Kolmogorov [2], E.N. Lorenz [3] and Henri Poincare' [4] have developed many methodologies and measures of chaos that have essentially created a new science that occurs everywhere in nature. In a review published in 1971, D.Ruella [5] first introduced the concepts of "strange attractors" and "routes to chaos" for dissipative dynamic systems. Then came Feigenbaum's [6] discovery of the scaling properties and universal constants in one-dimensional mappings and renormalization group theory [7]. Another stream of events

leading to the domain of chaos, was the study of nonintegrable Hamiltonian systems in classical mechanics [8]. By the end of the last century, the success of relativity and quantum theory as well as the foundation of statistical mechanics resulted in the development of the Kolomogorov-Arnold-Moser (KAM) theorem on nearly integrable Hamiltonian systems [9]. To describe a system as being chaotic means that the system measurands behave in an aperiodic manner or that the observed behaviour varies unpredictably. The observations are said to be chaotic when there is no discernable regularity or order. One very important point to note is that chaotic dynamics do not imply random stochasticity, rather it refers to a deterministic development with chaotic outcome. The evolution of the chaotic behaviour can be described by known physical laws and relationships. Any system that is dependent on initial conditions is potentially chaotic. Recent chaos studies relating to the onset of turbulent behavior in dissipative systems give conclusive findings that no matter what the size of the system phase space, motions in sub-spaces of lower dimension called attractors can be used to describe the characteristics of the system from its transient state of quasi-periodicity to turbulence. All physical systems exhibit dissipation phenomena; hence, when modelling these systems, it is possible to obtain the model of the attractors as well as the pattern of the system trajectory, that is its phase portrait.

3.2 Nomenclature

A = Area of the workpiece normal to the heat flux (m^2)

C = Specific heat of the workpiece (kJ/kgK)

C_I = Constant of integration

D = Distance travelled in the x-axis direction (m)

ε = System perturbation

f_o = f_o is a mapping function such that f_o: $IR^2 \rightarrow IR^2$

f_1 = f_1 is a T_t-periodic function such that f_1: $IR^2 \times T_t \rightarrow IR^2$

$f\mu(x)$ = One dimensional logistic mapping function

η = System efficiency (%)

k = Thermal diffusivity (m^2/sec)

K = Thermal conductivity (W/mK)

M = Isocline gradient

$M(t_0)$ = Melnikov function

P = Power (W)

q = Heat source per unit volume (kJ/m^3)

Q = Heat flux (kJ)

ρ = Specific density of the workpiece (kg/m^3)

R = Reflectivity of the material

t = Time (sec)

T = Temperature (K)

T_t = Period of oscillation (sec)

V = Velocity of cut (m/sec)

$\dot{x}$ (t) = Next x mapping point

ω = Frequency of perturbation (Hz)

3.3 Laser-material processing

A well controlled laser cut has high precision and reproducibility - as determined by the kerf width and heat affected zone measurement. In fact the precision of a laser cut has been quoted [10] as +/- 0.05 mm in 20 mm gauge stainless steel. Hence lasers are used as machine tools in industry. However, laser-material processing is a highly non-linear interaction. The behaviour of

material processing with a laser depends upon many variables, most of which are difficult to control. The effects of parameters such as : mode structure, surface reflectivity, heat transfer losses ... are difficult to quantify precisely. To date, many theories have been established to predict the approximate value of significant parameters such as the temperature distribution on the material surface, the velocity of cut together with the basic operating parameters for cutting or welding. These approaches can be broadly classified as :

(i) Analytical solution [11][12][13]

(ii) Numerical solution [14][15][16]

(iii) Semiquantitatve solution [17]

In the research conducted by the author, a new prediction scheme utilising a genetic algorithm [18] is adopted for the determination of the optimal laser cutting parameters. A hybrid decision support system for the automatic control and tasking of the laser system was also developed [19]. During the actual cutting process, it was observed that at a certain threshold of cutting rate, slight deviation of the predicted cut control parameters resulted in chaotic behaviour. The purpose of this paper is hence to quantify this observation as well as to develop an aid for approximating the laser cutting parameters in relation to this behaviour.

3.4 The chaos phenomenon

During the laser cutting process of stainless steel SS304, pre-set process control parameters were used. When a stainless steel plate of thickness 4mm was cut, it was observed that a good or reasonable cut was not possible, every slight modification in the cutting rate resulted in a transient chaotic behaviour (i.e. the cut was very bad). However, when the laser gas nozzle height was offset from 0.6mm to 1.5mm above the workpiece surface, a good cut was obtained with a feedrate of 800mm/min. This observation can be related to the concept of Hopf bifurcation [20]; the cut criteria for stainless steel for the range of thicknesses from 1mm to 3mm is furthermost from the fixed attractor for a laser nozzle offset of 0.6mm. Any further deviation, i.e. thicker material results in the cut criteria leaving the limit cycle of the attractor, this causes the laser-material interaction process to become chaotic. By changing the nozzle height to 1.5mm, the cut criteria is now within a new limit cycle where behavior is governed by a new attractor. This resulted in the attainment of a stable cut, see the experimental results in table 3.1 and Figure 3.1.

Thickness (mm)	Nozzle Height(mm)	CW Power (kW)	Assist gas pressure (bar)	Cut velocity (mm/min)
1.25	0.6	1.2	2	4000
2.0	0.6	1.2	2	2200
3.0	0.6	1.2	2	1250
3.0	1.5	1.2	2	1150
4.0	1.5	1.2	2	810
5.0	1.5	1.2	2	640

Table 3.1 Tabulated results of experimental cutting rates for stainless steel at CW power = 1.2kW

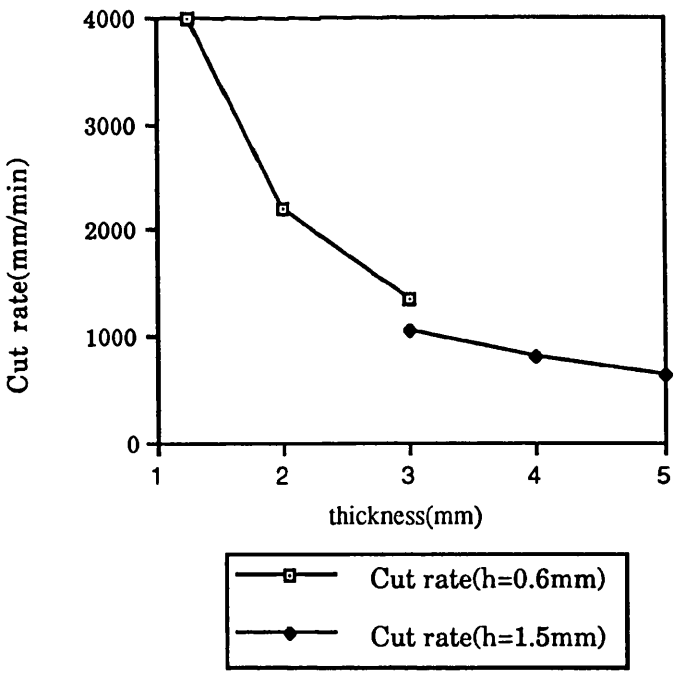

Fig 3.1 Cutting phenomena of stainless steel exhibiting chaotic effect (Experimental)

NOTE: h is the nozzle height above the workpiece surface.

3.5 Moving flux approach to laser-material modelling

Considering the interaction as a moving heat source within a metal target material:

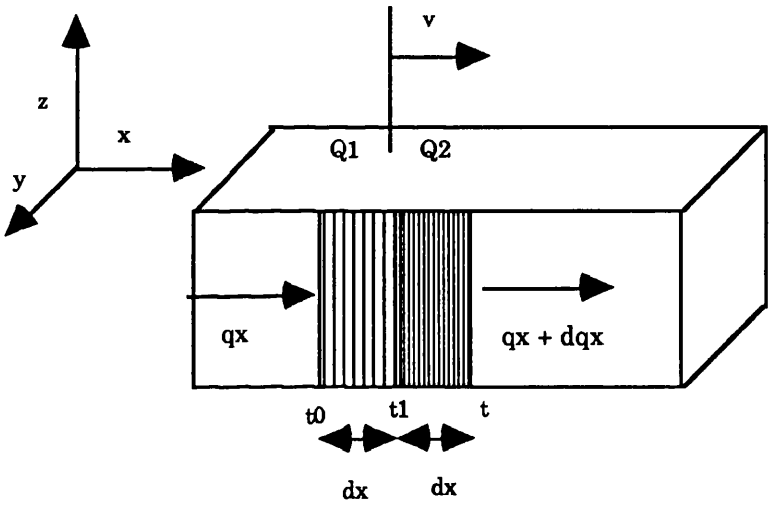

Fig 3.2 Diagram of moving flux in material

Assumptions:

a. The physical characteristics of the metal, i.e. thermal conductivity (K) and thermal diffusivity (k) are independent of the temperature.

b. The velocity of propagation V and the rate of heat input are constant.

Assuming thermal equilibrium;

$$\sum Q = 0,$$

Where Q = heat flux.

$$\left.\frac{dq_x}{dx}\right|_t + \frac{dq_y}{dy} + \frac{dq_z}{dz} + \rho C \left.\frac{dT}{dt}\right|_t - \rho C \frac{dT}{dt} = 0 \qquad (3.1)$$

let D = x(t) = Vt;

hence t = D/V;

Substituting D into equation (3.1);

$$-\{\frac{d}{dD}[K\frac{dT}{dD}] + \frac{d}{dy}[K\frac{dT}{dy}] + \frac{d}{dz}[K\frac{dT}{dz}]\} \qquad (3.2)$$
$$- \rho CV\frac{dT}{dD} + \rho C\frac{dT}{dt} = 0$$

$$-K\{\nabla^2 T\} - \rho CV\frac{dT}{dD} + \rho C\frac{dT}{dt} = 0 \qquad (3.3)$$

Since thermal diffusivity,

$$k = \frac{K}{\rho C} \qquad (3.4)$$

$$\nabla^2 T + \frac{V}{k}\frac{dT}{dD} - \frac{1}{k}\frac{dT}{dt} = 0 \qquad (3.5)$$

Considering a one dimensional model , i.e. in the D direction, and a quasi-stationary condition;

$$\frac{dT}{dt} = 0;$$

equation (3.5) becomes;

$$\frac{d^2T}{dD^2} + \frac{V}{k}\frac{dT}{dD} = 0 \qquad (3.6)$$

3.6 Melnikov resolution to chaos

Consider the perturbed Hamiltonian system in IR^2 Euclidean space described by;

$$\dot{x}(t) = f_o(x(t)) + \varepsilon f_1(x(t), t) \qquad (3.7)$$

The associated unperturbed system equation of equation (3.7) is;

$$\dot{x}(t) = f(x(t)) \qquad (3.8)$$

For ε=0, f(x(t)) is a homoclinic saddle point in that equation (3.7) possesses a homoclinic orbit $O^0(t)$ connecting $x(t_0)$ to itself.

Next, defining the Melnikov function [21];

$$M(t_o) = \int_{-\infty}^{\infty} f_o\left\{O^o(t - t_o)\right\} \Lambda\ f_1\left\{O^o(t - t_o)\right\} dt \tag{3.9}$$

Referring to equation (3.6),

$$T'' + \frac{V}{k} T' = 0 \tag{3.10}$$

where

$$T' = \frac{dT}{dD} \ , \ T'' = \frac{d^2T}{dD^2}$$

Let

$$Y = T' \tag{3.11}$$

$$\dot{Y} = T'' \tag{3.12}$$

Substitute equation (3.11) and (3.12) into equation (3.10),

$$\dot{Y} + \frac{V}{k} Y = 0 \tag{3.13}$$

Equation (3.13) is a mapping function of the general form.

$$\dot{X} = f_{\mu}(X) \tag{3.14}$$

Where μ is a mapping parameter and $X \in IR^n$. Equation (3.14) is referred to as a trajectory; significantly, the trajectory depends on the initial conditions.

To find the fixed attractor at this point for the evolution equation (3.13),i.e., $f_{\mu}(X) = 0$. The fixed attractors were found to be [0, $-\frac{V}{k}$].

If there is a small velocity perturbation from V of the form;

$$V_{\varepsilon} = \varepsilon V \cos \omega t \tag{3.15}$$

For a real physical laser machining process, it is possible to perturb k as a result of the temperature fluctuation, hence equation (3.10) is now;

$$T'' + \varepsilon\left[\frac{V}{k}\right]T' + \varepsilon V \cos \omega t = 0 \tag{3.16}$$

The unperturbed system (for ε=0) is

$Y = T'$;

$\dot{Y} = T'' = 0$;

$$M(t_o) = \int_{-\infty}^{\infty} \dot{Y}(t-t_o)\left\{-\left(\frac{V}{k}\right)\dot{Y}(t-t_o) - V\cos\omega t\right\}dt \tag{3.17}$$

But,

$$\lim_{t\to 0}\int_{-\infty}^{\infty} -\left(\frac{V}{k}\right)\left\{\dot{Y}(t-t_o)\right\}^2 dt \equiv 0$$

$$M(t_o) = -\int_{-\infty}^{\infty} \dot{Y}(t-t_o)\{V\cos\omega t\}dt \tag{3.18}$$

where $\dot{Y}(t-t_o)$ is either a homoclinic or heteroclinic orbit. The solution to equation (3.18) is of the form;

$$M(t_o) = A\cos\omega t + B\sin\omega t \tag{3.19}$$

where

$$A = -\int_{-\infty}^{\infty} \dot{Y}(t-t_o)\cos\omega t dt \tag{3.20}$$

$$B = -\int_{-\infty}^{\infty} \dot{Y}(t-t_o)\sin\omega t dt \tag{3.21}$$

Condition to prove that chaos exists; for sufficiently small ε.

lemma 1:

For $\exists A \to A \in 0$ *and* $\exists B \to B \notin 0$;

$M(t_o)$ *has a simple zero at* $\omega t_o = n\Pi|_{n=1,2,3,..}$

lemma 2:

For $\exists A \to A \notin 0$ *and* $\exists B \to B \in 0$;

$M(t_o)$ *has a simple zero at* $\omega t_o = \frac{1}{2}(2n+1)\Pi|_{n=1,2,3,..}$

In accordance to Chirikov [22], Holmes [23], from proving $M(t_0)$ has a simple zero, it can be concluded that the stable and unstable manifolds associated with the Poincare' map P_ε^t: IR^2->IR^2 intersect transversally. Hence equation (3.16) possesses a unique hyperbolic periodic orbit set with a Smale-Birkhoff horseshoe type of chaos.

The phase-portrait of the laser material interaction is shown in Figure 3.3;

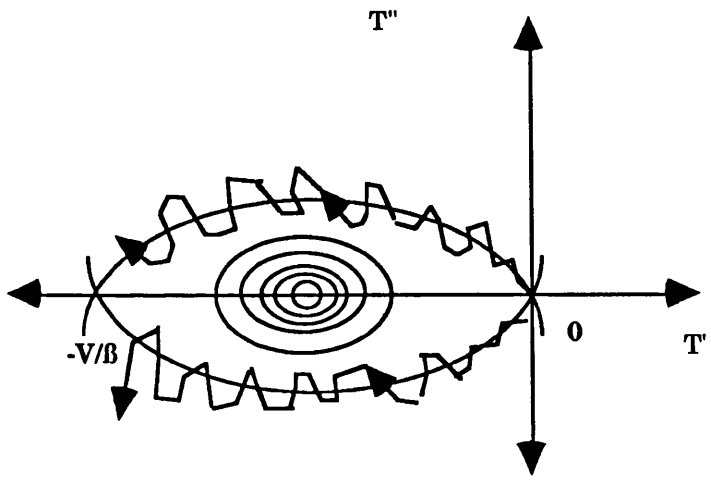

Fig 3.3 Phase portrait of the laser-material interaction

Hence, chaos would occur in the form of horseshoe for ε, sufficiently small.

3.7 Limit cycle as a tool for approximation

A stable fixed point acts as an attractor, hence it attracts all nearby initial points towards itself. Local repulsion and global attraction of the K-flow results in the formation of a closed curve. This closed curve is called a limit cycle and corresponds to a periodic motion of the system. By working the system within its limit cycle, an approach for retrieving information about the system

dynamics, in this case, the velocity plots for laser-material processing is presented.

Referring to equation (3.6);

$$\frac{d^2T}{dD^2} + \left[\frac{V}{k}\right]\frac{dT}{dD} = 0 \qquad (3.6)$$

Since,

$$q = -K\frac{dT}{dD} \qquad (3.22)$$

Where q is the rate of heat transfer per unit area;

Substitute equation (3.22) into equation (3.6);

$$-\frac{dq}{KdD} + \left[\frac{V}{k}\right]\left\{-\frac{q}{K}\right\} = 0 \qquad (3.23)$$

but;

$$\frac{dq}{dD} = \frac{dq}{dT} \cdot \frac{dT}{dD} = \left[-\frac{q}{K}\right]\frac{dq}{dT} \tag{3.24}$$

Equation (3.23) is rewritten in the form;

$$\left(\left[\frac{q}{K^2}\right]\frac{dq}{dT}\right) - \left[\frac{Vq}{kK}\right] = 0 \tag{3.25}$$

Simplifying;

$$\left(\left[\frac{1}{K}\right]\frac{dq}{dT}\right) - \frac{V}{k} = 0 \tag{3.26}$$

Since q = $\frac{\eta(1-R)P}{A}$;

Rewriting equation (3.26),

$$\frac{\eta(1-R)}{KA}\frac{dP}{dT} - \frac{V}{k} = 0 \tag{3.27}$$

Integrating equation (3.27);

$$P_{1,2} = \frac{KAV}{\eta(1-R)k}T_{1,2} + C_I \tag{3.28}$$

To establish the working limits of the trajectories of the laser-material interaction, the process phase portrait is constructed. Setting M = $\frac{dP}{dT}$ then shows that the isoclines of equation (3.28) are the lines M=$\frac{KAV}{\eta(1-R)k}$. Representative isoclines are shown in Figure

3.4. Short inclined lines have been added to these isoclines to indicate the direction of the tangents to the integral curves that intersect the isoclines; their angles of inclination have the magnitude arctan(M). The pattern of these tangents associated with the isoclines shows the direction taken by the trajectory equation (3.28).

3.7.1 Phase portrait construction

1. Derive the trajectory equation describing the deterministic behaviour of the dynamic system.

2. Set a variable denoting the isocline of the trajectory equation.

3. Plot a table of isoclines and its direction of slope (see table 3.2 - 3.6).

4. Mark on the isoclines, short crosslines to indicate the value of the slope. These crosslines are horizontal when the isocline variable is equal to 0 and vertical when the variable is equal to infinity.

5. Draw the phase trajectory so that it is always tangent to the isoclines.

6. Integrate the trajectory equation and mark off the relationship obtained by taking account of the constant

of integration for specific trajectory curves.

In this particular work a phase portrait of specific material thicknesses is investigated to obtain a prediction of cutting rates.

The material under investigation is stainless steel (C34 SS304 2B), properties are:

(a) K= 0.26 (w/cmK)

(b) k = 0.054 (cm^2/s)

(c) T = 1490K

(d) R = 0.81

(d) A = Area of material (m^2)

V(m/s)	M	arctan M
0.01	0.542	28.457
0.02	1.084	47.308
0.03	1.626	58.408
0.04	2.168	65.238
0.05	2.711	69.752

Table 3.2 Tabulated values of cutting rates and isoclines for stainless steel of thickness = 1.25 mm

V(m/s)	M	arctan M
0.01	0.867	40.943
0.02	1.735	60.043
0.03	2.602	68.980
0.04	3.470	73.919
0.05	4.337	77.017

Table 3.3 Tabulated values of cutting rates and isoclines for stainless steel of thickness = 2 mm

V(m/s)	M	arctan M
0.01	1.301	52.459
0.02	2.602	68.981
0.03	3.904	75.632
0.04	5.205	79.125
0.05	6.506	81.262

Table 3.4 Tabulated values of cutting rates and isoclines for stainless steel of thickness = 3.0 mm

V(m/s)	M	arctan M
0.01	1.735	60.043
0.02	3.470	73.924
0.03	5.205	79.125
0.04	6.940	81.802
0.05	8.675	83.421

Table 3.5 Tabulated values of cutting rates and isoclines for stainless steel of thickness = 4.0 mm

V(m/s)	M	arctan M
0.01	2.168	65.246
0.02	4.337	77.018
0.03	6.506	81.262
0.04	8.675	83.424
0.05	10.844	84.731

Table 3.6 Tabulated values of cutting rates and isoclines for stainless steel of thickness = 5.0 mm

In accordance with step 5, the phase portrait is plotted,

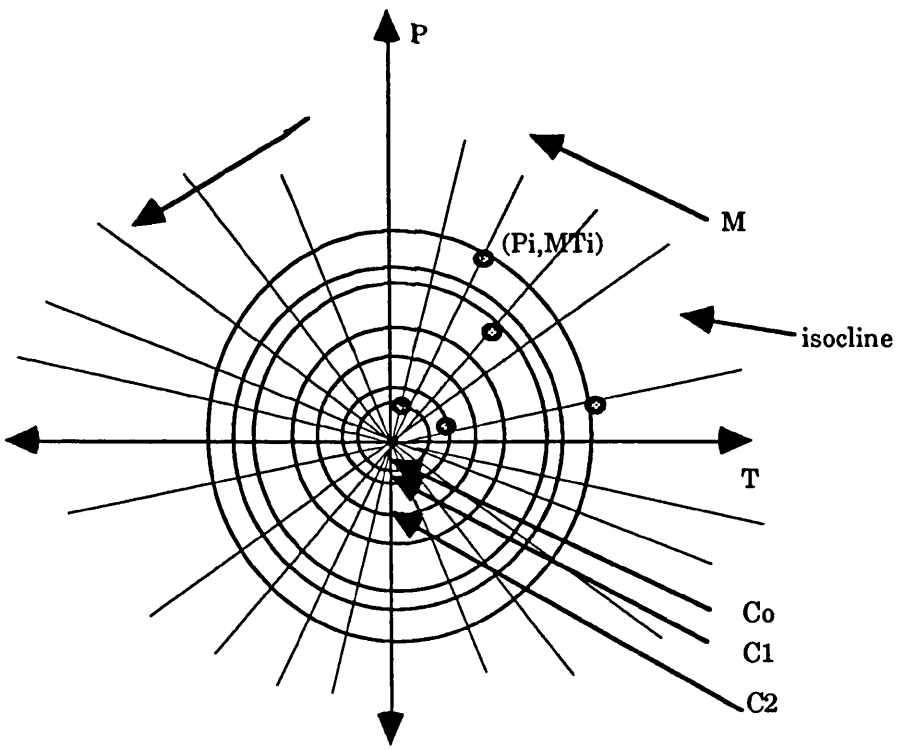

Fig 3.4 Phase portrait of the laser-material process (stainless steel thickness = 1.25mm)

From Figure 3.4, the initial conditions for cutting velocity and power for laser material processing can be established.

Taking the constant of integration as C_I, the cutting rate can be obtained by using the trajectory equation (3.28).

$$P_{1,2} = \frac{KAV}{\eta(1-R)\beta} T_{1,2} + C_I \qquad (3.28)$$

C_I is the intercept value of the limit cycle with the power axis of phase portrait plotted;

hence equation (3.28) becomes,

$$V = \frac{\eta(1-R)\delta}{KAT_{1,2}} \{ P_{1,2} - C_I \} \qquad (3.29)$$

Phase portraits of stainless steel of thicknesses of 1.25mm to 5mm were plotted for a CW laser power of 1.2 kW. The following values of limit cycle intercepts C, and predicted cutting rates were obtained (see table 3.7 and 3.8).

Thickness (mm)	Intercept C(W)	Experimental Velocity (mm/min)	Theoretical Velocity (mm/min)	Error(%)
1.25	-1320	4000	4218	-5.507
2.0	-1297	2200	2612.4	-18.9
3.0	-1108	1250	1598.4	-28.9
4.0	-1060	910	1271.2	-44

Table 3.7 Table of actual and predicted velocities for stainless steel thickness from 1.25mm to 4.0mm

It can be observed from table 3.7 that as the range of thicknesses increases, the prediction error increases. At the stainless thicknesses of 4mm, the error in velocity prediction is about 44%. By changing the nozzle height from 0.6mm to 1.5mm, the energy cycle of the cutting process is shifted. Hence, by considering a new trajectory for the cutting rates for stainless steel of thicknesses 3mm, 4mm and 5mm. A new set of cutting rates is obtained, see table 3.8.

Thickness (mm)	Intercept C(W)	Experimental Velocity (mm/min)	Theoretical Velocity (mm/min)	Error(%)
3.0	-500	1150	1191.79	-3.63
4.0	-500	810	852.6	-5.26
5.0	-500	640	687	-7.33

Table 3.8 Table of actual and predicted velocities for stainless steel thickness of 3.0mm, 4.0mm and 5.0mm

This approach was used to approximate power and cut velocities for a set of stainless steel plates of thicknesses ranging from 1mm to 5mm using a Ferranti MFKP CO_2 laser giving 1.2 kW of CW power. The results from table 3.7 and table 3.8 are plotted in graphs 3.1 and 3.2.

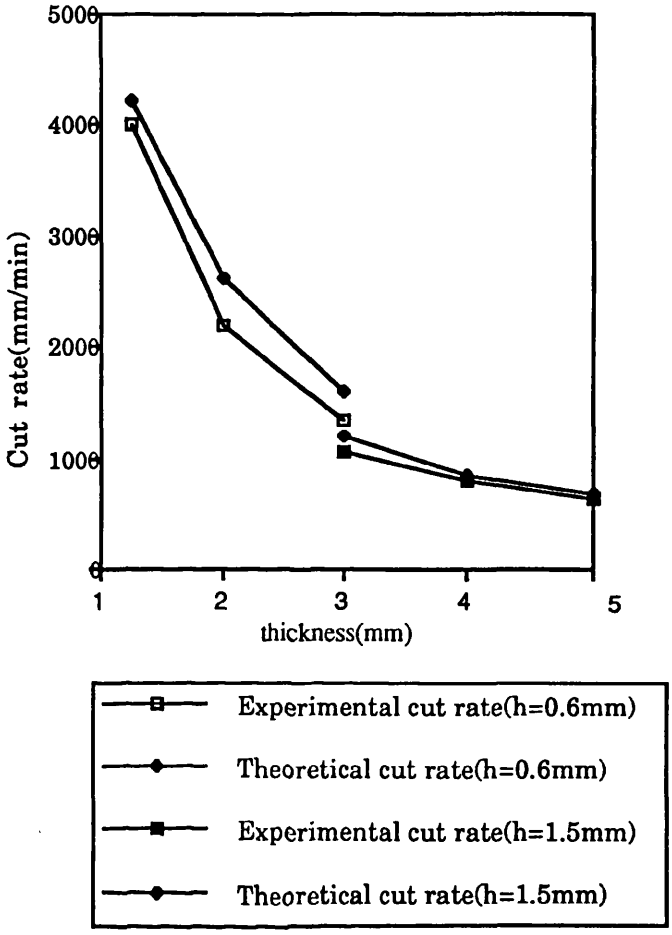

Graph 3.1 Graph of predicted velocities against actual cut velocities for various thicknesses of stainless steel at CW power = 1.2 kW

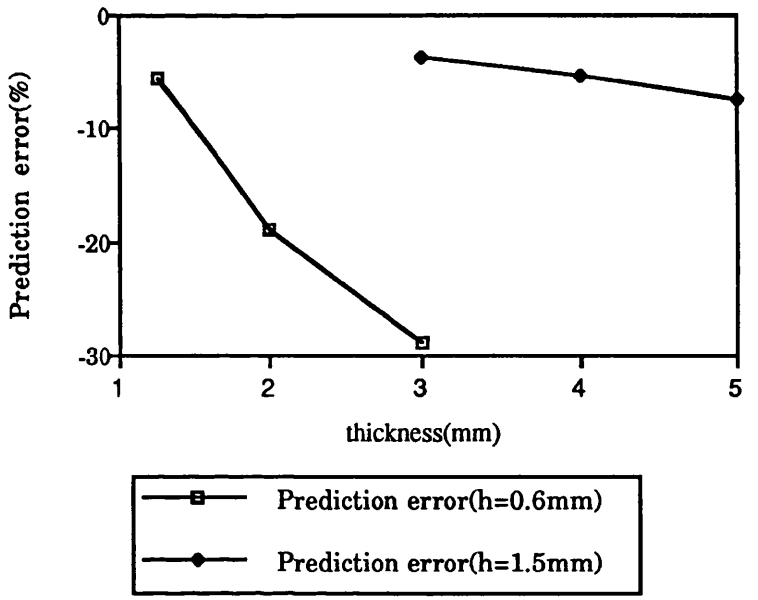

Graph 3.2 Graph of predicted velocity error against amended predicted velocity error for various thicknesses of stainless steel at CW power = 1.2 kW

3.8 Conclusion

Laser materials processing is a highly non-linear process. Chaotic dynamics can be observed when the cutting control parameters are set to particular values. An investigation was thus conducted into the existence of chaos as well as the possibility for process parameter prediction using the information stored in the phase portrait of the dynamic system. A one-dimensional heat transfer model was derived and using the property of the Melnikov integral, the condition for the onset of chaos was verified for small perturbations in the cutting rates and thermal properties of the material. By using the isoclines approach, a method of approximating the initial cutting rates from the system phase

portrait was established. The predicted cutting rates were tested against actual cutting rates. The error of prediction increases in relation to the increment of thicknesses of stainless steel in an approximately exponential manner which can be characterized by the Lyapunov exponent of chaotic dynamics. The divergence of the error of prediction can be explained by Hopf bifurcation where the predicted laser processing parameters starts to move away from a deterministic energy cycle towards a higher energy cycle, see graph 3.2. The predicted cutting rates for stainless steel (C34 SS304 2B) agree extremely well with the experimental results. This in conclusion hence proves the suitability of using the proposed method as a prediction mechanism for laser cutting.

REFERENCES

[1] S. Smale, "Differentiable dynamics systems" , Bull. A.M.S., 73, pp 747 - 817(1967).

[2] A.N. Kolmogorov, Dokl. Akad. Nauk., SSSR 98, 5, pp 27(1954).

[3] E.N. Lornez, "Deterministic nonperiodic flow", J. Atmos. Sci., 20, pp 130(1963).

[4] H. Poincare', "Methodes Nouvelles de la Mecanique Celeste" , English Trans. , Dover Publications, New York(1957).

[5] D.Ruelle and F.Takens, "On the nature of turbulence" , Commun. Math. Phys, 20, 167,23, pp 343(1971).

[6] M.J. Feigenbaum, "The Universal metric properties of non-linear transformations" , J. Stat. Phys, 21,pp 669(1979).

[7] M.J. Feigenbaum, "Quantitative Universality for a class of non-linear transformations" , J.Stat Phys, 19, pp 25(1978).

[8] A.N.Kolmogorov, Russian original Akad. Nauk, SSSR Doklady 98, 527(1954), "Preservation of conditionally periodic movements with small change in Hamiltonian function" , translation by H.Dahlby, Lect. Notes in Physc, 93, pp 51(1979).

[9] G.H. Walker and J. Ford, "Amplitude instability and ergodic behavior for conservation nonlinear oscillator systems" , Phys. Rev., 188, pp 416(1969).

[10] Atkey M., "Machinery and Production Eng." , 133, 3441, pp 23(1978).

[11] J.N. Gonsalves and W.W. Duley, "Cutting thin metal sheets with the CW CO2 laser" , J. Appl. Phys, 43,11, pp 46 - 84(1972).

[12] D.Schuocker, "Dynamic Phenomena in laser cutting and cut quality" , Appl. Phys B40, 9, pp 74(1986).

[13] P.S. Myers, .A. Uyshara. and G.L. Borman, "Fundamentals of heat flow in welding" , UK Welding Research Council Bulletin, July, 123(1967).

[14] J.Mazumder and W.M. Steen, "Heat transfer model for CW laser material processing" , J. Appl. Phys 51(2), 9, pp 41(1980).

[15] M.Lax, "Temperature rise induced by a laser beam" , J. Appl Phys., 48, 9, 39, pp 19(1977).

[16] J.Mazumder, "Mathematical modelling of laser surface treatments ", LTM 86, USA, 1, pp 86(1986).

[17] Dutta M., PhD Thesis, Birmingham University(1974).

[18] Lim See Yew and C.R. Chatwin, "Evolutionary process prediction and optimization for laser-material interaction" , to be publish.

[19] Lim See Yew and C.R. Chatwin, "The design of a Second Order PID Knowledge Based Management System for process control" , ICRAV'92, Singapore, CO.7.4.1-CO.7.4.5(1992).

[20] E. Hopf, "A mathematical example displaying features of turbulence", Commun. Pure Appl. Math., 1, pp 303(1948).

[21] V.K. Melnikov, "On the stability of the center for time periodic perturbations" , Trans. Moscow Math. Soc., 12, pp 1(1963).

[22] B.V. Chirikov, "Instability of dynamics systems with several degree of freedom" , Dokl. Akad. Nauk. SSR., 156, pp 9(1979).

[23] J. Guckenheimer and P.J. Holmes, "Non-linear Oscillations, dynamic systems and bifurcations of vector fields" , Appl. Math. Sciences, pp 42(1983).

4 ARTIFICIAL INTELLIGENCE AS AN ALTERNATIVE APPROACH TO SYSTEM UNDERSTANDING AND CONTROL

4.1 Introduction

In theory, physical systems are supposed to be predictable, but in practice, it always seems that there are inbuilt limits in predicting the future at all levels of complexity. It was the development of chaos theory [1] that enabled researchers in many disciplines to realise that in addition to a universe that is deterministic; obeying the fundamental physical laws, there exits a predisposition for disorder, complexity and unpredictability. Chaotic behaviour exists in all systems, i.e. engineering, astronomy, population dynamics .... To cope with these characteristics of system change, many abstract bounded modelling and adaptive modelling techniques have evolved [2]. Coupled with readily accessible computer power, these

techniques allow a revelation of the subtle behaviour of chaotic systems as they can follow their trajectories over many steps. This leads to the establishment of computer-aided systems [3]. The three phases of computer usage are: acquisition, processing and presentation of knowledge. The three levels of software engineering are: mechanisation, automation and cybernation. The third level; i.e. cybernation, involves self-learning capabilities for the system in addition to self-regulating features [4]. It is in this specific domain that the third level of software engineering evolves into the area of intelligent control (IC). Computer-aided systems can be decomposed into four main groups, they are:

(i) model generation and/or referencing
(ii) model acceptability
(iii) model processing, and
(iv) behaviour processing (Figure 4.1)

These models have been integrated with existing artificial intelligence technology into a real-world domain with many sucesses [5][6][7][8]. In the development of these intelligent control systems, many new knowledge representation formalisms have evolved. These formalisms are relatively similar to the traditional mathematical modelling formalisms used in computerised simulation [9][10][11]. The developing sciences of cybernetics, knowledge engineering, system behaviour and theories of computation were combined to form the discipline of Artificial Intelligence (AI). The official inception was at a summer research project held at Dartmouth College in the year 1956. Fundamentally, the main goal of artificial intelligence is in the replication of the

functionality of the human mind. To this end, many replicate-the-brain approaches have evolved by simulating their evolution in computer models - neural networks [12], parallel computing [13], fuzzy approximations [14], and knowledge based management systems [15]. Over the years, the range of AI applications have included, *inter alia* : machine vision - an application which aims at recognising patterns in much the same way as the human visual system does; robotics - which focusses on producing mechanical devices capable of controlled motion; speech processing - which aims at recognising and synthesising spoken human speech; theorem proving - which attempts to automatically prove theorems in mathematics and logic; AI self-tuning control - which adapts the system dynamics to the stability dead zone. The research carried out for this thesis is in the area of AI self-tuning control. The domain is in the tasking and control of a medium power 1.2 kW CO_2 gas laser. Because of the wide variety of contexts in which, the AI discipline resides, the major theme of this chapter focusses on the existing concepts and applications in the field of AI.

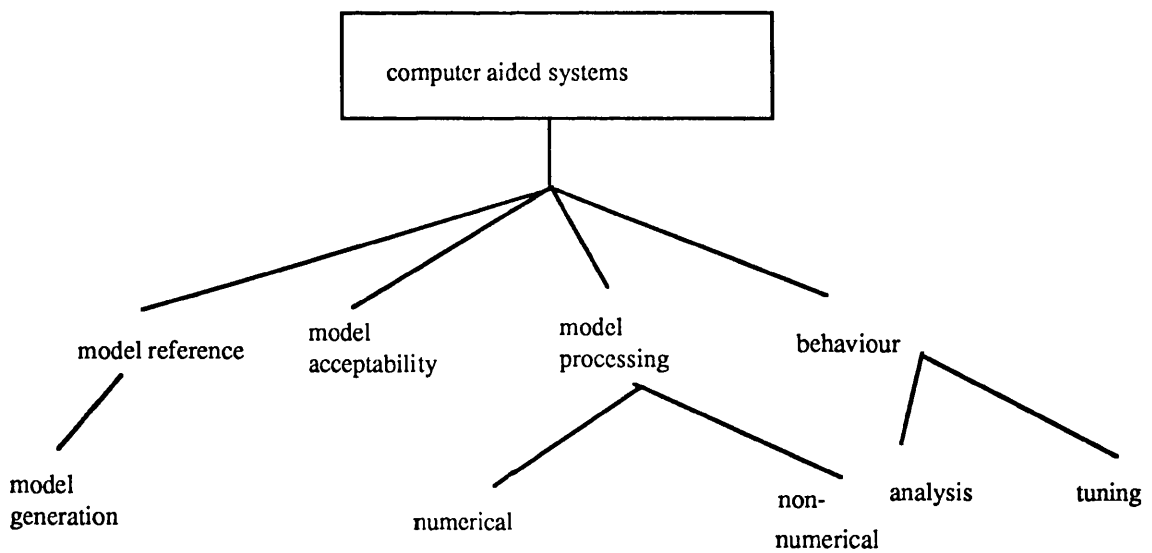

Fig 4.1 Computer-aided system models

4.2 Foundations of Artificial Intelligence

The success of AI systems (expert systems) provides one of the major lessons that has been learned in AI, namely, that general purpose reasoning, by itself, is not powerful enough to produce acceptable levels of performance in many tasks. To achieve success in performing difficult tasks, we need to focus on specific knowledge and adaptive inference.

The basic concepts necessary in understanding AI and expert systems are explained as follows:

(a) Knowledge and knowledge representation

(b) Knowledge organisation and manipulation

(c) Knowledge acquisition

(d) Machine learning

4.2.1 Knowledge and knowledge representation

AI systems derive their power from knowledge. Knowledge can be defined as the body of facts and principles accumulated by humans or the act, fact, or state of knowing [16]. In order to represent knowledge in a machine, it must be possible to define objective versions of knowledge for each domain of interest. These AI systems must deal with knowledge that has been structured and

codified. Basically, there are three knowledge representation paradigms [17] : logical, structural and procedural. The logical paradigm equates the knowledge base with a theory (i.e. First Order Logic, FOL), here the knowledge base is a set of theorems which can be obtained from a set of stored axioms using a set of general purpose inference mechanisms. The structural paradigm emphasizes the organisation of facts composing the knowledge base. The facts are obtained from the semantic units using predefined rules (i.e. semantic nets [18], frames [19], E-R approach [20], etc). The knowledge base structure of the procedural paradigm is composed of active agents with definable reaction patterns. The use of the knowledge is to reduce the reaction of those agents to a given situation according to the procedural rules in the knowledge base. The functionality of knowledge representation can hence be viewed as an approach whereby a kernel of shared parameterised theories can be used to build other theories, a concept commonly known as theory mappings [21] Knowledge and its relational attributes are stored into knowledge representations. The first type of knowledge structure is a fact. Facts can be ascribed as either permanent or temporary knowledge.

i.e. Apples are delicious.
Steel contains carbon atoms.

The next knowledge structure is a rule. Usually, the formal representations are in the form of IF [antecendents] THEN [consequences]. This representation is usally termed a production rule [22].

i.e. IF

The inflation is high.

THEN

The unemployment rate is high.

When combined with the facts, rules can be used to acheive a conclusion, which is composed of a set of new facts (theory mappings).

i.e.

CONCLUSION:

Unemployement is high.

is true, if the fact

Inflation is high.

is true (Figure 4.2)

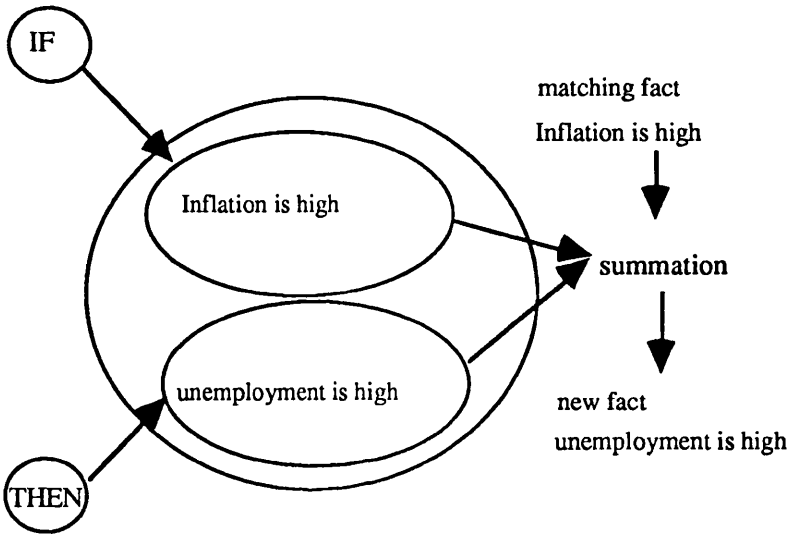

Fig 4.2 Theory mapping

Knowledge can be arranged in a hierarchical structure by facts linkage. An example might be in expressing the family relationship of fatherhood (Figure 4.3).

i.e.

Jim is the son of David.
Mary is the grand-daughter of David.
David is a retired businessman.
Tom is the son of Jim.

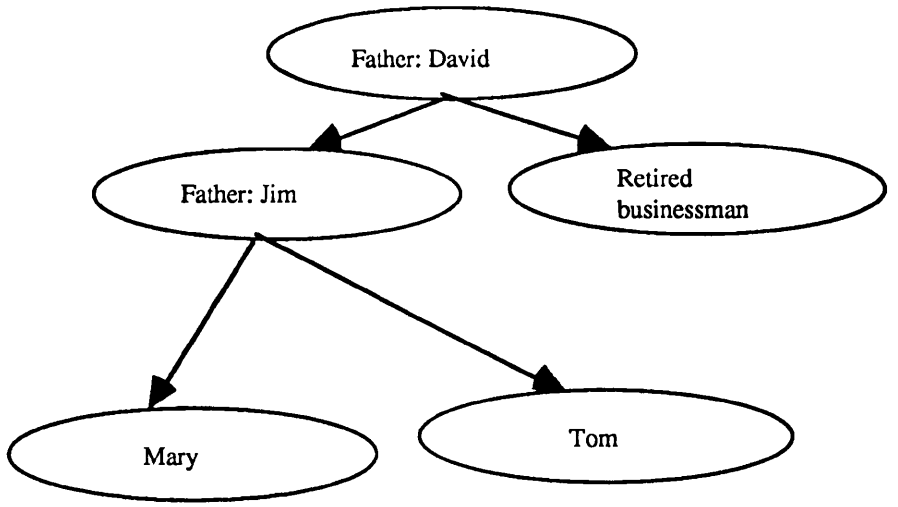

Fig 4.3 Heirarchy knowledge structure of a family

Other representations of knowledge schemes include fuzzy logic [23] and object-oriented methods [24]. Fuzzy logic is a generalisation of predicate logic, developed to permit a varying degree of some property. In classical boolean logic, a predicate can be TRUE or FALSE, but in fuzzy logic, a predicate can be partially true. An object-oriented representation hides these facts by packaging an object together with its attributes and functions. Operations are performed by sending messages between the objects.

4.2.2 Knowledge organisation and manipulation

In addition to methods of describing objects and their relations, methods exist for organising objects into conceptual categories. Knowledge can be organised in memory for easy access by a method known as indexing [25]. Some experimental findings [26] suggest that long term memory can be viewed as a collection of categories nested with a large hierarchy. As a result, the search for

some specific chunk of knowledge is limited to the group only, a fraction of the knowledge base rather than the whole memory. The two main organisation and manipulation techniques are:

(a) Search and control strategies

(b) Matching techniques

4.2.2.1 Search and Control Strategies

Problems can be characterised as a state space plane of states and operators that map one state to other states. One search method is to represent the search space as a diagram of a directed graph or a tree. Each node or vertex in the graph corresponds to a problem state, and arcs between nodes correspond to a transformation or mapping between the states. An AND/OR graph or tree (Figure 4.4) is a special type of representation for a problem that can be reduced to a set of sub-problems, all of which must be solved. The AND node serves as a requirement constraint for all sub-problems concluding towards a solution whilst the OR node serves as enumerating choice of solution search path. To generate the process of searching for a solution, a node must be expanded (i.e. tracing of attached nodes). Searching can be conducted either in a blind/uninform search where no information is used to determine the preference of one node over another, or directed/informed search, where *a priori* information of the problem space and its association with a particular node is known.

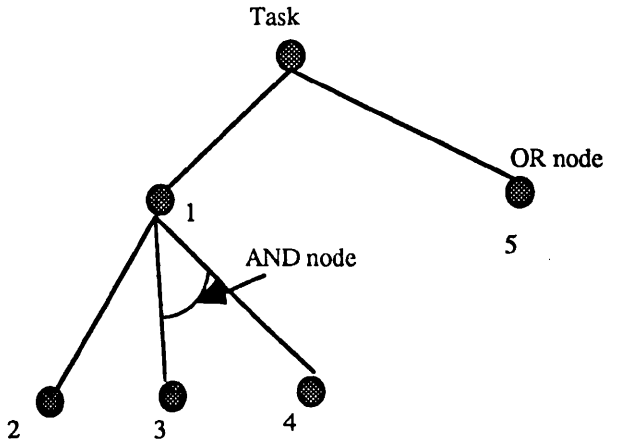

Fig 4.4 Example of AND/OR tree

In a blind search, nodes in the space are explored mechanically until a goal is found, a time limit has been reached, or failure occurs. In a worst case, it may be necessary to explore the whole space before finding a solution. Examples of blind searches are:

(a) Depth-first iterative deepening

Depth-first iterative deepening search is performed as a form of repetitive depth first search moving to a successively greater depth with each iteration until a goal node is found or some maximum depth is reached

(b) Breadth-first

Breadth-first search is performed by exploring all nodes at a given depth before proceeding to the next level

(c) Depth-first

Depth-first search is performed by diving downward into a tree as quickly as possible. It does this by generating a node from the most recently expanded node. This process continues until a goal is found

If *a priori* knowledge of the search domain is available, the informed search techniques based on some cost functions are used to select the most cost effective path to the solution. Examples are:

(a) General best-fit

Using *a priori* knowledge, the nodes are computed and the best valued node is explored

(b) Hill climbing

At each point in the search path, a successor node that leads to the goal is selected for exploration.

(c) Branch-and-bound

This method accumulates all the node path lengths and selects the shortest path for further exploration

(d) Optimal AND/OR heuristic search (OA*)

This is a search which is formulated to heuristically choose the shortest path through the nodes for exploration

4.2.2.2 Matching techniques

Matching is the process of comparing two or more structures to discover their similarities or differences. Matching is used in the control on the sequence of operators, to identify/classify objects or to retrieve items from a database.

Matching can be broadly classified into two main catagories. Matching by variables or matching by measures.

4.2.2.3 Matching by variables.

Knowledge structures are constructed from basic elements such as numbers or characters. By comparing these basic objects with an input pattern, a cross correlation test can be conducted. Uncorrelated features would denote a failed match whilst a cross correlation between the knowledge structure and the input pattern would signify a match.

4.2.2.4 Matching by measures.

The similarity between two structures is a measure of the degree of association or likeness between the objects attributes and other characteristic parts. Hence by evaluating the distance between the predicate and the input pattern, the qualitative approximation of the match can be noted. Methods of measuring evaluations are:

(a) Distance metrics

(b) Probabilitistic measures

(c) Qualitative measures

(d) Similarity measures

(e) Fuzzy measures

4.3 Knowledge Acquisition.

A number of approaches to knowledge acquistion exists. The three basic approaches are as follows : (Figure 4.5)

(a) Interviewing

In this approach, a knowledge engineer obtains knowledge from the human expert through a series of interviews and encodes it in the AI system

(b) Learning by Interaction

Experts directly interact with a computer program that helps to capture their knowledge

(c) Learning by Induction

A computer program synthesises knowledge by examining data and example

The acquired knowledge may consist of facts, concepts, rules, relations, plans, and procedures. Examples of expert systems [27] that use knowledge acquisition are MYCIN [28], DENDRAL, PROSPECTOR and XCON.

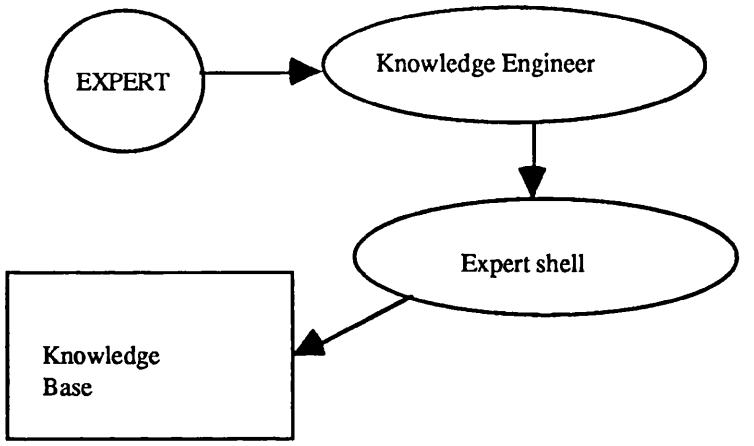

Fig 4.5(a) Learning by interview

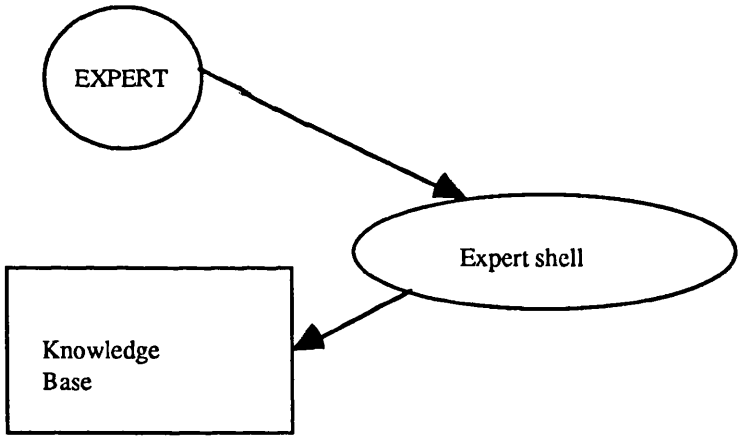

Fig 4.5(b) Learning by interaction

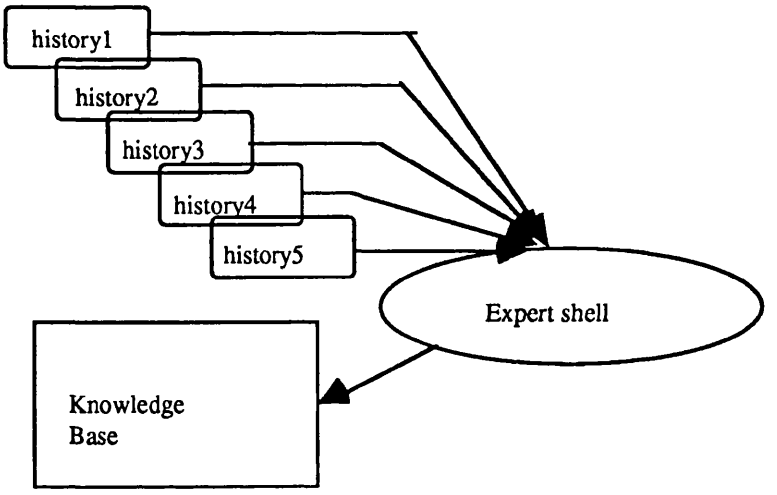

Fig 4.5(c) Learning by induction

There is no consensus of how the process should take place as knowledge acquisition is highly dependent on the domain of the expert system. Some common methods [29] are as follows:

(a) Protocol analysis

(b) Card-sorting and other psychology techniques

(c) Task analysis

(d) Examining re-orders

(e) Machine induction

4.4 Machine learning

Autonomous learning systems are self-adaptive systems which modify their own structures in an attempt to produce an optimal

response to some input stimuli. Numerous approaches have been developed in the area of machine learning since the 1950s, the most successful ones are :

(a) Network of neurons (i.e. Perceptron [30])

(b) Rote learning [31]

(c) Self-adaptive stochastic automata models

(d) Genetic evolution systems (i.e. Genetic Algorithm [32])

Fundamentally, machine learning can be divided into two basic elements - description language and training set. The description language or rule language is the notation or formalism which expresses the knowledge of the system. The training set is important in testing the efficiency of the learning machine. Typically there is a database of examples for which the solutions are known. The system works through these instances and develops a set of rules for associating input descriptions with output decisions. Now, the same system is tested against a test set (i.e. a database of the same example domain but containing unseen data). If the new rules also apply successfully to these fresh cases, the machine learning mechanism can be validated.

Machine learning can be applied through techniques like optimization, scientfic discovery, programming by examples, etc. But the commonest theme of generate-and-test provides a unifying principle.

4.5 Artificial Intelligence in control

Real-time control system - ranging from small simple controllers in home applicances to large, complex systems for industrial and/or military purposes - are used in more applications than ever before. However, the complexity of these controllers is increasing not only in numbers of functions controlled but also in the kinds of factors that must be considered before a correct decision can be made. This increasing complexity has generated considerable interest in using knowledge based techniques for controller applications. In the design of control systems, both the robust control approach and the adaptive control approach can be used. Robust design methods give fixed compensators with satisfactory performance over a specific range of system parameter variations. Adaptive design methods extract knowledge from the system parameters on line and redesign the control law (Figure 4.6 and Figure 4.7). Usually, most of the system dynamics are difficult to model, hence adaptive control is usually recommended. Direct coupling of AI techniques to adaptive control has greatly improved the adaptive controller response and sensitivity to system design adaptation. An important contribution to the field of adaptive control systems is the computer controller system developed by R.E. Kalman [33]. Since then, many applications of Intelligent control have evolved [34][35][36].

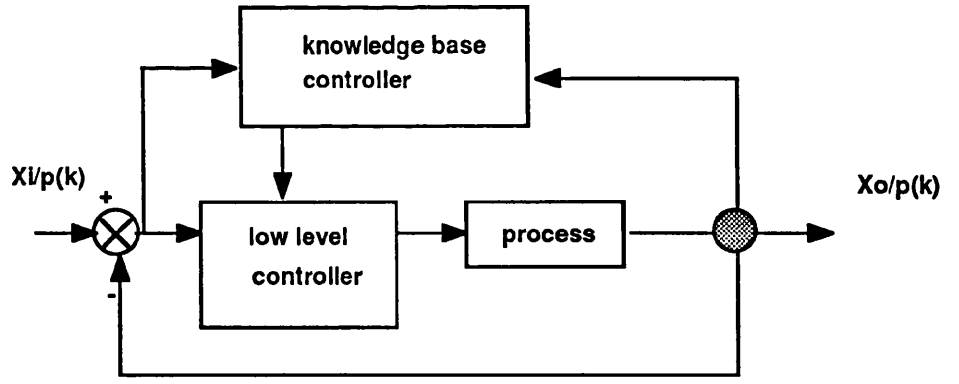

Fig 4.6 Parametric adaptive intelligent control system

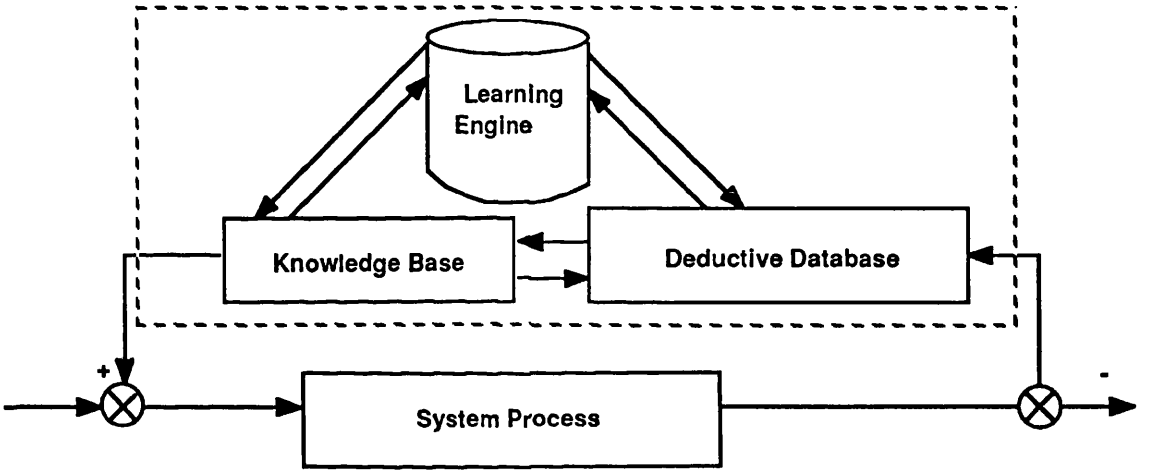

Fig 4.7 High level intelligent control

To gain a better understanding of AI in control, we need to review the areas of AI applications in system process control. There are three main areas in which AI is applied to process control:

(a) Model processing

A form of AI integration in model processing is in the design of a knowledge based system for computer-aided design in the control domain which provides selection

and recommendation of control methodology for specific control problems [37]. This function of the AI system would enable a greater flexibility and combination of control techniques to be applied to a system. Another area would be in the modelling of the process dynamics domain using tools and evaluation functions provided by the expert system. The tools are represented in terms of transfer functions and control elements. Automatic evaluation of the process can be done by the expert shell via algorithmic computation. Validity of the process model could then be justified by the responses from the expert shell user-interaction facilities.

(b) Knowledge management systems

In knowledge management systems, the AI system deals with the representation, acquisition, and the use of knowledge, i.e. with knowledge management [38][39]. Many expert systems already exist as applications of AI. An expert system for fuzzy self-tuning of a dynamic system [40] is an example.

(c) Behaviour generations

There are two groups of possibilities for AI behaviour generation: (1) simple behaviour generation, and (2) sensitivity analysis. Both of the cases involve two types of behaviour:

(i) point behaviour

In point behaviour, the model is processed either numerically (i.e. in optimisation using either hill-climbing or genetic algorithm) or non-numerically (as in searches of the knowledge representation system or symbolic processing) to generate point behaviour in one or multidimensional solution space.

(ii) trajectory behaviour

Trajectory behaviour is the common behaviour for modelling and simulation of dynamics systems. The AI system here is used as an on-line model reference to adaptive control. As a result of model processing, one may get either point or trajectory behaviours of the model. In the analysis of the point behaviour, AI comes into play by providing multi-criteria decision making. In trajectory behaviour, AI techniques [41] can be used in data selection and compression, i.e. statistical or surface fitting.

In the research carried out herein, an object oriented Knowledge Based Management System (KBMS) architecture based on the concept of Proportional-Integral-Differential (PID) control with self-learning

capabilities is proposed for the high level control of complex control systems. The architecture comprises: an enhanced KBS with tight coupling to a deductive database which allows both bottom-up and breadth-wise search strategies to be implemented in an optimal combination. This management system selects both the set-point and the independently controllable variables; the independent variables can then be modified by an inductive process. The knowledge base extracts the deduced properties and functional attributes of data abstracted from the deductive database and converts them into an object-oriented representation for inductive selection. The principles of the PID-KBMS architecture, the deductive semantic-algorithms and the inductive engine are described in detail. The resultant system utilises experimental data for the tasking and control of a CO_2 laser manufacturing system.

4.6 Artificial Intelligence in Computer Integrated Manufacturing

The continuous development of computer technology has created opportunities for manufacturing industry in both the areas of numerical machine control and manufacturing management. The uses of digital computers in numerical control (NC) can be classified into three main topics: (1) computer numerical control (CNC), (2) Direct numerical control (DNC) and (3) adaptive control. Computer integration involves the replacement of the conventional hard-wired NC controller unit by a small computer. The small computer is then used in performing some of the basic NC functions by programs stored in its read/write memory. One of the distinguishing features of CNC is that one computer is used to

control one machine tool. This contrasts with the second type of computer control, direct numerical control. DNC involves the use of a larger computer to control a number of separate NC machine tools. The third control topic, adaptive control, does not necessarily require a digital computer for implementation, instead, a hardwired control circuit may be used. Adaptive control machining denotes a control system that measures one or more process variables (such as cutting force, temperature, horse-power, etc.) and manipulates feed and or speed in order to compensate for undesirable changes in the process variables. Its objective is to optimise the machining process, something that NC alone cannot accomplish.

The manufacturing environment can be decomposed into 9 basic parts:

(a) Engineering and manufacturing database

(b) Material requirement planning

(c) Capacity planning

(d) Inventory planning

(e) Shop floor control

(f) Cost planning and control

(g) Sales forecasting and market trends prediction

(h) Personnel i.e. man management

Many schools of thought have been established to provide an insight into the optimisation of the CIM environment i.e. JIT, OPT. Readily available software packages such as MRPI, MRPII provide tools for evaluating and controlling flow within the manufacturing environment. AI shells integrate into the CIM software a dynamic knowledge structure and provides expert insight into the management of the inventory, manufacturing processes and sales prediction. An AI interfaced manufacturing system usually provides parameteric feature modelling facilities and material selection facilities for components manufacturing. Intelligent network interfacing of the DNC is also an area in which AI has established itself. By providing a distributed knowledge based system, information selection and recommendation can be pipelined to the relevant department as required. The knowledge representation for the CIM environment commonly used is the petri nets topological modelling technique. Petri nets modelling allows a closer insight to the control flow of information in CIM. In conclusion, the integration of knowledge engineering/concepts into CIM provides a manufacturing control environment that displays high flexibility and adaptability, as has been seen demonstrated in successful applications [42][43].

REFERENCES

[1] Hao Bal-Lin, "Chaos", World Scientific Publishing Co. Pte Ltd (1984).

[2] Grahma C. Goodwin and Kwai Sang Sin, "Adaptive filtering prediction and control", Prentice-Hall Information and System Science Series(1989).

[3] M.L. Minsky, "Matter, mind, and models", Proceedings of IFIP Congress, Vol 1, Spartan books, pp 45 - 49(1979).

[4] T.I. Oren,"Concepts for advanced computer-assisted modelling", Methodolgy in systems modelling and simulation, North-Holland, Amsterdam, pp 31(1979).

[5] S. Dickhoven, " Strategies for standardization in socio-economic modelling", Methodolgy in systems modelling and simulation, North-Holland, Amsterdam, pp 161 - 181(1979).

[6] Lim See Yew and C.R. Chatwin," The design of a second order PID knowledge based management system for process control", Proceedings of the second international conference on Automation, Robotics and Computer vision, ICARCV'92, pp CO.7.4.1 - C.O. 7.4.5,6-18 Sep(1992).

[7] Kenneth De Jong,"Adaptive System Design: A Genetic Approach", IEEE Trans. on Systems, man, and cybernetics, Vol SMC - 10, No.9, pp 566 - 574, Sep(1990).

[8] T. Takgi and M. Sugeno, "Fuzzy identification of systems and its application to modelling and conrol", IEEE Trans. on Systems, man, and cybernetics, Vol 15, pp 116 - 132(1985).

[9] E. Janus,"Time requirements for time-driven system using augmented petri nets", IEEE Trans on Software Engineering, 9, pp 603 - 616, Sep(1983).

[10] L.T. McCathy and N.S. Sridharan,"The representation of an evolving system of legal concepts: Logical template", Proceedings of the third Biennial Conference of the Canada Society for Computation studies of Intelligence, Victoria, Canada, pp 304 - 311(1980).

[11] Lim See Yew and C.R. Chatwin,"Knowledge control modelling (KCM): The bond graph unification approach to design", submitted for review, Journal of knowledge and data engineering(1992).

[12] D.H. Ackley, G.E. Hinton and T. Sejnowski, "A learning algorithm for Boltzmann machines", Cognitive science, Vol 9, pp 147 - 169(1985).

[13] J.L. McClelland and D.E. Rumelhart, "An interactive activation model of context effects in letter perception: Part I, An account of basic findings", Psychological review, vol 88, pp 275 - 407(1981).

[14] Bellman, R.,Kalaba M., and Zadeh, "Fuzzy sets", information and control, Plenum Press, NY(1964).

[15] R.J. Brachman and H.J. Levesque," What makes a knowledge base knowledgeable? A view of database from the knowledge level", First international workshop on expert database system, pp 67 - 78(1986).

[16] A. Hart, "The role of induction in knowledge elicitation", Knowledge Acquisition for expert systems: A Practical Handbook, Plenum Press, NY(1987).

[17] J. Mylopoulous and M.L. Brodie, "AI and databases: Semantics vs computational theories of information", New Direction for Database systems, Ablex Publishing Co., Norwood, NJ(1985).

[18] P.P.S Chen, "The Entity-relationship model - towards a unified view of data", ACM trans. on database system, Vol 1, No 1, pp 9 - 36(1976).

[19] P.J. Hayes, "The logic of frames", Frames conceptions and text understanding, Walter de Gryter and Co., Berlin, pp 46 - 61(1979).

[20] R. Hull and R. King, "Semantic database modelling: Survey: Applications, and research issues",Computer surveys, vol 19, No. 3, pp 201 - 260(1987).

[21] J. Goguen and R.Burstall, "Introducing institutions", Logics of programs, Lectures notes in computer science, Vol 164, Springer-Verlag, Berling(1984).

[22] F. Flayes-Roth, "Rule-based systems",Communications of the ACM, Vol 28(1985).

[23] L.A. Zadeh, "The role of fuzzy logic in the management of uncertainty in expert systems", Fuzzy sets and systems, vol 11, No 3(1977).

[24] M. Stefik and D. Bobrow, "Object- oriented programming: Themes and variations", AI magazine, vol 6, No. 4(1986).

[25] W.A. Bousfield, "The occurence of clustering and the recall of randomly arranged associates", Journal of general psychology, vol 49, pp 229 - 240(1953).

[26] E.E. Smith, E.J Shoben and L.J. Rips,"Structure and process in semantic memory: A feature model for semantic decisions", psychological review, vol 81, pp 214 - 241(1974).

[27] J.L. Alty and M.J. Coombs, "Expert systems - concepts and examples", NCC publications(1984).

[28] E.H. Shortliffe,"Computer-based medical consulations: MYCIN", NY(1979).

[29] A. Kidd, "Knowledge acquisition for expert systems: A practical handbook", Plenum Press, NY(1987).

[30] F. Rosenblatt, "The perceptron: a probabilistic model for information storage and organisation in the brain", psychological review, vol 15, pp 386 - 408(1958).

[31] T. Forsyth and R. Radar, "Machine learning: Applications in expert systems and informations retrieval", Ellis Harwood(1986).

[32] T.M. Holland,"Adaption in natural and artificial systems", University of Michigan press(1975).

[33] R.E. Kalman, "Design of a self-optimising control system", ASME trans, vol 89, pp 486 - 478(1975).

[34] J. Taylor and R.Fredrick,"An expert system architecture for computer aided control engineering", IEEE Proceedings, vol 72, pp 1795 - 1805(1984).

[35] J. Lieslehto, "An expert system for interaction analysis of mulitvariable system", International journal of adaptive control and signal processing, vol 5, pp 41 - 62(1991).

[36] R. Sutton, "A design of a self-orgainising fuzzy logic controller", Proceedings of Internal Mech. Engr., Part C, vol 200, pp 59 - 69(1986).

[37] B.Akhatib, B. bergeon, "SECOA: A knowledge based system for control design", Proceedings of the second international conference on Automation, Robotics and Computer vision, ICARCV'92, pp CO.7.7.1 - C.O. 7.7.5, 16-18 Sep(1992).

[38] N.V. Findler, "Associative networks: representation and use of knowledge by computers", Academic press, NY(1979).

[39] S. Ohsuga, 'Theoretical basis for a knowledge representation system", Proceedings of the sixth international joint conference on artificial intelligence, pp 676 - 683(1979).

[40] Zhang Hua-Quang and Chai Tian-You,"A fuzzy self-tuning control approach for dynamic systems", Proceedings of the second international conference on Automation, Robotics and Computer vision, ICARCV'92, pp CO.13.3.1 - C.O.13.3.5, 16-18 Sep(1992).

[41] J.C. Stansfield, "Qualitative reasoning about time series", Proceedings of the third Biennial Conference of the Canada Society for Computation studies of Intelligence, Victoria, Canada, pp 41 - 48(1980).

[42] T.M. Tirpak,"A note on fractal architecture of modelling and controlling flexible manufacturing systems", IEEE trans on SMC, vol 22, No 3, pp 564 - 568(1991).

[43] Opas Chutatape, "A simulation and control of a real-time multitasking manufacturing process by two pcs", Proceedings of the second international conference on Automation, Robotics and Computer Vision, ICARCV'92, pp IA-7.5 - IA 7.5.5, 16 - 18 Sep(1992).

5 ASSOCIATIVE ARTIFICIAL INTELLIGENT REAL-TIME SYSTEM MODELLING

5.1 Introduction

For some engineering systems, the general control theory defines the system framework and a major part of its structure. Providing parameter estimation procedures are adequate, parameters may be determined by straightforward experimental methods, minor uncertainties in the structure are quantified by using final validation arguments and iteration through the procedures. For some very complex systems - like laser materials processing and biosystems - in addition to the parameters, a large part of the structure may be unknown due to softness; even details of the framework may be ill defined and hence unavailable. As a consequence, control engineering techniques must be combined with expert insight to infer unknowns in the framework and

structure from the available information. Current computer based control has evolved many new inference techniques, for example: expert shells, fuzzy systems, artificial neural nets. Many of these have proven to be highly efficient for particular control applications. This treatise proposes the use of: unified bond graph theory in knowledge control modelling (KCM) for the construction of state space artificial intelligent systems for process control. In KCM there are three stages in the design of an intelligent control system: physical representation, bond graph representation and the state space bonding graph (SSBG). This unification of both the intelligent system and process models using bond graphs allows design of the flow of both data and system events. This approach was used in the design of a second order PID-Knowedge Based Management System (PID-KBMS) for laser control.

In the classical modelling approach, a control model is completely defined if the specification illustrated by Figure 5.1 can be determined. An improvement on this specification is summarised in the modelling approach outlined in Figure 5.2. The specification requires:

(i) The system framework: boundary conditions; input and output variables: u(t), y(t); disturbances d(t)

(ii) The system structure : functional relations f, g, h, etc; dimensionality of the state vector; noise characteristics

(iii) The system parameter coefficients

In the design of an intelligent system for on-line/off-line control, clear classification of the expert intelligent system must be achieved in order to produce an efficient architecture for control [1]. A PID-KBMS was proposed [2], which differentiated the intelligent systems into three main modes of data fusion. This chapter proposes a common topological methodology using the bond graph theory to unify the PID-KBMS modules with the process control. The objective of this approach is to enable computer scientists and control engineers to realise a unified design topology in the construction of an intelligent system for process control.

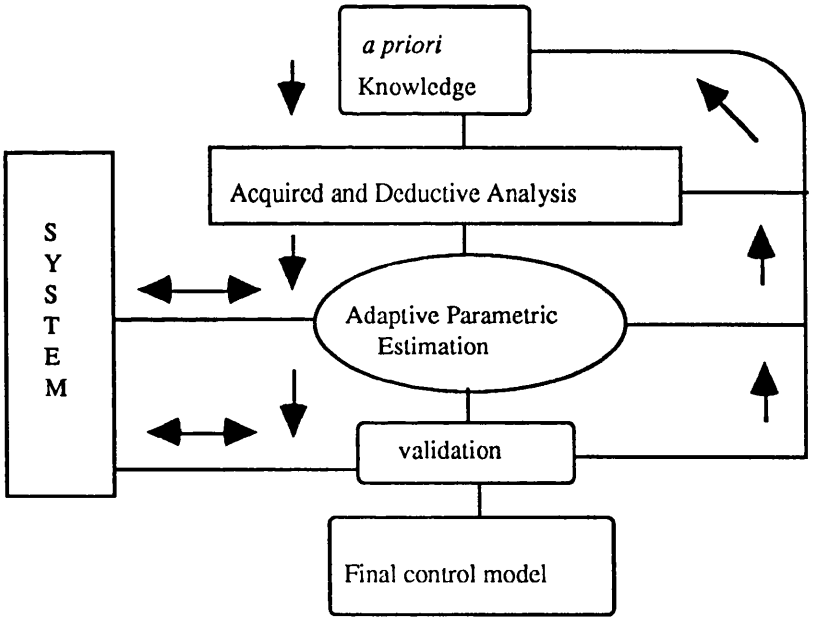

Fig 5.1 Classical approach to mathematical modelling

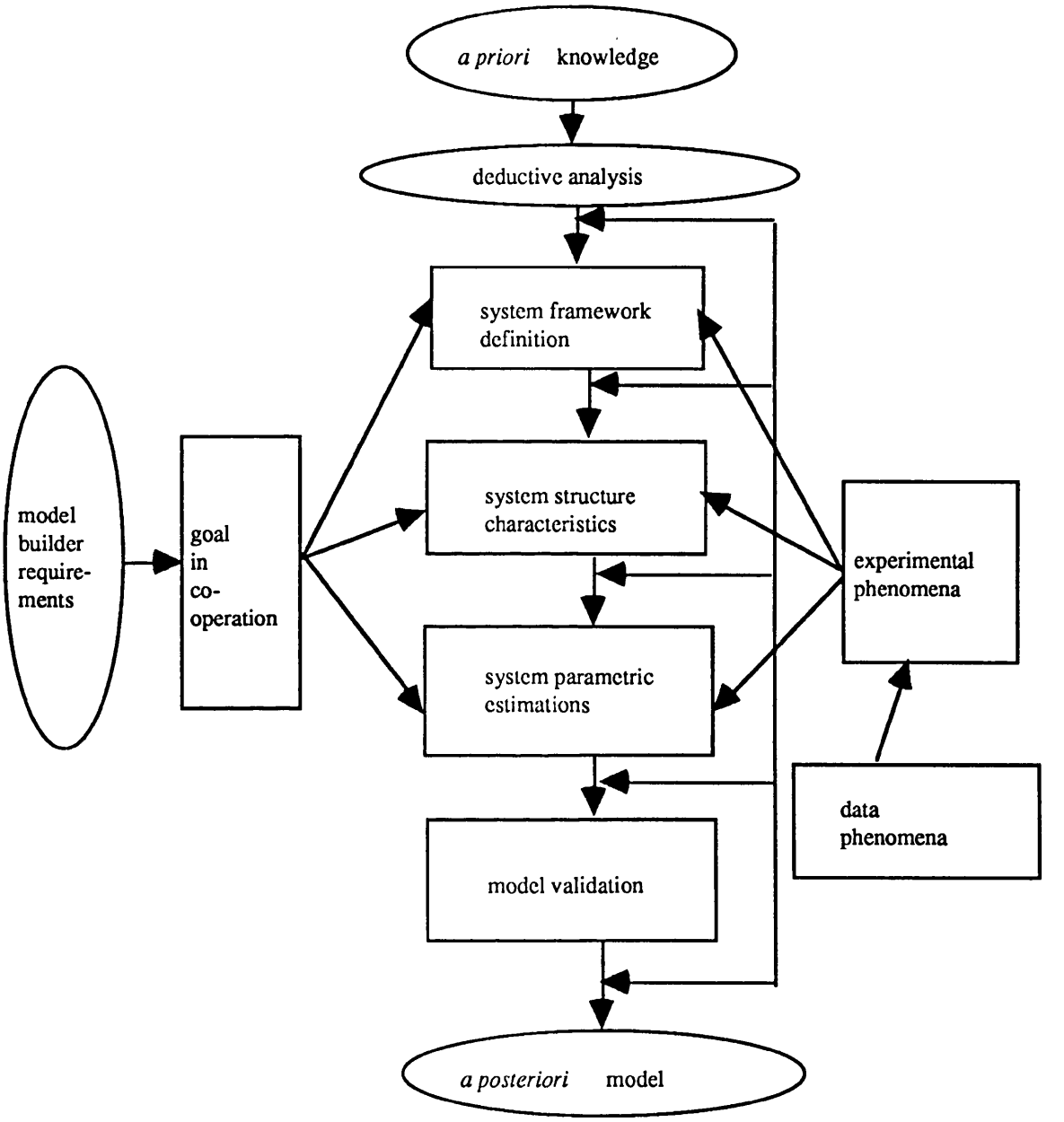

Fig 5.2 Current approach to mathematical modelling

5.2 Nomenclature

A = Workpiece cross sectional area (m^2)

ß() = State space bond graph tuple representation

C = Specific heat capacity (kJ/kgK)

C_m = Thermal capacity (kJ/K)

δ = Absorptivity (1/m)

e = Bond graph effort representation

f = Bond graph flow representation

f{} = Laser heat source function (kJ/m^3)

h = Overall heat coefficient (W/m^3K)

k = Thermal conductivity (W/mK)

m = mass of material (kg)

P = Power (W)

ρ = Specific density of the material (kg/m^3)

r = Kerf width (m)

R = Bond graph resistance representation

R_f = Reflectivity of the material

S_e = Bond graph effort source representation

t = Time (sec)

t_z = Thickness of material (m)

T = Temperature (K)

T_{amb} = Ambient temperature (K)

T_{kerf} = Temperature at the underside of the cut (K)

V = Velocity of cut (m/sec)

ω = Laser beam waist diameter at $1/e^2$ the beam intensity (m)

5.3 Brief outline of bond graph modelling

Bond graph modelling [3] is a topological methodology developed by Paytner and later improved by Karnopp and Rosenberg [4]. In all types of system analyses, the fundamental step to the attainment of stable solutions is to create a model, which can be analytical, graphical or numerical. The analytical model is a model derived

from the history of the system variables so that relations can be derived to form constitutive laws (i.e. V= IR). Where the physical system is described by differential equations that have no analytical solution, numerical representation of the governing equations and their boundary conditions must be utilised. The last model is the graphical approach, commonly block-diagrams/schematic-diagrams or signal flow graphs are used to produce a state space solution. Mathematical analyses are then used to approximate expressions for the model variables. The bond graph topological method to system modelling belongs to this category. Bond graphs use a small number of standard element features to represent system dynamics. Bond graphs are models which rely on the concepts of energy translation and conservation. The approach of bond graph modelling is, strongly related to the thermodynamic Onsager reciprocal relations [5] which relate driving forces to energy flows. The translation of energy is via power flow. Power flow is a product of the flow of the system variables and the effort or force associated with these variables. In bond graph modelling there are seven basic elements, effort (e(t)), flow (f(t)), time integral of effort (momentum(p)), time integral of flow (displacement(q)), capacitance (C), resistance (R) and inductance (L) (see table 5.1).

Bond graph variables	Topological representation
Effort	e(t)
Flow	f(t)
momentum	p=integral(e(t))
Displacement	q=integral(f(t))
Capacitance	C
Resistance	R
Inductance	L

Table 5.1 Table of bond graph elements

Transitional operators exist in bond graph modelling. A passive operator; a gyrator (GY) - relates one form of linear energy to another. The structure of the bond graph (b.g.) is linked by 1-bond (the algebraic summation of the effort is zero) and O-bond (summation of the flow is zero). The half arrow (see Figure 5.3) represents the power bond and points towards the function where power is supplied. Bond graphs need to be causally augmented, i.e. numbered and given a causal stroke. The numbering allows identification whilst the causal stroke denotes the direction of the effort, the stroke is always placed in the direction of the applied effort.

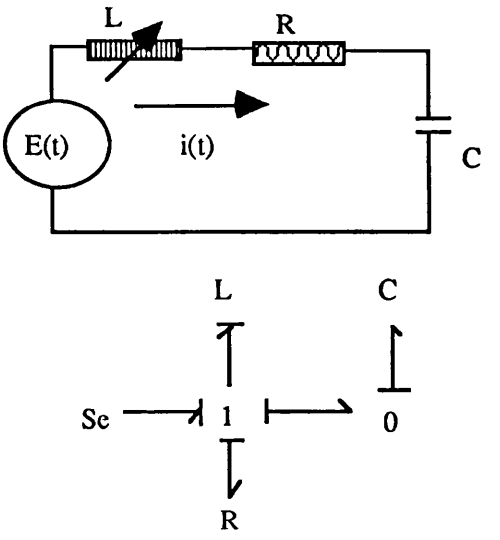

Fig 5.3 Bond graph representation of a simple electrical circuit

5.4 Knowledge control modelling (KCM)

KCM [6] is a proposed knowledge modelling topology that can be used with the bond graph topology in the design of computer based artificial intelligent process controllers. KCM comprises basically three stages: the physical representation stage, the bond graph representation stage and the state space bonding graph (SSBG) (see Appendix B) This integration of topologies can be related to the data fusion theory. The efforts, here for data integration, are the rules or inferences; whilst the flows from a node of the knowledge matrix to another are dependent on the validity of the data (see Figure 5.4 and Figure 5.5). After KCM modelling, a full flow schedule of the data management can be obtained. In real time system applications, by following the SSBG and the bond graph, traceability of dynamic variables can be maintained with ease.

Additional advantages of using KCM are in the persistence and robustness of the data management. The method is used to implement the PID KBMS in the tasking and control of a laser manufacturing workcell. The independent variables are the power and velocity of cut, whilst the dependent variables are the reflected power and temperature during the laser/material interaction process. Physical implementation of the system is already near its final stage; however, a process simulation has been completed using the designed PID KBMS. The response bandwidth proves that the AI system designed is efficient.

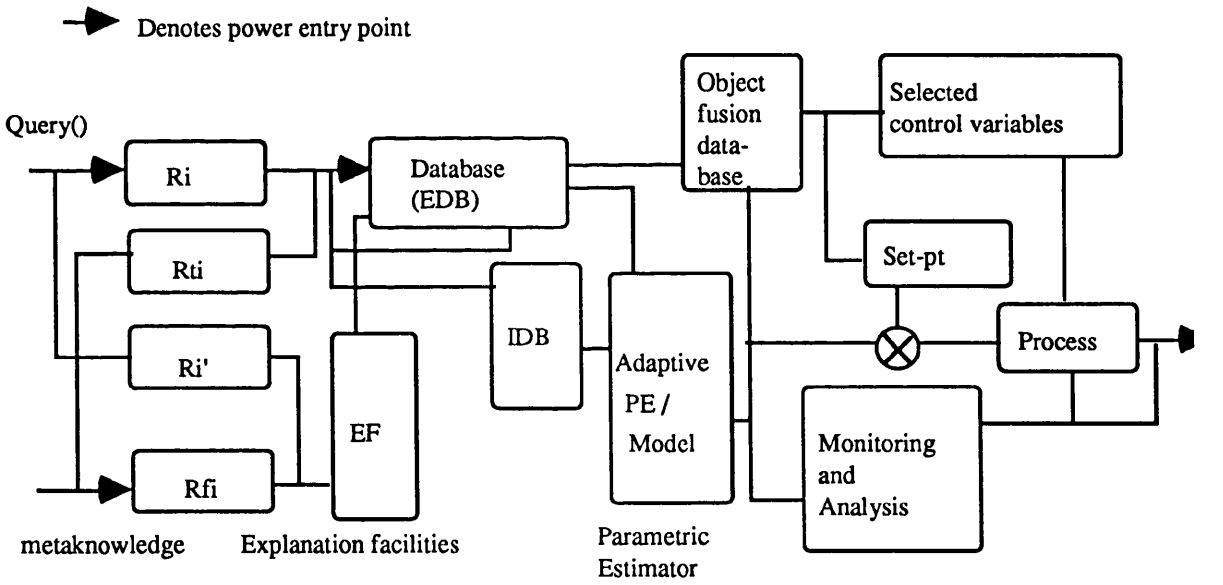

Fig 5.4 Block diagram of a proposed intelligent control system

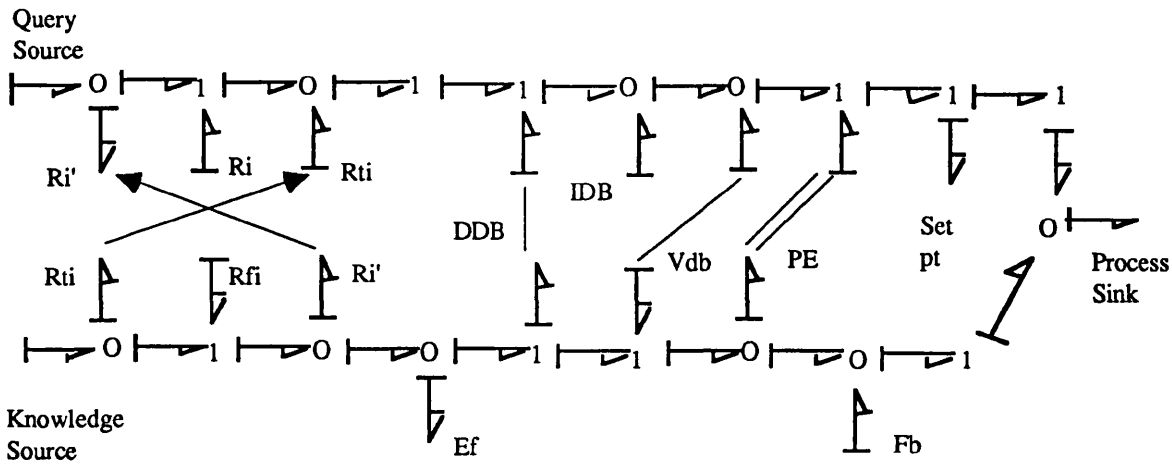

Fig 5.5 KCM ladder bond graph of the intelligent system

5.5 Deductive database

A deductive database [7][8] (DDB) is a database in which new facets can be derived from the existing facets and explicitly stored by using an inference engine. The database can be subdivided into an extensional database (EDB) and intensional database (IDB). The EDB is basically a factual model whilst the IDB comprises deductive rules. Many evaluation methods for recursive queries in the domain of deductive databases have been studied, for example: Actifs Graphs Connections (AGC), Rules/Goals Graphs (RGG), System Graphs (SG), Transitions Petri Nets (TPN) and Resolution Graphs [9]. This research work proposes modelling the deductive database attributes as a control module with its queries achieved utilising resolution theory. The recursive mechanism of the bond graph modelling of a DDB is satisfied by a resolution factoring tree and Robinson Inference Theory [10]. When first building a model it is

essential to understand the workings of a system; hence, a physical identification model must be drawn first (Figure 5.6).

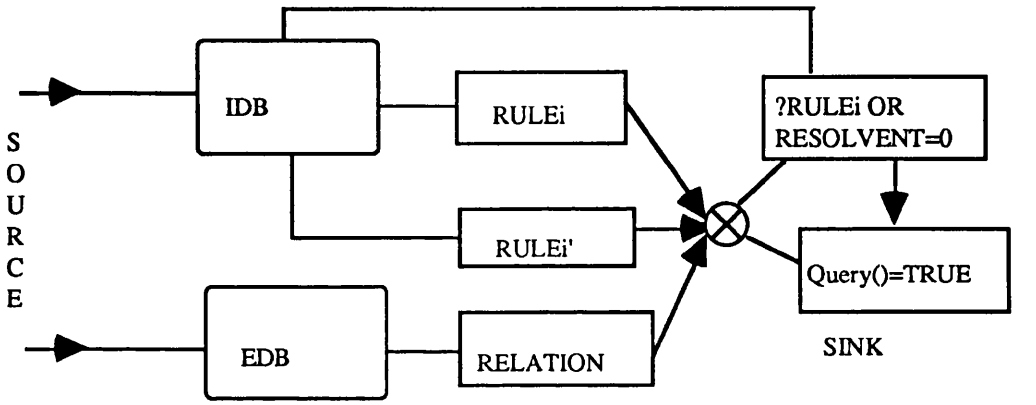

Fig 5.6 Block diagram for the database physical domain

The modelling process can be visualised via an example; consider the following database of company employee data. EDB is a functional attribute of employee name, salary and age as well as job description. The IDB consists of rules relating to the staff appointment.

EDB

: (Relation 1) emp(name, salary, age).

: (Relation 2) job(name, dept)

IDB

: (Rule 1) Manager(X1) <- emp(X1,Y1,Z1), Salary(2000)

: (Rule 2) Staff(X2) <- emp(X2,Y2,Z2), Salary(500)

Now, consider the query "Find all employees that are managers with salary between 3000 to 4000". Modelling with the bond graph approach leads to Figure 5.7.

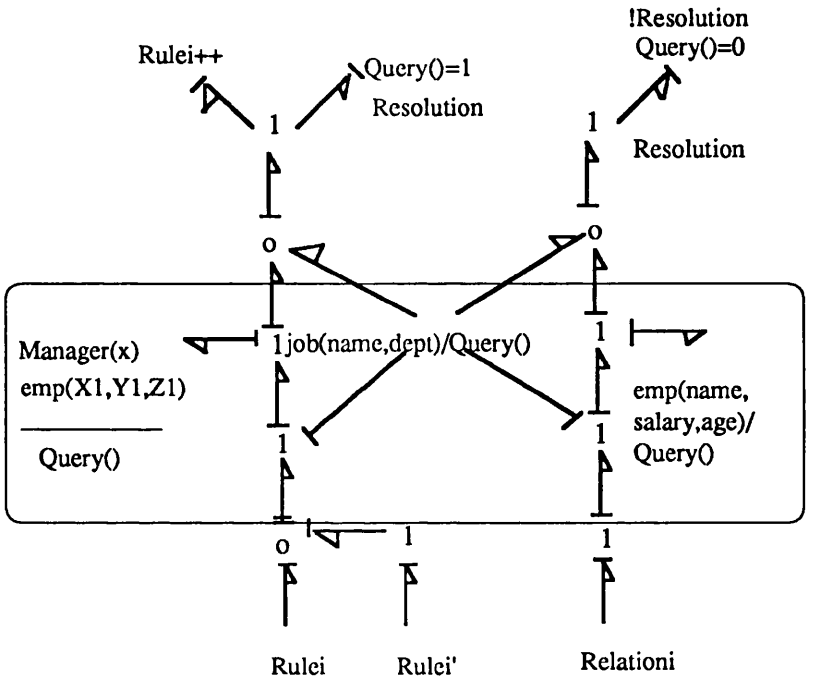

Fig 5.7 Bond graph modelling of the database

: Rule fired for system (Ri).(where i denotes the rule number).

: Complementary or negation rules (Ri').

: Query function (Query()).

By following the bond graph modelling, if the rules have been exhausted or if the resolvent of the query is zero, then the query would be valid. The bond graph allows an easy recursive search through i=1 to N, where N is the total number of rules, by validating the EDB and IDB sequentially. The next stage is to draw the state space bonding graph to trace the architecture of the design implicitly. There are basically three main steps to drawing a SSBG (see Figures 5.8, 5.9, 5.10 and Appendix B).

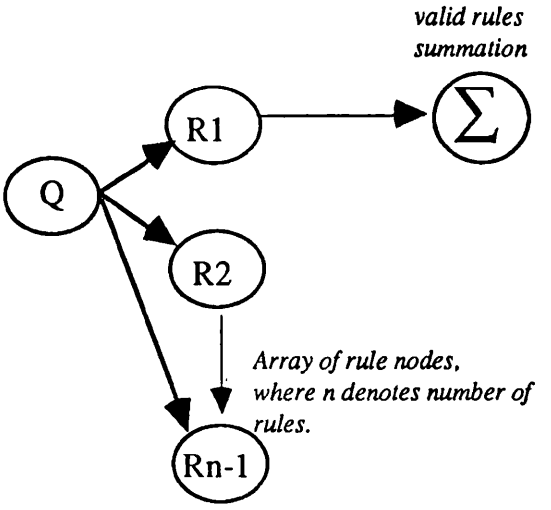

Fig 5.8 SSBG of ß(query, rules)

Step 1:

logic bonding:

Query:

Q: (?Manager(name,age,dept), salary(3000 - 4000))

Rules

*R1:Manager(X1)<-emp(X1,Y1,Z1), salary(2000 - 3000).

R2:Staff(X2)<-emp(X2,Y2,Z2), Salary(400 - 500)

Summation:

$\forall Rule : \exists Manager\ (X) <- emp\ (X,Y,Z), (2000 < salary < 3000)$

(Where * denotes valid rule);

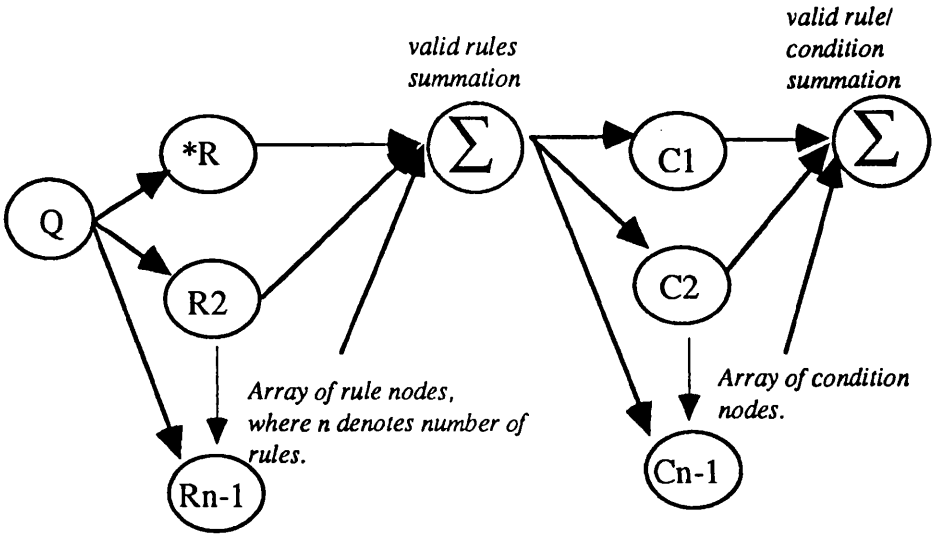

Fig 5.9 SSBG of ß(query, rules, conditions)

Step 2:

logic bonding:

Query	Rules	Conditions
Q:(?Manager(name,age, dept), salary(3000 -4000)	*R1:Manager(X1) <-emp(X1,Y1,Z1), Salary(2000)	C1: manager:C(name, (salary(2000)) C2:manager:C(name, (salary(3000)) C3:staff:C(name, (salary(500))

Summation:

$$\forall C: \sum \forall(\exists manager\ (X,Y,Z) <- emp\ (name, Y, salary):((salary) \wedge (salary\ (3000-4000)))$$

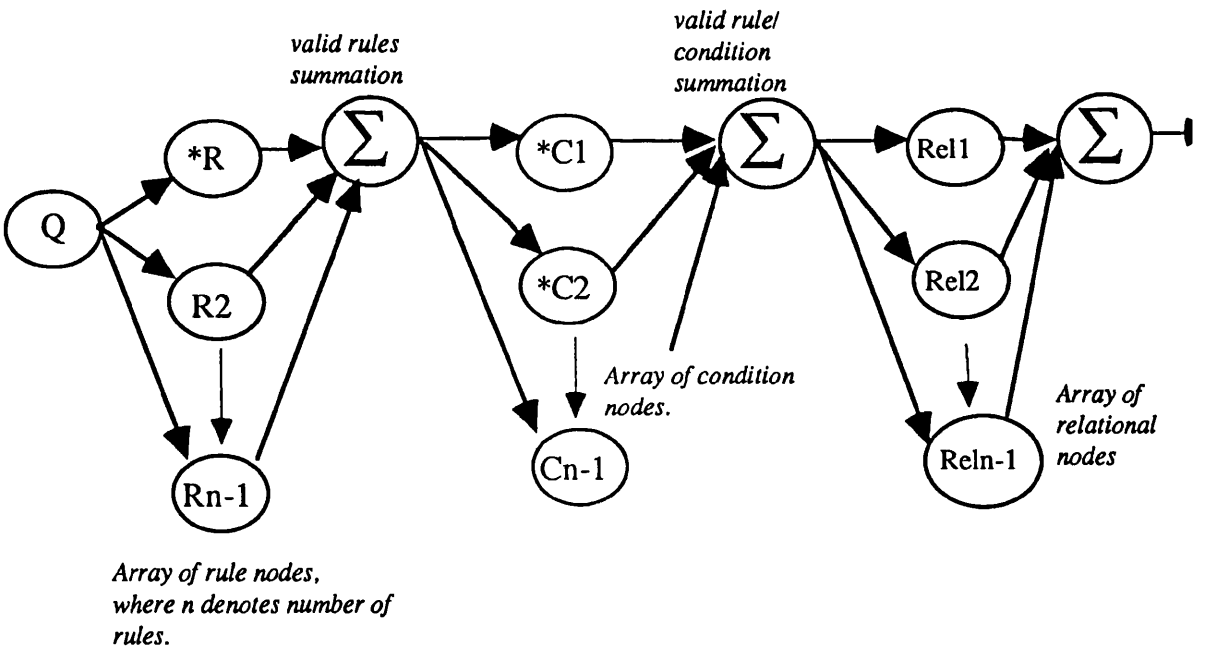

Fig 5.10 SSBG of ß(query, rules, conditions, relations)

Step 3:

logic bonding:

Query	Rules	Conditions	Relational
Q:(?Manager(	*R1:Manager(X1)	*C1:manager:C(	Rel1:
name,age,	<-emp(X1,Y1,Z1),	name,	manager:Rel(
dept), salary(3000	(salary > 2000).	(salary(2000))	name, salary,age)
- 4000)	*R5:Manager(X1)	*C2:manager:	:2000<salary<3000)
	<-emp(X1,Y1,Z1),	C(name,	Rel2:
	(salary < 3000)	(salary(3000))	manager:
		C3:staff:C(name,(	Reljob(name,
		salary(500))	dept)

Summation:

Q:(?*Manager* <– *emp* (*X*,*Y*, *Z*), *salary* (2000 < *salary* < 3000) =

$\forall$ *Manager* : $\exists$ *Manager* (*X*) <– *emp* ((*X*, *Y*, *Z*), (2000 < *salary* < 3000))

$\vee$ (*C*: *Manager* (*name*, (2000 < *salary* < 3000))

$\vee$ (Rel : *emp* ((*X*, *Y*, *Z*) $\wedge$ *emp* (*name*, *age*, *salary*)

$\wedge$ *job* (*name*, *dept*))

Hence, the resolution to the query is: " there exist managers whose name is name($\sum$ X) of age($\sum$ Y) in the dept($\sum$ Z) with the salary range from 2000 to 3000 pounds.

where

name($\sum$ X) = names of managers who satisfy the query.

age($\sum$ Y) = age of managers who satisfy the query.

dept($\sum$ Z) = department of the managers who satisfy the query.

Note: The KCM can also be used in designing a database system, in this particular case, the rule predicates are not included in the construction stages. i.e. the SSBG tuples is now ß(Query, Conditions, Relations).

5.6 Transient laser-material interactive model

A three dimensional transient analysis [11] is used to model a laser, with a TEM00 (Gaussian mode) power distribution, interacting with the surface of an opaque material (see Figure 5.11). Some incident radiation is reflected while the rest is absorbed. A molten pool of material is then formed as a result of the interaction, causing a surface tension gradient. This gradient coupled with the rate of evaporation causes a kerf to propagate through the material.

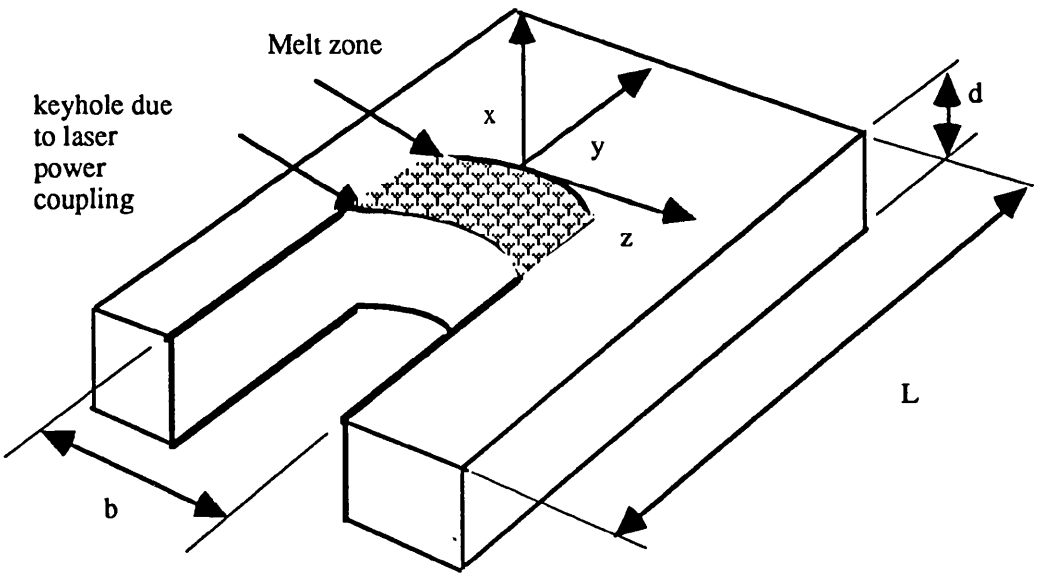

Fig 5.11 Physical diagram for laser material interaction

Assumption

1. *All properties of the liquid metal and solid metal are constant, i.e., they are independent of surface temperature.*

2. *Linear flow of melt.*

3. *The material is homogenous and isotopic.*

Mathematical formulation

$$\rho C \frac{\partial T}{\partial t} = k \nabla^2 T + f\{x, y, z, t\} \qquad (5.1)$$

where f{x,y,z,t} is the laser energy input source.

Rewriting equation (5.1)

$$\rho C \frac{\partial T}{\partial t} = \frac{\partial}{\partial x}\left(k \frac{\partial T}{\partial x} \right) + \frac{\partial}{\partial y}\left(k \frac{\partial T}{\partial y} \right) + \frac{\partial}{\partial z}\left(k \frac{\partial T}{\partial z} \right) + f\{x, y, z, t\} \qquad (5.2)$$

Solving equation (5.2),
considering the boundary conditions at the upper and lower workpiece surface;

(a) Surface, x= 0;

$$-k \frac{\partial T}{\partial y}\Big\|_{x=0} = F(t) - h_{overall}(Tx - Tamb) \qquad (5.3)$$

Where

F(t) denotes the beam intensity.

(b) At x = thickness of material;

$$-k\left.\frac{\partial T}{\partial y}\right|_{x=d} = h_{overall}(Tx - Tamb) \tag{5.4}$$

Assuming a Gaussian beam and ignoring convective and radiation losses.

we have

$$\rho C\frac{\partial T}{\partial t} = \frac{\partial}{\partial x}\left(k\frac{\partial T}{\partial x}\right) + \frac{\partial}{\partial y}\left(k\frac{\partial T}{\partial y}\right) + \frac{\partial}{\partial z}\left(k\frac{\partial T}{\partial z}\right) + f(P,v) \tag{5.5}$$

where

f(P,v) is the transform function of f{x,y,t}.and

$$f(P, v) = \left[1 - R_f\right]\frac{Power}{\pi w^2}\exp\left\{\frac{(Vt - r)^2}{r^2}\right\}\exp\{-\delta x\}$$

For the construction of a bond graph model, a schematic diagram is first drawn to enable a better understanding of the process. Particularly for a linear system (see Figure 5.12), a signal flow diagram is commonly drawn. A bond graph is then drawn (see Figure 5.13).

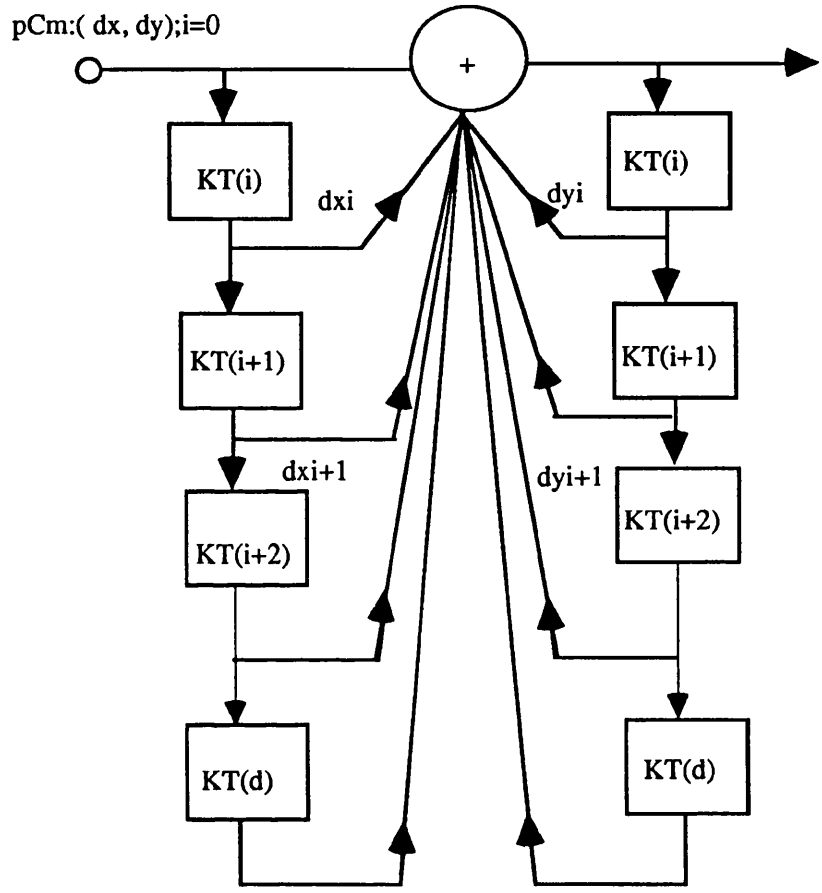

Fig 5.12 Schematic diagram of heat transfer

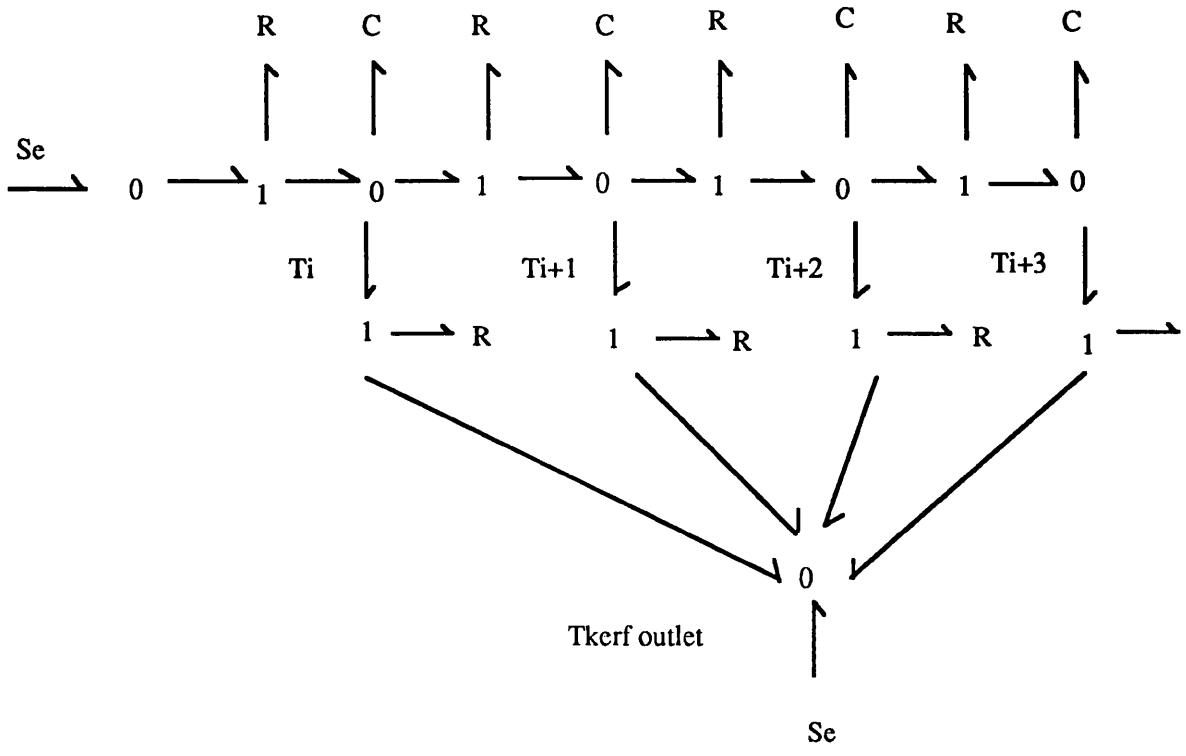

Fig 5.13 Bond graph representation

Simplifying the bond graph into bond argumentation and taking the kerf temperature, T_{kerf} at equivalent to ambient temperature (Figure 5.14).

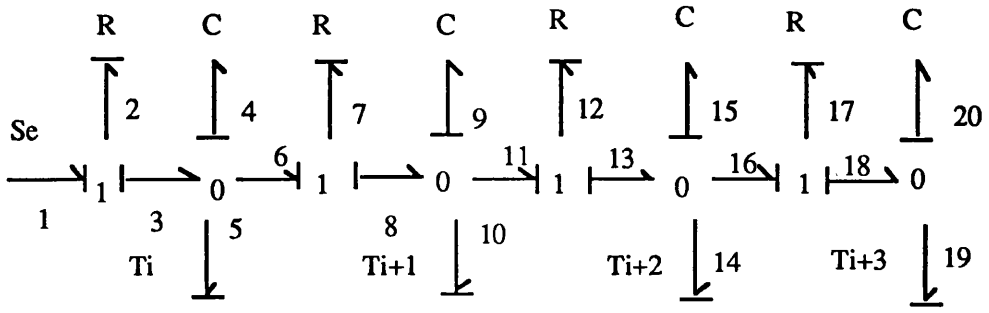

Fig 5.14 Causal bond representation of heat transfer

To analyse any depth of cut, we can consider the energy balance at any one of the bond graph nodes

$Q_9 = f_8 - f_{10} - f_{11}$

$= e8/R8 - e9/R10 - e12/e12.$

The thermal capacity C is given by:

$C_m = mc$; and

the resistance to the flow is

$R = t_z/kA$

relating the bond graph derivation to equation (5.1);

$$\rho C \frac{\partial T}{\partial t} = \frac{\partial}{\partial x}\left(k \frac{\partial T}{\partial x} \right) + \frac{\partial}{\partial y}\left(k \frac{\partial T}{\partial y} \right) + \frac{\partial}{\partial z}\left(k \frac{\partial T}{\partial z} \right) + f(P, V, t)$$

$$\rho C \frac{\partial T}{\partial t} - f(P, V, t) = k\left\{ \frac{\partial}{\partial x}\left(\frac{\partial T}{\partial x} \right) + \frac{\partial}{\partial y}\left(\frac{\partial T}{\partial y} \right) + \frac{\partial}{\partial z}\left(\frac{\partial T}{\partial z} \right) \right\}$$

$$k = \frac{\rho C \frac{\partial T}{\partial t} - f(P, V, t)}{\left\{ \frac{\partial}{\partial x}\left(\frac{\partial T}{\partial x} \right) + \frac{\partial}{\partial y}\left(\frac{\partial T}{\partial y} \right) + \frac{\partial}{\partial z}\left(\frac{\partial T}{\partial z} \right) \right\}} \qquad (5.6)$$

Relating equation (5.6) to the bond graph resistance;

$$R = \frac{L}{A \dfrac{\rho C \frac{\partial T}{\partial t} - f(P, V, t)}{\left\{ \frac{\partial}{\partial x}\left(\frac{\partial T}{\partial x} \right) + \frac{\partial}{\partial y}\left(\frac{\partial T}{\partial y} \right) + \frac{\partial}{\partial z}\left(\frac{\partial T}{\partial z} \right) \right\}}}$$

$$R = \frac{L\left\{ \frac{\partial}{\partial x}\left(\frac{\partial T}{\partial x} \right) + \frac{\partial}{\partial y}\left(\frac{\partial T}{\partial y} \right) + \frac{\partial}{\partial z}\left(\frac{\partial T}{\partial z} \right) \right\}}{A\left[\rho C \frac{\partial T}{\partial t} - f(P, V, t) \right]} \qquad (5.7)$$

In this relationship between power, velocity of cut and the bond graph resistance R, R can be used in the bond graph analogy to determine a suitable value of incident power and cut velocity. Possible methods for solving the equations (5.6, 5.7) [12] are by:

(a) Linearizing the equation as discrete quasi-steady variables

(b) Numerical finite differential analysis

(c) Empirically

For simplicity, only the top level of the bond graph analogy is considered, .i.e., port 1,2, 3.

For this work, in designing an intelligent laser manufacturing workcell, the last choice is selected. This selection is based on the fact that the laser material interaction is to be implemented in real time, hence, heuristic and stochastic approximations would enable a more accurate and reliable negative feedback control.

5.7 System functional characteristics

The KCM unification approach is implemented in the design of a second order PID-KBMS for the control of a laser manufacturing system. The system provides adaptive control through genetic and functional approximations as well as an analytical evaluation of the cutting process. Knowledge of the material properties, laser processing parameters as well as inventory information of the material is logged into the system sub-databases. At a regular interval, the system samples a temperature sensor using an A/D converter. The A/D bit value is then converted to temperature units. The value is then compared with the desired set point selected *a priori* by the expert system. If it is within acceptable limits, nothing is done. If the temperature is too high or too low, the system rectifies the process by functionally predicting

a new set of processing parameters to adapt the process environment back into the desired trajectory for a good cut.

Formal representation of SSGB.

* A set "E" of environments in which a complex process must operate.

* A set "C" of selected control inputs providing the initial and adaptive strategy for modifying the behaviour of the process.

* A set "R" of rules providing the inference for the system prediction and operation.

* a set "S" of solution trajectories satisfying the query and process control.(i.e. S: $S_{traj}(\exists(CxR)\text{->}(Q \wedge FVT^1(E=0))$

* a set "Q" of user input queries.

* a set "Cond" of condition constraints providing the antecedents of the inference engine.

* a set "DBrel" of the laser process parameter and material specifications relations.

**

FVT^1 denotes Final Value Theorem.

SSBG structural flow (see Figure 5.15)

Query: Material -

(a) What are the purchase and cost details?

(b) What are its laser process parameters?

(c) What is the material temperature at thickness t_z?

Formal query:

Q: ∃ material(thickness=x,area=A) ∧ Cond(cut(c), power(P:peak power (pk), pulse length(pl), pulse frequency(pf), feedrate(Fr), Temperature(T)) ∧ material(manufacturer information(mi), unit cost(uc), thickness(t_z), area(A)) ∧ T(material, T).

at Rules node,

R1: ∃material:(C->Ro)∧ P(pk,pl,pf).

R2: ∃material:(C->Ro)∧ T.

R3: ∃material:(C->Ro)∧ Fr.

R4: ∃material:(C->Ro)∧ material(mi,uc).

where Ro denotes the resolution of the rule to the qurey.

at Condition node,

Cond1: ∃ R(∃ material->∀(area⊗thicknessxP(pk,pl,pf))).

Cond2: ∃ R(∃ material->∀((area⊗thicknessxT)).

Cond3: ∃ R(∃ material->∀((area⊗thicknessxFr)).

Cond4: ∃ R(∃ material->∀((area⊗thicknessxucxmi)).

at Database relation node,

$\Phi db1$: $\forall$(P(material, area, thickness, pk,pl,pf).

$\Phi db2$: $\forall$(manufacturer(material, address, contact number, area, thickness).

$\Phi db3$: $\forall$(T(material, area, thickness).

$\Phi db4$: $\forall$(Fr(material, area, thickness).

$\Phi db5$: $\forall$(material(conductivity, specific heat capacity, latent heat of fusion, specific density).

Rules and conditions are decomposed into validated and invalidated first order logic sets (FOL) and mapped to the relational databases. Invalidated FOL sets are used to provide the system explanation facilities whilst validated FOL provides the system operations.

at the Summation node (input to process).

S: Straj: $\exists$ E: $S_{control}$->(material(manufacturer information, pk, pl, pf, T, Fr)$\otimes$A$\otimes t_z$) C->FVT(0).$\wedge$ Straj: $S_{analytical}$->(Td,A,t_z).

The two S trajectory sets are evaluated individually, the adaptive set Scontrol carries out the process control whilst Sanalytical pipelines into the node of the bond graph model in which the material thickness is at t_z. In respect of the derived relation between the bond graph resistance and capacitance, the theoretical temperature of cut at depth t_z can be evaluated.

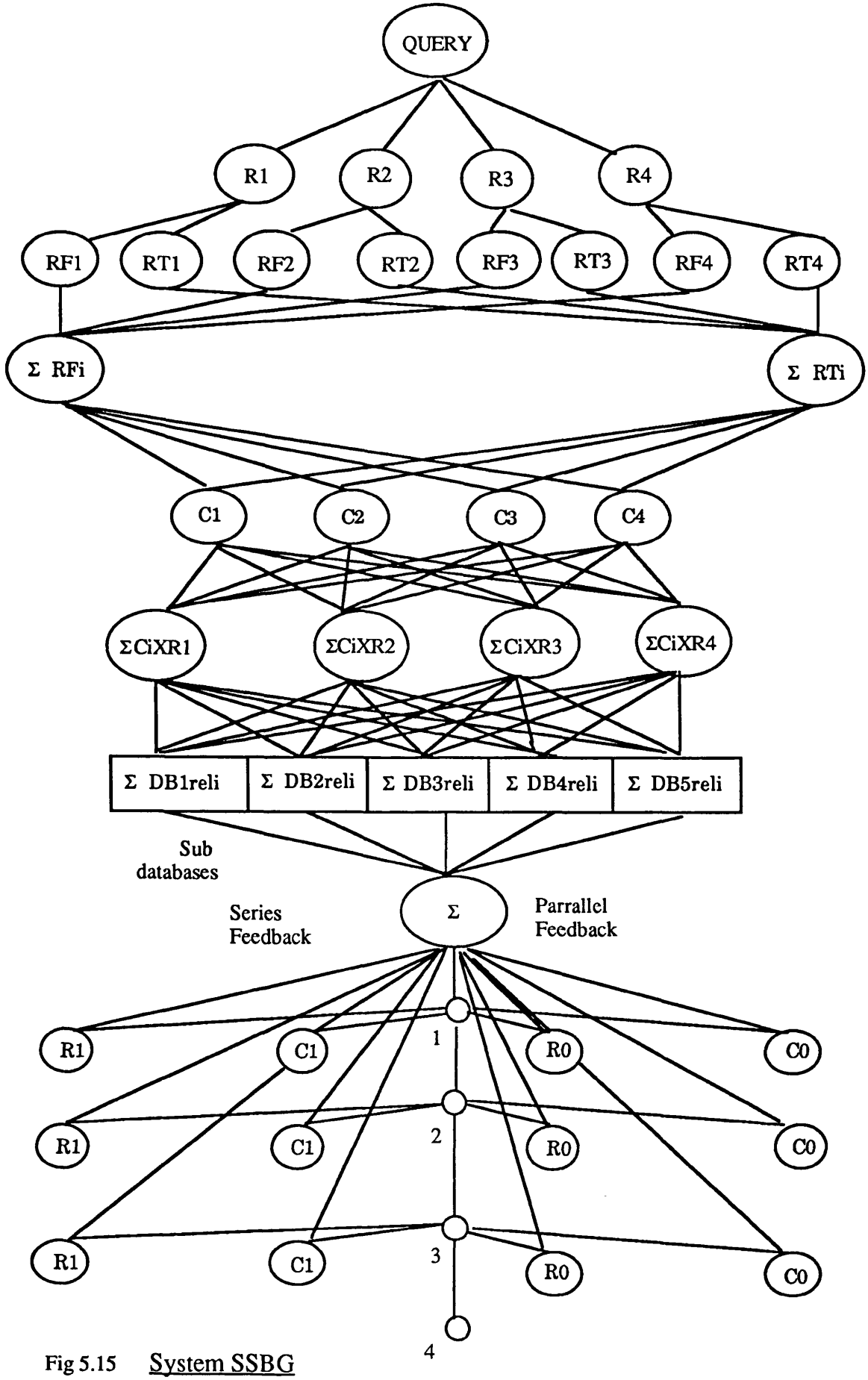

Fig 5.15 System SSBG

5.8 Conclusion

A knowledge control modelling technique has been presented which achieves data fusion for systems by bonding using the bond graph unified theory. Stages of implementation are reviewed and a bond graph model for a laser material interaction is derived. The topologies are then used to implement an autonomous laser manufacturing system. The actual physical implementation is currently under development by the Laser and optical Systems Engineering Group (LOSEG) at the University of Glasgow. Pre-trial testing of the system with a simulated laser cutting process reflects the high sensitivity of the designed system. The final design structure allows easy data traceability as well as system understanding.

REFERENCES

[1] Gian Piero Zarri, "A proposal for integrating artificial intelligent and database techniques", Database and Expert System Application, Proceedings of the International conference in Vienna, Austria, pp 307 - 314(1990).

[2] Lim See Yew and C.R. Chatwin, "A Second Order PID Knowledge Based Management Systems for process control, ICARCV'92, Proceedings of the Second International Conference on Automation, Robotics and Computer Vision, Singapore, pp CO.7.4.1- CO.7.4.5(1992).

[3] J. Franklin, "Bond graph in control: Physical state variable and observers", Inst 308, No. 3, pp 219 - 234(1979).

[4] Karnopp, D.C and Rosenberg, "System dynamic, a unified approach", John Wiley, N.Y(1974).

[5] I.L. Onsager, "Reciprocal relations in irreversible process", Physical Review, Vol 37, pp 405 - 426(1931).

[6] Lim See Yew and C.R. Chatwin, "Knowledge Control modelling (KCM): The bond graph unification approach to design", to be published.

[7] F.L. Bauer, "AI and software engineering", Proc 2nd Int. Conf on software engineering, Oct(1976).

[8] A. Albano, "Type hierarchies and semantic data model", Proc ACM, SIGPLAN Symposium on programming languages Issuses in software systems, ACM SIGPLAN, Vol 18, No. 6, pp 178 - 186(1983).

[9] J.A. Robinson, "A Machine-Oriented logic based on the resolution principle", Journal of the ACM, VIZ, NZ, pp 23 - 41(1965).

[10] Yeol Song, Hyoung-Joo Kim, Petra Geutner, "Intensional query processing:A three step approach", Proceedings of the International Conference in Vienna, Austria, pp 541 - 549 (1990).

[11] D.Chan and J.Mazumder, "Application of lasers in material processing", ASM, pp 150(1983).

[12] H.S. Carslaw and J.C. Jaeger, Conduction of heats in solids, Second Edition, London, Oxford University press(1959).

6 PROCESS AUTONOMOUS IDENTIFICATION AND CONTROL

6.1 Introduction

Laser machining provides a useful production method for difficult to machine materials and special applications such as micromachining. Hence, even with the high capital and operating cost for laser machining systems, high dimensional accuracy, good surface finish quality and a high degree of repeatability make these systems economically attractive. For laser material processing applications, operating parameters for the optimum machining rate and quality are found through *ad hoc* 'trial and error' procedures, involving time - consuming calibration experiments to determine laser/material behaviour. Although several heat transfer models exist that predict the laser/material interaction characteristics [1][2], they are not

sufficiently accurate for final process tuning; furthermore, they are only accurate for a limited range of duty cycles. Optimum prediction of laser/material processing operating parameters, which is important to minimise production costs, is an active area of research [3][4]. Since laser/material processing is a non-linear process, an alternative solution to parameter prediction and control is in the utilisation of the science of artificial intelligence [5][6]. This research concentrates on the laser/material interaction process using a Ferranti MFK 1.2 kW CO_2 laser. A second order PID Knowledge based management system [7] has been built to predict the operating parameters required for a specific material via parametric adaptation. As most ferrous materials, when cut by a laser, produce a well defined conical shower of sparks consisting of superheated material, it is possible to characterise the exit spark cone utilising image processing.

6.2 Nomenclature

A_c = Effective area of the plate (m^2)

$\hbar$ = Regression step size

I_{real} = Real image array

I_{ref} = Reference image array

μ = Arithmetric mean

MC = Effective heat capacity of the plate (kJ/kgK)

N = Total number of samples

q = Energy at the plate (W/m^2K)

σ^2 = Variance

T_a = Ambient temperature (K)

T_p = Plate temperature (K)

U_L = Overall heat loss coefficient (W/m^2K)

6.3 Proportional-Integral-Differential (PID) knowledge based management system

In conventional control systems, the parameters are measured against and directed towards a pre-defined local control set-point. The stability of the systems are maintained by a local hardware controller which produces a corrective gain This gain, which is used to maintain the set-point, originates from a differential signal based on the difference between the desired and actual output, i.e. the error deviation. Utilising this error signal, the independently controllable variables are then modified. Furthermore, as most of the actual control parameters are in dynamic states, hardware controllers must also condition the signal for noise.

Conventional low level controllers are relatively difficult to utilise as fully stable control instrumentation due to their inflexibility. A possible solution is to provide a high level KBMS controller (see Figure 6.1) that delivers the required set-point-signal to maintain stable process control [8]. The proposed design of a PID-KBMS allows self-tuning, self-induced learning and inference with two intelligent engines based on deduction semantics from first order logic (FOL) [9] and knowledge manipulation from first principles [10].

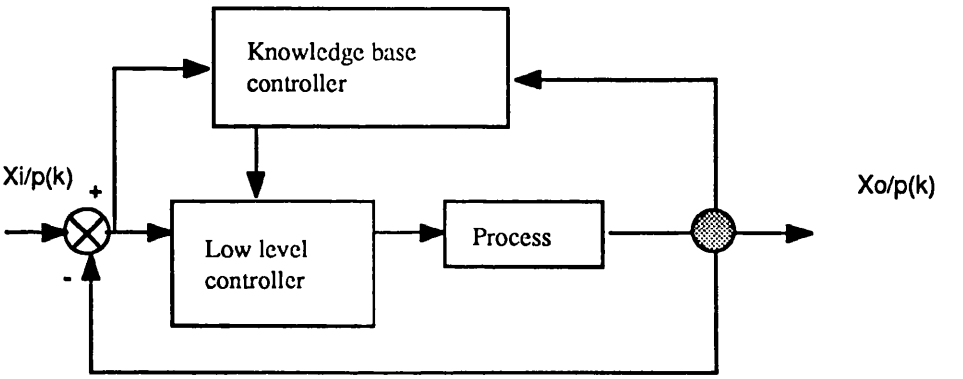

Fig 6.1 Conventional parameter-adaptive intelligent control system

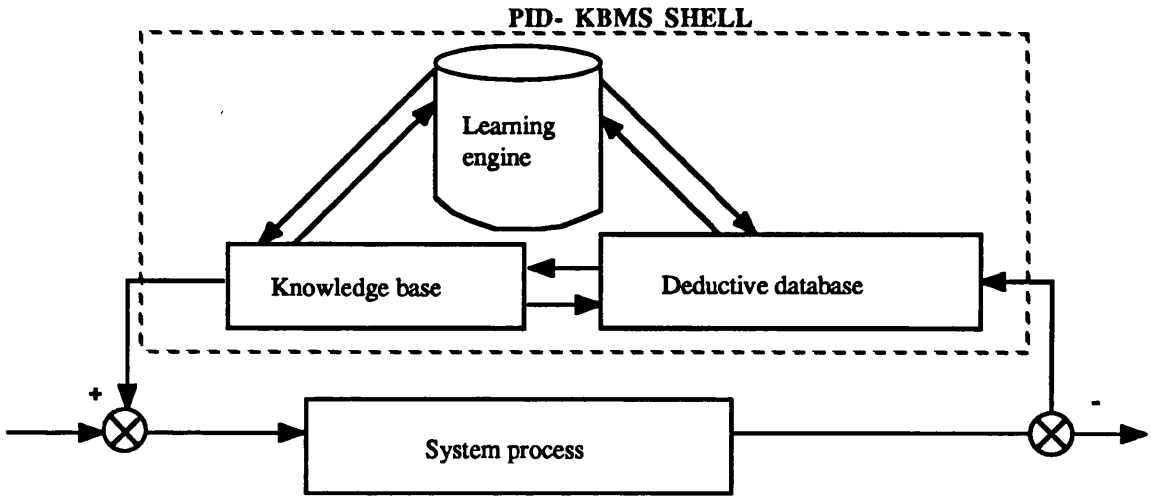

Fig 6.2 Proposed PID-KBMS high level intelligent control system

In a real time system, various design approaches and tools (bode diagrams, phase plane methods, linearisation techniques, etc) are used in order to find a suitable compromise in adjusting the parameters of the low level process controller. This leads to rigidity in the design and selection of a controller. In the design proposed, the proportional control is provided by an inductive fuzzy approximation based on a Gaussian probability distribution which resides in the deductive database. This selects the set-point whilst the integrating function originates from the part of the system's knowledge base which is structured in logic algebra (see Figure 6.2). The deductive database, which is based on First Order Logic (FOL) [11] , forms the differential function module of the PID-KBMS.

6.4 Characteristics of proportional control algorithm

In process control, it is important to find the functional relationships between the process dependent variables and the process independent control parameters. Commonly, the true type of functional relationships are unknown; however, it is often convenient to fit a polynomial to the data, this is of the form:

$$y_c = a0 + a1x_c + a2x_c^2 + \ldots \qquad (6.1)$$

Where c is the number of observations, it is possible to fit a polynomial up to (c - 1) degrees of freedom.

Now, the analytical approach of the proportional engine learns in two stages. One by linear approximation and the other via probability logic.

The approach for the approximation is based on the fact that all the system's dependent and independent variables have functional relations with respect to each other. Regardless of the functional complexity of adjacent points on the process output signal, it is acceptable to assume a straight line approximation. If the points are in very close proximity to each other, the accuracy of prediction is high. The principle of approximation is based partly on heuristic-iterative extrapolation and interpolation. The Lagrange three point approximation is used because the use of more points often results in divergence from the real process trajectory [12]. This numerical method is based on the fact that any three adjacent points can be

approximated by a quadratic curve. The accuracy criteria used to control the iteration process is embedded in the knowledge base

The basic mathematical model is defined by assuming $f(x)$ is a continuous function in the interval of $x0 \leq x \leq x2$ and $f(x0) = y0$, $f(x1) = y1$ and $f(x2) = y2$ with $x0 \leq x1 \leq x2$. Then the approximated value of $f(x)$ for $x0 \leq x \leq x2$ is given by :

$$f(x) \cong -\frac{(x - x1)(x - x2)}{(x0 - x1)(x0 - x2)} y0 + \frac{(x - x0)(x - x2)}{(x1 - x0)(x1 - x2)} y1 \qquad (6.2)$$

$$+ \frac{(x - x0)(x - x1)}{(x2 - x0)(x2 - x1)} y2$$

This method has the advantages of not requiring the three points $x0, x1, x2$ to be equally spaced and allows both interpolation and extrapolation. It is inadvisable to use Lagrange numerical approximation for more than three points since this can lead to a large error. This comes about because this method fits a higher order polynomial to the points in question which force the interpolation curve into large oscillations about the selected points.

In this approach, by using randomised block sampling, by the law of averages, it is possible to obtain accurate control variable data that will control the steady state response. During the process, the PID-KBMS selects the appropriate control variables based on polynomial approximations of the available experimental data. In the event that the selected control variables are so inaccurate that the system diverges from the required steady state process, the proportional engine will prompt the knowledge base to initiate corrective rules

which reselect the initial values of the control variables. The self-tuning alogrithm continues until the controlled process reaches a steady state. The data generated is stored in the main database and kept for future inference for further process control of the specific system. As the gain control is continuous, the controlling PID-KBMS learns continuously. The PID-KBMS is hence a self-learning and self-tuning system which does not require process modeling as a design pre-requisite of the system control.

The proportional engine (see Figure 6.3) utilises offline fuzzy logic, this serves mainly as a user interface and a prediction mechanism for the PID-KBMS. The data collected from the process is assumed to be a standardised uniform probability distribution (historically known as a Gaussian distribution). By mathematically modelling the probability distribution, a first approximation of the desired dependent variable set-point and it's related controllable independent variables can be obtained prior to actually running the process. The reason that this distribution is not incorporated in the real-time selection of the process variables is that it requires excessive computational time which is not available when engaged in real time control.

The set-point and initial value selection assumes a probability distribution $P(x)$ for the interval $-\infty \leq x \leq \infty$, where $P(x) \geq 0$ and has a mean value (μ) given by:

$$\mu = \int_{-\infty}^{\infty} x P(x) \partial x \tag{6.3}$$

Variance :

$$\sigma^2 = \int_{-\infty}^{\infty} \|x - \mu\|^2 P(x) dx \tag{6.4}$$

Hence by satisfying a standardised probability distribution which results from the PID-KBMS engine learning from collected data, we can assume the probability distribution is described by:

$$P(x) = \frac{1}{\sqrt{2\pi\sigma^2}} \exp\left(-\frac{(x-\mu)^2}{2\sigma^2}\right) \tag{6.5}$$

for $-\infty \leq x \leq \infty$

By ascribing the probability of occurrence of both the set-point and initial values of control variables into the system, an accuracy assessment tool is provided.

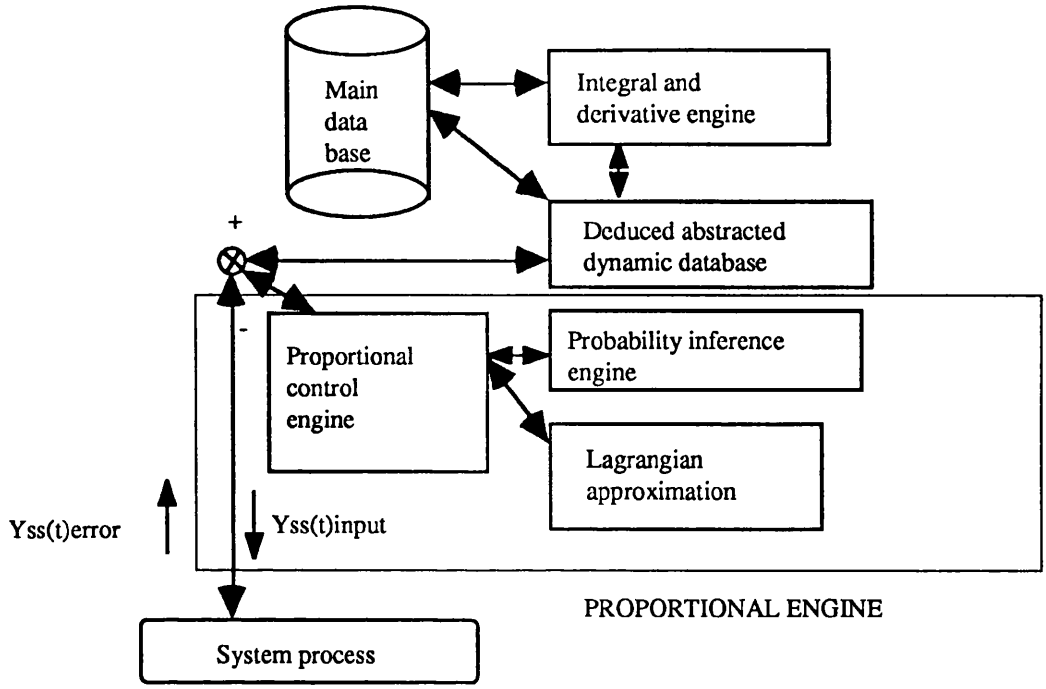

Note : Yss(t) is the response variable.

Fig 6.3 Architecture of the proportional engine

In this system, learning is of a heuristic nature and is based on both deduction and induction which are the two main artificial intelligence techniques for self-learning.

6.5 Characteristics of the integral engine (KNOWLEDGE BASE)

The knowledge base (see Figure 6.4) relies for its intelligence on the representation provided by two sets of production rules. One set are the prediction rules that select the criteria for the proportional engine, whilst the other set are the alarm rules which monitor the actual control variables and set-point and hence the initialisation of the PID-KBMS.

The "object-attribute-value" (OAV) tuples are defined individually as the process variables (i.e. dependent and independent), their value is specified as is their relationship with other tuples. The rules are embedded in the working memory (WM) and hence allow a high level of modularisation in the PID-KBMS.

Since the proposed PID-KBMS is a real-time system controller, the structure of the rules is based on forward chaining which is known as a data driven approach. Assuming that there are N data points for each function F_i where i=0,1,2,...,N, the prediction rule specifies the first approximation of the set-point ($y_{ss}(t)_d$) and the initial values of the independent control variables for the proportional engine. In the event that the first approximation is unable to maintain process stability, alarm rules automatically change the PID parameters in real time to maintain stability.

The first order logic (FOL) syntax for the rules is as follows:

/* Fired initialised rules for deductive database */

$$1. \ldots\ldots IF\left(\neg\, y_{ss}(t)_d \wedge \neg \sum_{i=0}^{i=N} F_i\right) THEN$$

$$\ldots\ldots\left\{\cdot\ get\ \cdot \forall\,(y_{ss}(t)_d) \sum_{i=0}^{i=N} F_i\right\}$$

$$\ldots\ldots \forall\,(y_{ss}(t)_d) \sum_{i=0}^{i=N} F_i \cup \exists\,(y_{ss}(t)_d)\left\{\sum_{i=i-1} F_i \cup \sum_{i=i+0.5} F_i \cup \sum_{i=i+1} F_i\right\}$$

/* Do iterative approximation during process */

$$2.\ldots\ldots Do \cdot \int_{i=0}^{i=N} f(x) - Lagrange \cdot approximation .$$

/* Output stable response for real-time process */

$$3.\ldots\ldots\left(selected \sum_{i=0}^{i=N} F_i \rightarrow (y_{ss}(t)_d) \rightarrow stable \cdot system \right)$$

$$\ldots\ldots\left\{ Output \cdot \forall (y_{ss}(t)_d) \sum_{i=0}^{i=N} F_i \right\}$$

Since the system must operate in real time, it is important that the PID parameter selection is done within one sampling period. In view of this, the d-step constraint is introduced in order to represent the process data oscillation in the course of continuous data generation. The following are the alarm rules used in the design.

1. IF (search $\neg \sum_{i=0}^{i=N} F_i$ in deduced database) THEN iterate using Recursive Weighted Least Square Method (RWLS) for initial prediction in the proportional engine.

2. During process, if (Iteration for d-step of about 100 samples does not converge)THEN (use final value as new trial values but do not update in abstracted database) AND (redo iteration).

3. IF (process ended) THEN (update abstracted database AND tagged probability density).

The knowledge base WM is kept as small as possible as this makes more memory available for use by the graphical user interface (GUI). This displays the initial values of the control variables and set-points and provides an explanation of the initial choice. The number of rules for specification of the system depends largely on the number of process dependent and independent variables involved. If the number of independent and dependent control variables is A and B respectively, then there should be minimum array size of A⊗B rules.

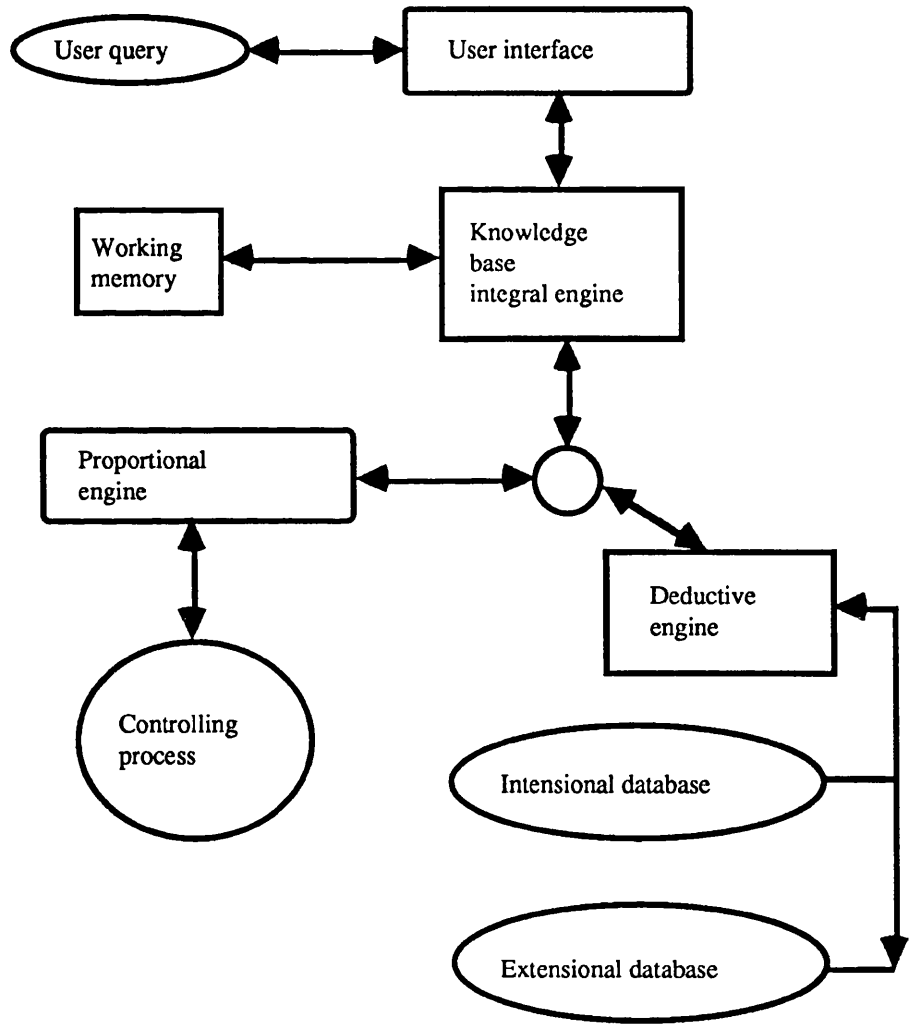

Fig 6.4 Architecture of the integral knowledge base

6.6 Characteristics of the differential deductive database

Since it's establishment in 1970, Database Management Systems (DBMS) have evolved from basic structures of heirarchies or networks to a relational model. DBMS and KBMS are mainly implementations of logic based models (FOL).

For high level menu driven programming of database operations, there is a high processing overhead [12]. The best way to reduce this problem is to access data in the main memory (large cache memories). This can be done via dynamic construction and destruction of data storage using an object oriented approach [13].

In this engine, there exists two types of database; firstly the extensional database (EDB) and secondly the rules or intensional database (IDB) which is composed of deduced relationships. By using the Proof theoretical approach [10], the subset of axioms which defines the EDB are basically positive ground atomic formulas made up of the data from both the collection of steady state variables (set-point and control parameters) and process specifications. The IDB are sets of virtual relations of FOL derived from the EDB predicates using non-grounded logical formulas. The reason for using the deductive database approach instead of incorporating the rules into the knowledge base is to increase the bandwidth and allow the PID controller to be broken down into modules.

The mechanism of deduction is activated by the IDB upon initialisation of the PID-KBMS. Upon specification of the expected output of the response, the IDB abstracts a randomised block of

process variables kept previously in the EDB. This abstracted and deduced database is then integrated by the knowledge base into the PID-KBMS controller system. As the process proceeds, the IDB updates the abstracted database so as to provide a continuous dynamic database. Upon completion of the process trial, the IDB then selects the data which has the highest probability of success, this is used to update the EDB. The FOL of the source code is validated by Robinson Inference Theory [10] (see Figure 6.5). The architecture of the deductive database can be seen in Figure 6.6.

**Proof:

Axioms are :

1. ... $Control\,(factor \cdot level \cdot database)$.

2. .... $Set\_pt\,(stable) \wedge Control\_select\,(stable, factor \cdot level \cdot database)$.

3. .... $\forall\, x\,(Set\_pt\,(x) \wedge \exists\, y\,(Control\_select\,(x, y) \wedge Control\,(y)$
$\rightarrow System\_stable\,(system, x)$.

(Where x represent the set-point and y the controlling parameter).

**(note: Here only 1 pair of relationships are proved, however the theorem can be extended to more than one set)

Applying Robinson Inference Theory on the predicate;

$\forall\, x\,(\neg\, Set\_pt\,(x) \vee \forall\, y\,(\neg\, Control\_select\,(x, y) \vee \neg\, Control\,(y)$
$\vee\, System\_stable\,(system, stable)$

Redefining the predicate in clause form:

1. ... *Control (factor · level · database)*.

2.... *Set _ pt (stable)*.

3.... *Control _ select (stable , factor · level · database)*.

4.... *Set _ pt (x) ∨¬ Control _ select (x , y) ∨ ¬ Control (y)*
..... *∨ System_ stable (system, stable)*.

5.... *¬ System_ stable (system, stable)*.

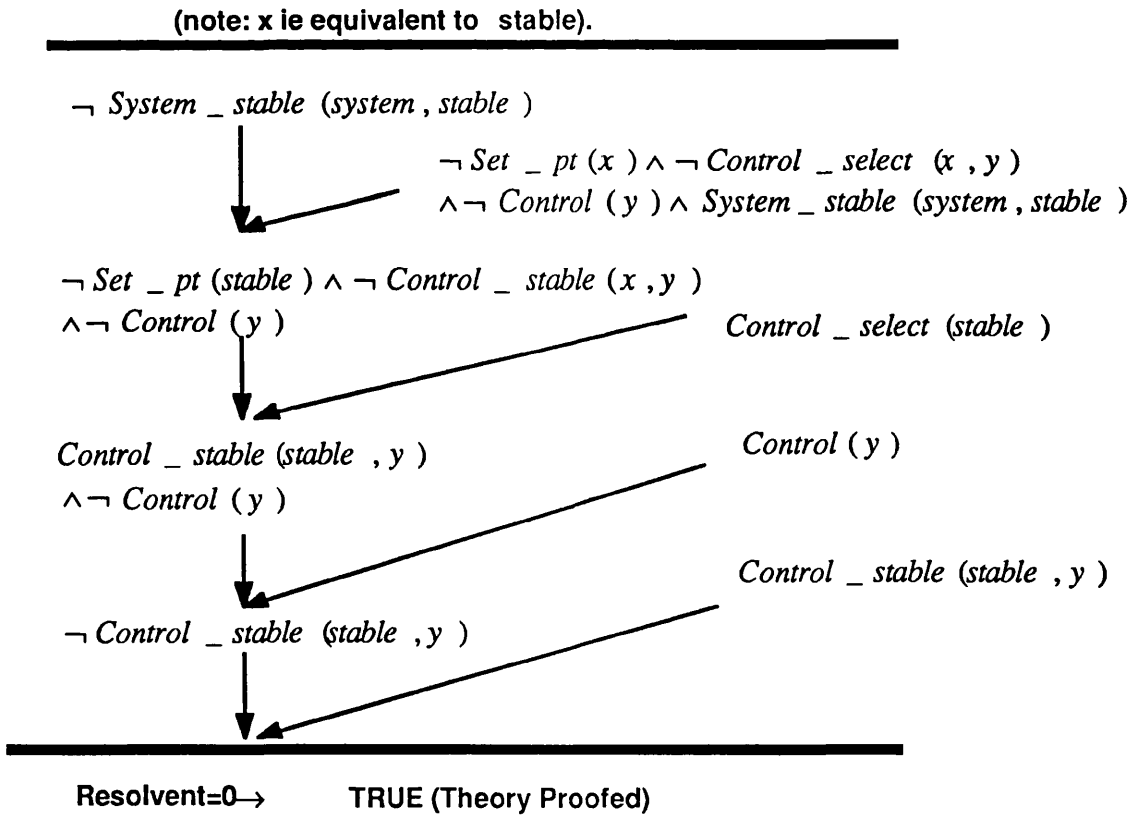

Fig 6.5 Resolution tree for deductive database

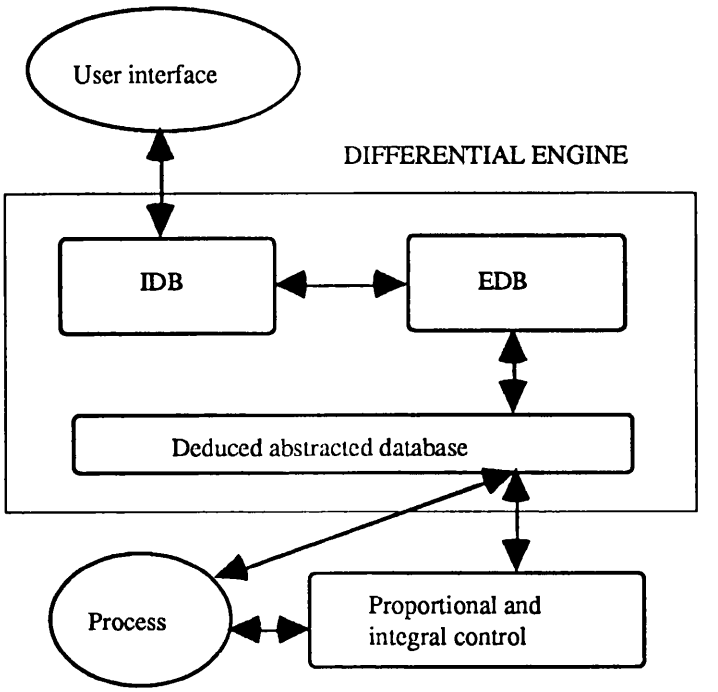

Fig 6.6 Architecture of the Deductive Database

6.7 Simulation

To evaluate the performance of the proposed KBMS implemented by the PID approach, a simulation of a laser cutting process has been developed in a C environment. This simulation however does not reside in the PID-KBMS and is used only as a validation tool for the proposed control system.

Hence, the respective engines were statistically tested against a model(equation 6.6) of the heat transfer process. The measurands are the laser power and temperature of a simulated laser cutting process, the controlling parameter being the surface temperature of the metal being processed.

Heat Energy =

$$(MC)_p \frac{dT_p}{dt} = A_c[q - U_L(T_p - T_a)] \tag{6.6}$$

Integrating equation (6.6),

$$\exp\left(\frac{A_c}{MC}(t_2 - t_1)\right) = \frac{q_2 - U_L[T_p - T_a]_2}{q_1 - U_L[T_p - T_a]_1} \tag{6.7}$$

But as the change in time is very small, $T_a \equiv$ constant.

$$1 = \frac{q_2 - U_L \Delta T_2}{q_1 - U_L \Delta T_1} \tag{6.8}$$

Therefore,

$$\Delta q|_1^2 = U_L[\Delta T_1 - \Delta T_2] \tag{6.9}$$

Results from the simulation were then plotted together with the results from the process model as shown :

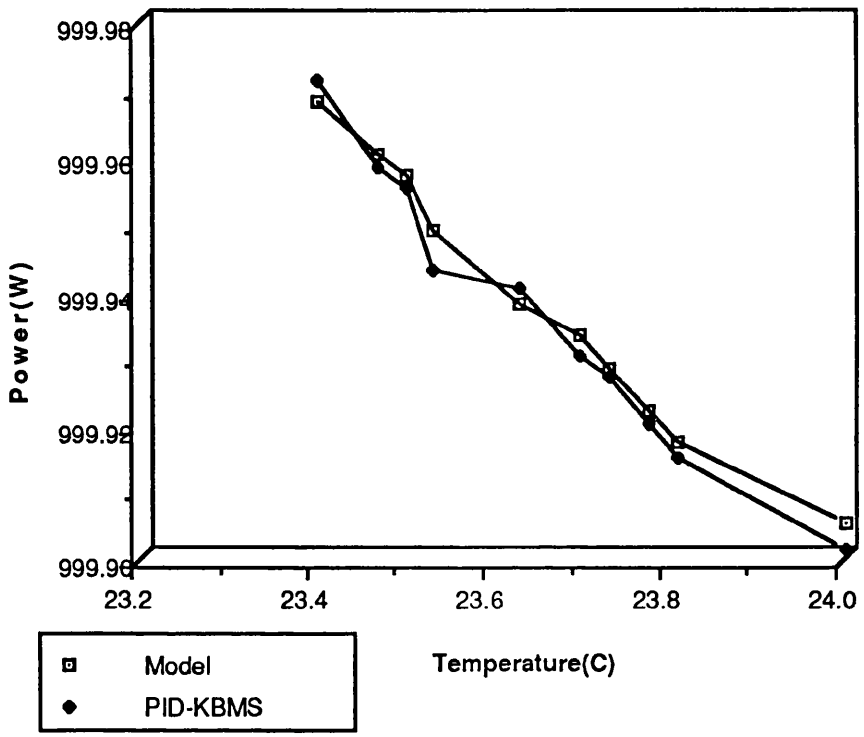

Fig 6.7 Model laser power /PID-KBMS laser power versus Temperature

From Figure 6.7, it can be observed that at the activation of the alarm calls, resulting from the deviation of the measurand from the control set-point, the PID-KBMS control algorithm alters the laser so as to minimize the difference. This was done by using the control error deviation, i.e. between the temperature set-point and the actual temperature being measured in process, as a correcting factor with which to adjust the laser power. For this simulation, the number of iterations necessary to obtain steady state control is never greater than ten. This further proves the high sensitivity of the KBMS.

6.8 Image acquisition system setup

The image acquisition setup is as shown in Figure 6.8. Although the material ejected from the underside of the workpiece is a highly transient dynamic phenomenon, it emits a relatively homogenous irradiance signature which has three distinct conical zones. The cone (Figure 6.9 and Figure C-2) characterises the physical relationship between the cut quality and the rate of material removal and hence is used as a parameter for the decision support system (PID-KBMS) when justifying a good cut. The set up consists of a CCD camera mounted on an aluminium holder attached to the laser head. The focus length is set at 500mm and the camera is focused on the surface of the material to be cut. The camera is mounted in a fixed position such that the laser cutting process is always in the field of view. From the histogram of the cone scene acquired during cutting 3mm mild steel, it can be observed that there exists three clusters of pixel grey levels showing the presence of three distinct cone regions (Figure 6.10).

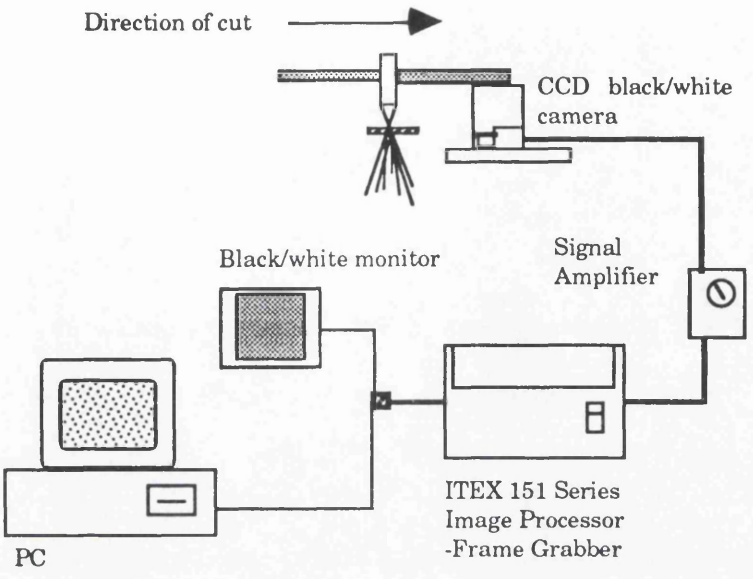

Fig 6.8 **Image Acquisition System Setup**

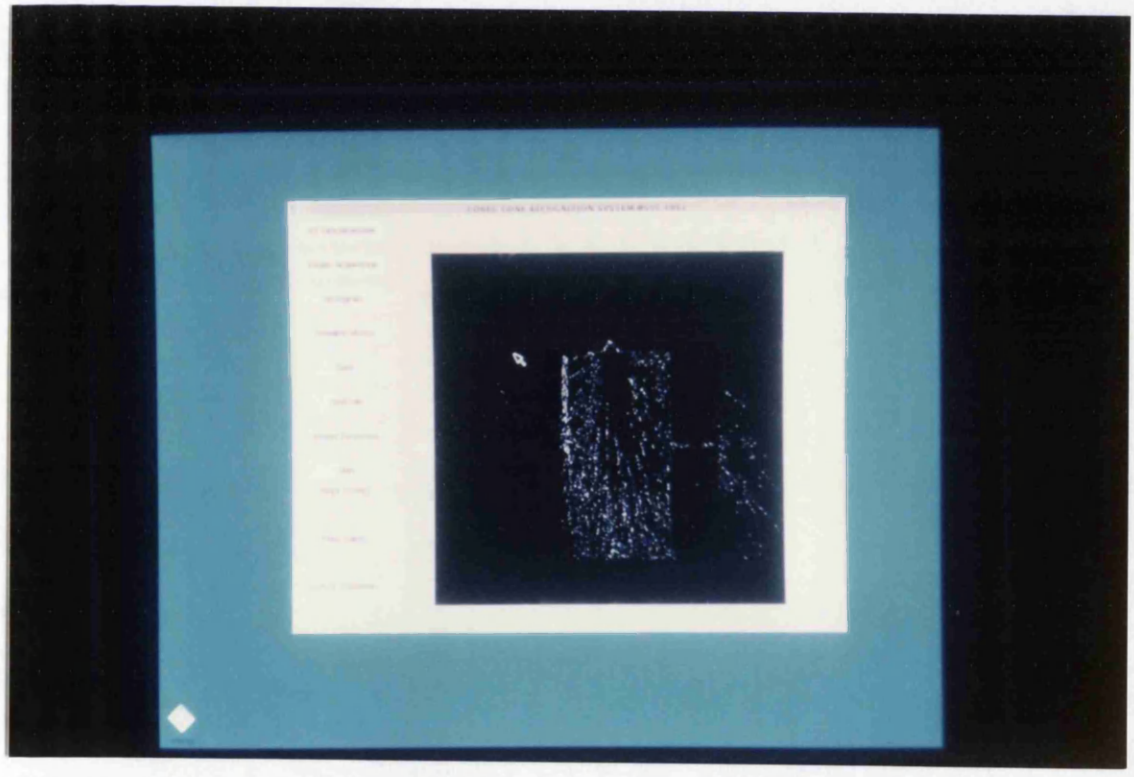

Fig 6.9 **Image of a spark cone**

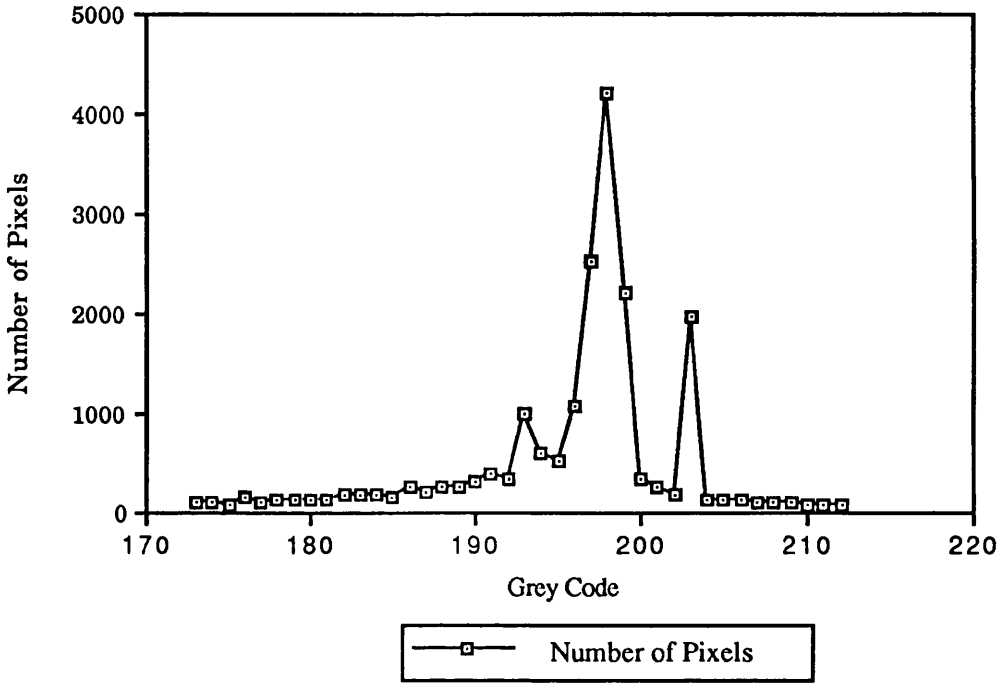

Fig 6.10 Histogram of the cone for 3mm thick mild steel

Note: Only the histogram of the cone area is plotted

6.8.1 Cone analysis

Several image processing techniques [14] were reviewed for use in the analysis of the cone. The Hough transform[15] and the angular section [16] technique were tested but were found to be too slow to be useful for the analysis of the laser interaction process. It was thus decided to produce an alternative algorithm for the image analysis. The image analysis task can be segmented into three parts, they are;

(i) Edge detection using a 'swinging pendulum' algorithm

(ii) Calculation of the cone angle

(iii) The template matching

6.8.2 Edge detection and calculation of the cone angle

As seen from the histogram plotted, there exists three distinct grey levels of significant intensity in the spatial distribution of the exit cone. Only the most intense pixel grey level value is used to characterise the exit cone. A pendulum algorithm was developed which takes into account the presence of the specified cone pixel and ignores the rest of the image. The method hence allows a fast computation of the cone angle. The 'pendulum' algorithm for the cone angle calculation is as follows; Let Nx and Ny denote the spatial length of the image. Let Pnxi, and Pnyj denote the pixel local location. For every grey level value, let F(G)-> F(G) $\exists$ $(\sum_{G=0}^{G=255} F(G)^{Nx,Ny})$:{ Pnx0, Pnx1, ..., PnxN Pny0, Pny1, ..., PnyN }^{T} denote the grey level cluster. Where G is the grey level code , i.e. ;

G->{0, 1, ... , 255}. Let A be a partial recursive function such that

Af: { Af(0,0): {x0,y0}:F(G) (nx,ny)

Af(n,n): {xn,yn}:F(G) (nx,ny)}.

Next, defining a constraint function;

$$F(G) = \{\ 1,\ Af(0,0) \parallel Af(n,n) :\ F(G)\{Pnx, Pny\}^{T} \qquad (6.10)$$
$$\{\ 0,\ Af(0,0) \parallel Af(n,n) :\ F(G)\{Pnx, Pny\}^{T}$$

The partial recursive function Af is tested in a 'swing' motion from a local origin of Nx/2, Ny/2. Upon detecting the first and last occurrence of a common pixel value, the function Af is indexed by 1 and the location of the pair of pixels is stored in an array. The recursion function is then stepped through the next layer of the image until the full image frame is processed. At each co-ordinate pair, the local gradient is calculated. When the gradient averages within a pre-set error limit, the angular orientation is calculated and set against the pixel location array. In order to decrease computation time, only the most intense cone half angle is calculated (i.e. the angle between the cone edge and the vertical, - see Figure 6.11 and Figure 6.12).

$$Af:\ F(G)\{\ P(Nx/2),\ P(Ny/2)\ \} \qquad (6.11)$$

$$Af{:}F(G)=1 \quad F(G)\{\ P0(x_{1i},y_{1j}),\ P0(x_{2i,2j})\ \} \qquad (6.12)$$
$$Af{:}F(G)=1 \quad F(G)\{\ Pn(x_{1i},y_{1j}),\ Pn(x_{2i,2j})\ \} \text{ else } F(G) = 0;$$

$$M:\quad F(G)=1 \rightarrow m\ \{\{\ \frac{\prod_{i=0}^{N} \Delta y}{\prod_{i=0}^{N} \Delta x}\ \}\ \exists\ error(\ \frac{\text{-------}}{M_{error}}\ )\} \qquad (6.13)$$

$$= \text{limit}_{F(G)=1}\ : TAN^{-1}(1/M) \qquad (6.14)$$

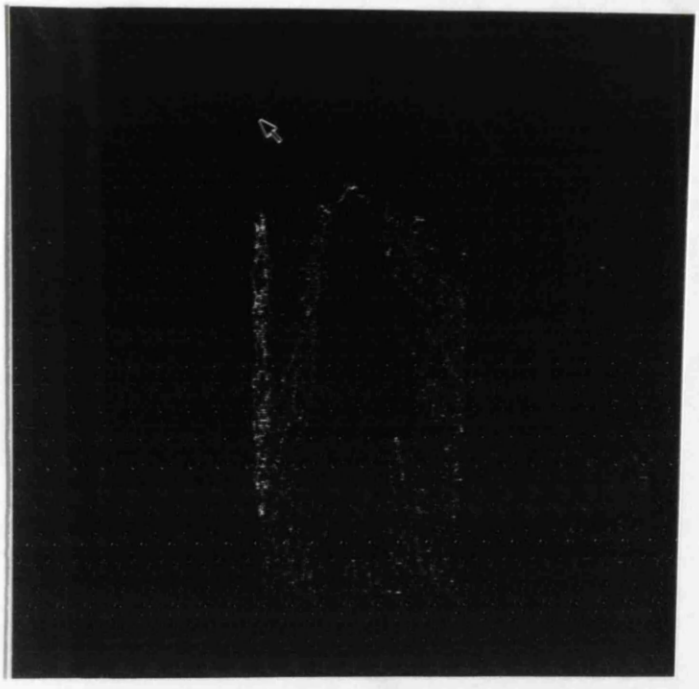

Fig 6.11 Exit Cone Image with cone half angle = 10.204 degrees

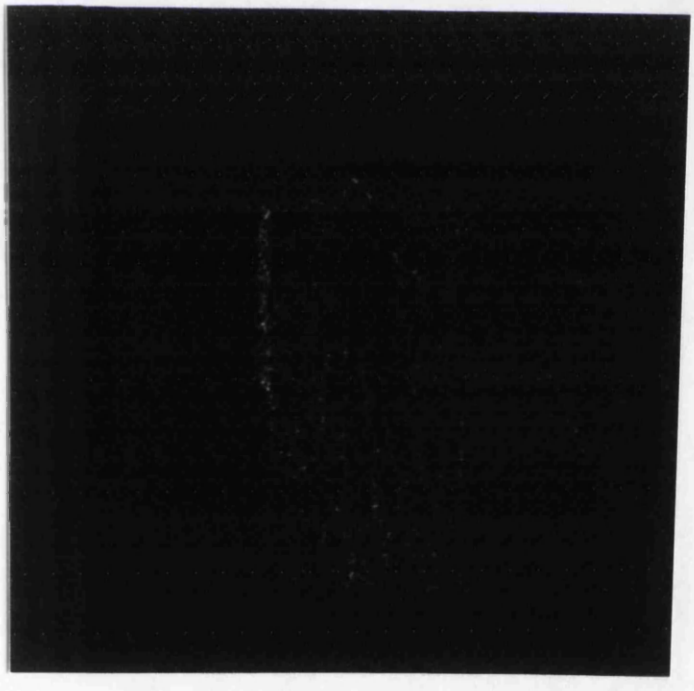

Fig 6.12 Exit Cone Image with cone half angle = 34.606 degrees

The cone analysis system developed acts as a support module for the PID-KBMS. The final hybrid system is to be used to train both the laser system and technicians in the real time judgement of cut quality. For every thickness of a specific material, there is an approximate ideal cone image; hence, for a range of thicknesses of the material as well as for a range of different materials, there is a need for a very large amount of data storage. This is of course not practical and hence a line representation of the cut cone is implemented for material cut classification. A two dimension representation is included in the system to provide a play back facility for the technician's cognition. The 'swinging pendulum' algorithm was used to produce the orientation and location array. The final array was then used to generate a spatial representation of the cone (Figure 6.13).

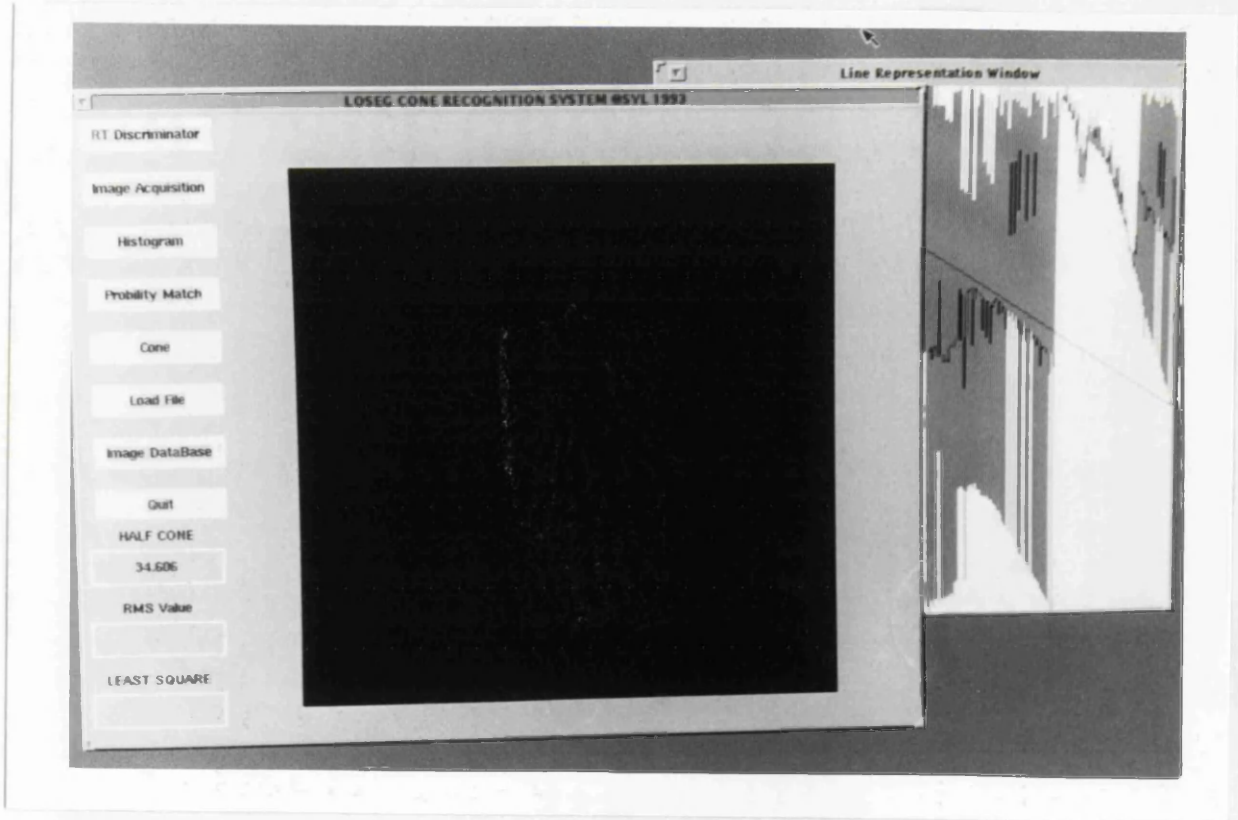

Fig 6.13 Line representation of the reference cone

Note: The black lines represent the rest of the pixel grey level.

6.8.3 Template matching

During the real-time processing of the material, the acquired image is compared with reference image data, to generate a cone error value. Two methods for the template matching procedure were considered. The correlation of the two images was initially carried out in the frequency domain but was found to be too computationally intensive. A least square algorithm was then used to calculate the deviation between the reference image and real time image. The calculated deviation provides a control signal for the cutting process via the PID-KBMS. The algorithm is as follows:

Let the real input image be Ireal and the reference image be Iref. The transform function that convolves the reference image with the real input image is Trf. Let N denote pixel location.

$$Ireal\ (i,j) = Trf(i,j)\ Iref(i,j) \qquad (6.15)$$

Let the regressor be R(i,j);

$$R(i,j) = [\ Iref(0,0),\ Iref(0,10,\ \ldots\ ,\ Tref(512,512)]^{T} \qquad (6.16)$$

Let the Transform function be T';

$$T' = [\ Trf(0,0),\ Trf(0,1),\ \ldots\ ,\ Trf(512,512)\ ]^{T} \qquad (6.17)$$

Rewriting equation (6.16);

$$Ireal = T'\ R(i,j) \qquad (6.18)$$

Let e_{LMS} be the least square error and $\hbar$ the step size for iteration. Writing in the least square parameteric equation;

$$T' = T'(i-1,j-1) + \hbar R(i,j)e_{LMS} \qquad (6.19)$$

$$e_{LMS} = \{1/\hbar R(i,j)\}(T' - T'(i-1,j-1)\ ) \qquad (5.20)$$

The LMS value hence serves as a quantifier for relating the cone to the quality of cut (Table 6.1).

Figures compared with Figure 6.11 (at the cone region only)	Mean Square Error	Root Mean Square Error
Figure 6.12	0.0044975	0.0676082

Table 6.1 LMS values of the images

6.8.4 System operations.

The PID-KBMS developed is structured on the architecture of knowledge based management system (see Figure 6.14). An expert

system is coupled into the PID-KBMS which provides the user with a consultation facility for identifying materials with particular machining properties. By providing a predictor mechanism and a deductive database, *a priori* approximation of the machining parameters can be obtained from past memories of true cut parameters. The user initiates the system after obtaining the approximate data values, these values are the process control variables that would enable a satisfactory material quality cut. An on-line system driver which operates both the laser pulser unit and the TNC 155AR (see Figure C-3) x-y table for the flying optics is incorporated into the PID-KBMS (see Figure C-4). The selected dependent and independent variables are automatically fed into the on-line system driver to set up the conditions for laser machining. Sensory input for control comes from the intensity probe attached onto the laser nozzle head (see Figure C-5). The intensity value of cut is then fedback to the PID KBMS for adaptive control of the cutting process (see Figure C-6). A CCD camera is attached to a frame that moves with a fixed focal length to the point of cut. Data acquisiton is done on the PC to provide the user with a rote training of the conditions of a good cut via the spark cone angle and spark distribution. In order to limit the PC working memory so that a good control response time is achieved, the interface for the cone acquisition and training is set on the Sun_4 (see Figure C-7), the results are displayed on the PC via the network (see Figure C-8).

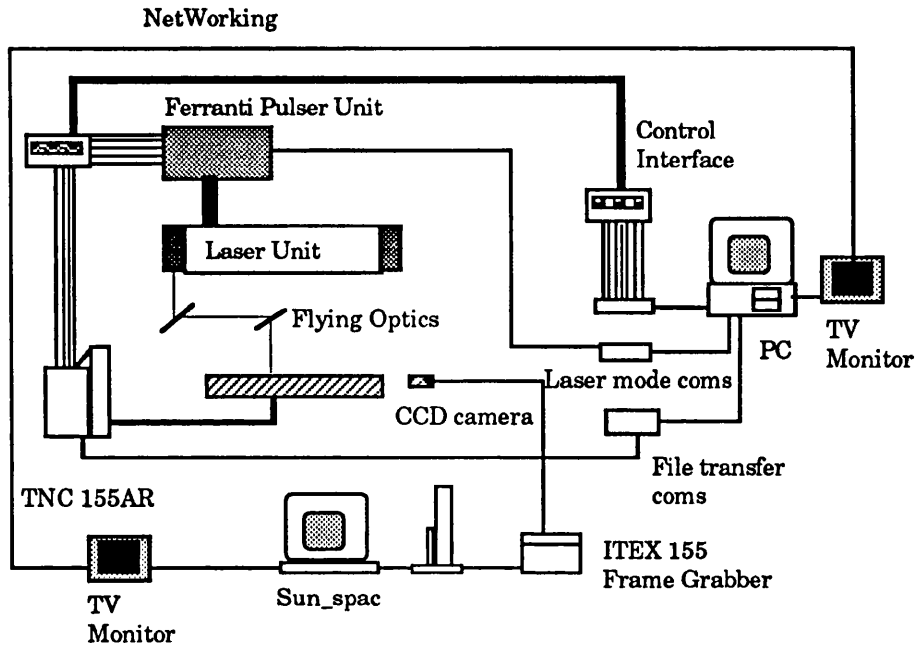

Fig 6.14 **Hybrid Decision Support System for the tasking and control of the MFKP CO2 laser for material processing**

6.9 Conclusion

The PID-KBMS was tested using a simulation of a laser cutting process. In this application, the material surface temperature is evaulated for a variable laser input power. However, for the proposed KBMS design, there is no constraint in the number of related process variables that can be considered. The data for the simulated EDB includes specification of the material as well as of the cut required. The whole system runs under a graphical virtual operating system created in object oriented code. The PID-KBMS was tested using a simulation model before its actual implementation. Whilst this treatise has of necessity described the

proposed design as a modular system which indeed it is, it must be emphasised that the system is tightly coupled in software architecture for the rapid collection and processing of real time data. Data acquisition is achieved utilising board-level algorithms. The system performed well in that a very close approximation to the prediction was obtained as the amount of data collected increased. A rapid image analysis algorithm for measurement of the exit spark cone has been developed for the final hybrid system. The edge detection algorithm utilises a swinging pendulum technique to perform edge detection on the spark cone. This method is very effective in compressing the amount of data, consequently subsequent data processing is rapid. For this application a least square template matching technique was adopted, cross correlation in the frequency domain was found to be too slow; however, we are currently investigating the possibility of optical cross correlation, which is an extremely fast technique. The error signal from the LMS matching and the calculated cone angle were input into cone decision support system (CDSS). The final combined system of the CDSS and PID-KBMS results in a hybrid intelligent decision support system (see Figure C-9) for the tasking, control and consultation for a laser manufacturing workcell.

REFERENCES

[1] Dieter Schuocker, "The physical mechanism and theory of laser cutting", The Industrial Laser Annual Handbook, David Belforte(ed.), PennWell Books, pp 65 - 80(1987).

[2] W.W. Duley, "CO_2 lasers, effects and applications", Academic Press, N.Y.(1976).

[3] Lim See Yew and C.R. Chatwin, "Evolutionary process prediction and optimization for laser - material interaction", to be published(1992).

[4] H.H. Martien Van Dikj, "Pulsed Nd.YAG laser cutting", The Industrial Laser Annual Handbook, David Belforte(ed.), PennWell Books, pp 52 - 65(1987).

[5] A.Hill and C.J. Taylor, "Model Based Image Interpretation using Genetic Algorithms", BMVC'91, Peter Mouforth(ed.), pp 266 - 275(1991).

[6] K.S. Ku, " Digital Pattern Recognition", Communications and Cybernetics (10), Springer-Verlay, NY (1976).

[7] Lim See Yew and C.R. Chatwin," The design of a Second Order PID Knowedge Based Management System for process control", Proceedings of the Second International Conference on Robotics, Automation and Computer Vision, pp 7.4.1-7.4.5(1992).

[8] Kang G. Shin, Xian Zhong Cui,"Design of a knowledge based controller for intelligent control system ", IEEE Transactions on system, man, and cybernetics, Vol 21, No. 2, pp 368 - 375 March/April(1991).

[9] Robinson J.A.,"A Machine-oriented logic based on the resolution principle", Journal of the ACM, JACM, VIZ, NY, pp 23 - 41(1965).

[10] A.Bahrami, "Designing artificial intelligence based software", Sigma Press(1988)

[11] D.W. Patterson, "Introduction to artificial intelligence and expert systems", Prentice Hall International(1990)

[12] A.M. Tjoa and R.Wagner, "Database and expert systems applications", Proceedings of the International conference in Vienna, Austria, Springer-Verlag, NY(1990)

[13] J.K. Annot and P.A.M Haen, "POOL and DOOM : the object oriented approach in : Parrallel computing : Object oriented, Functional, Logic", Wiley, pp 47-79(1990)

[14] B. Burg., "Smart laser cutting", Proceedings SPIE conference Innsbruck, Austria, Vol 650, Schuocker (ed.), SPIE, Bellingham, Washington USA, April 1986, pp 271-278(1986)

[15] R. Duda and P. Hart, "Use of the Hough Transform to detect edges and lines", Computer ACM, Vol 15, pp 11 - 15(1972).

[16] B.Zavidovique," Hey Robots ... Looking for cones", Proceedings of Computer Vision and Pattern Recoginition IEEE, pp 379 - 381(1985).

7 GENERAL CONCLUSIONS AND FUTURE WORK

7.1 General conclusions

For most engineering systems, the general control theory defines the system framework and a major part of its structure. Providing parameter estimation procedures are adequate, parameters may be determined by straightforward experimental methods, minor uncertainties in the structure are quantified by using final validation arguments and iteration through the procedures. For some very complex systems - like laser materials processing and biosystems - in addition to the parameters, a large part of the structure may be unknown due to softness; even details of the framework may be ill - defined and hence unavailable. As a consequence, control engineering techniques must be combined

with expert insight to infer unknowns in the framework and structure from the available information.

This treatise proposes the use of unified bond graph theory in knowledge control modelling (KCM) for the construction of state space artificial intelligent systems for process control. In KCM there are three stages in the design of an intelligent control system: physical representation, bond graph representation and the State Space Bonding Graph (SSBG). This unification of both the intelligent system and process models using bond graphs allows design of the flow of both data and system events. The PID-KBMS was initially tested using a simulation of the laser cutting process. In this application, the cut material surface irradiance and exit spark cone angle is evaluated for a variable laser input power. However, for the proposed KBMS design, there is no constraint in the number of related process variables that can be considered. The data for the simulated extensional database(EDB) includes specification of the material as well as the required cut quality. The whole system runs under a graphical virtual operating system created in object oriented code. The PID-KBMS was tested using a Fourier simulation model before its actual implementation.

Whilst this treatise has of necessity described the proposed design as a modular system, which indeed it is, it must be emphasised that the system is tightly coupled in software architecture for the rapid collection and processing of real time data. Data acquisition is achieved utilising board-level algorithms. The system performed well, in that a very close approximation to the prediction was obtained as the amount of data collected increased.

A rapid image analysis algorithm for measurement of the exit spark cone has been developed for the final hybrid system. The edge detection algorithm utilises a swinging pendulum technique to perform edge detection on the spark cone. This method is very effective in compressing the amount of data, consequently subsequent data processing is rapid. For this application a least square template matching technique was adopted and cross correlation in the frequency domain was found to be too slow; however, optical cross correlation is currently being investigated, as this is an extremely fast technique. The error signal from the least mean square(LMS) matching and the calculated cone angle were input into the Image Discriminator Decision Support System (IDDSS).

The final combined system of the IDDSS and PID-KBMS results in a hybrid intelligent decision support system for the tasking, control and consultation for a laser manufacturing workcell.

The prediction of the machining process control parameters for the expert system was done via genetic alogrithms. The genetic algorithm was then run on a Sun-4 Workstation to generate a range of pulse lengths and pulse separations for different values of laser mean power. The predicted pulse values and velocity were then used to cut the corresponding workpiece. Experimental results of the cut obtained show a favourable accuracy in relation to the predicted values.

Laser materials processing is a highly non-linear process. Chaotic dynamics can be observed when the cutting control parameters are

set to particular values. An investigation was thus conducted into the existence of chaos as well as the possibility for process parameter prediction using the information stored in the phase portrait of the dynamic system. A one-dimensional heat transfer model was derived and using the property of the Melnikov integral, the condition for the onset of chaos was verified for small perturbations in the cutting rates and thermal properties of the material. By using the isoclines approach, a method of approximating the initial cutting rates from the system phase portrait was established. The predicted cutting rates were tested against actual cutting rates. The predicted cutting rates for stainless steel (C34 SS304 2B) agree extremely well with the experimental results. This in conclusion validates the suitability of using the proposed method as a prediction mechanism for laser cutting.

7.2 Future work

A proposed development method for designing the information systems was presented in Chapter 5. The hybrid system, named "Lamarckism Implicit Expert System" (LIES) comprises the second-order PID KBMS and the IDDSS. The architecture of LIES was based on a knowledge based management system. Although the hybrid expert system works well for the tasking and control of the CO_2 laser, further improvement in the form of a neural-network like architecture is recommended.

In recent years, there has been an increasing interest in studying the mechanisms and structure of scheduling in a computer-integrated manufacturing (CIM) environment. This has led to the development of new scheduling models, such as petri-nets, time-augmented petri-nets, fuzzy scheduling model and neural net scheduling model. The basic underlying factor in scheduling is in the notion of synchronisation and an orderly approach to the command, control and communication (C^3) between each active node element of the overall CIM structure.

CIM scheduling can be vaguely regarded as a dynamic process control problem, whereby, the feedforward or feedback elements are the scheduling priorities that enable the manufacturing organisation to remain within a 'steady-state' profit margin. However, it is a fact that at each different hierarchy of the organisation, random phenomena in C^3 can be observed i.e. changes in a particular department or level causes a perturbation elsewhere along the chain of the manufacturing structure.

An important point to note is that even if a change in a department occurs, these changes are constrainted by the framework of rules pre-set by the organisation structure. Hence, these cause-and-effect phenomena can be viewed as deterministic changes or 'deterministic chaos'. By considering a KBMS architecture to replace the node of a neural net, chaotic dynamics can be controlled with a high efficiency via the individual KBMS junctions thus providing both tasking and controlling functions. Possible areas of application of the neural-KBMS architecture would be in the area of scheduling

of computer-integrated-manufacturing systems and system control in high level controllers.

In Chapter 2, the genetic algorithm was used to predict optimal cutting rates for a pulsed laser cutting process. A further extension of this new laser prediction scheme would be in the investigation of predicting the optimal nozzle height; gas pressure and laser focal height for laser-material processing.

In laser-materials processing, dynamic chaotic phenomena were observed, transient interaction characteristics were then proved to exist, Chapter 3. The phase portrait of the cutting process was then exploited to predict the laser machining parameters. Further research in the area of deterministic chaos should be pursued in:

(i) Reaction characteristics of the material thermodynamic properties and the machining parameters.

(ii) Comparison of different phase portraits and Poincare' maps for different materials.

APPENDIX A

System electrical circuits

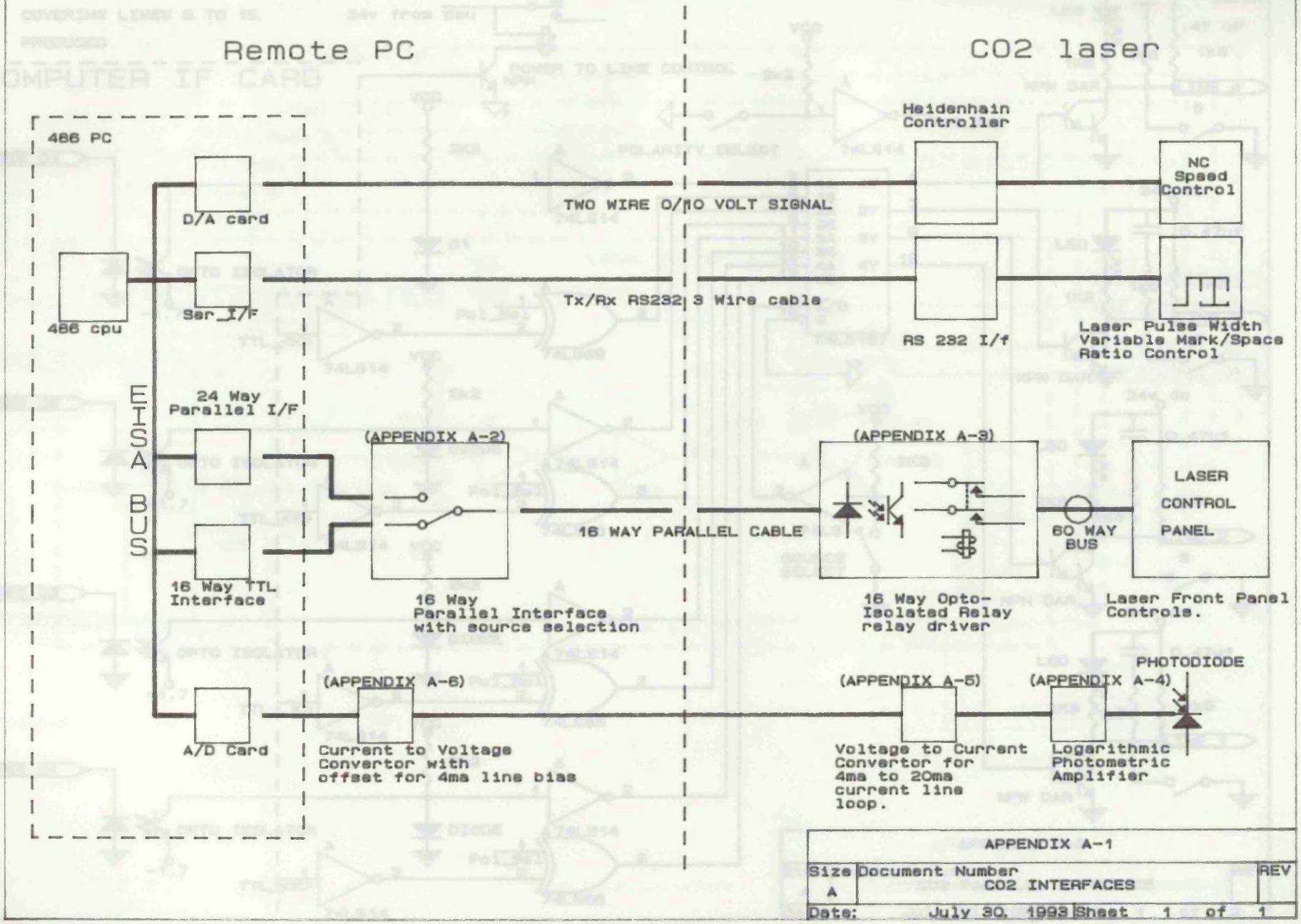
Remote PC
CO2 laser
486 PC
D/A card
486 cpu
Ser_I/F
EISA BUS
24 Way
Parallel I/F
16 Way TTL
Interface
A/D Card
Heidenhain
Controller
TWO WIRE O/10 VOLT SIGNAL
Tx/Rx RS232 3 Wire cable
RS 232 I/f
NC
Speed
Control
Laser Pulse Width
Variable Mark/Space
Ratio Control
(APPENDIX A-2)
16 Way
Parallel Interface
with source selection
16 WAY PARALLEL CABLE
(APPENDIX A-3)
16 Way Opto-
Isolated Relay
relay driver
60 WAY
BUS
LASER
CONTROL
PANEL
Laser Front Panel
Controls.
(APPENDIX A-6)
Current to Voltage
Convertor with
offset for 4ma line bias
(APPENDIX A-5)
Voltage to Current
Convertor for
4ma to 20ma
current line
loop.
(APPENDIX A-4)
PHOTODIODE
Logarithmic
Photometric
Amplifier
APPENDIX A-1
Size
A
Document Number
CO2 INTERFACES
REV
Date: July 30, 1993
Sheet 1 of 1

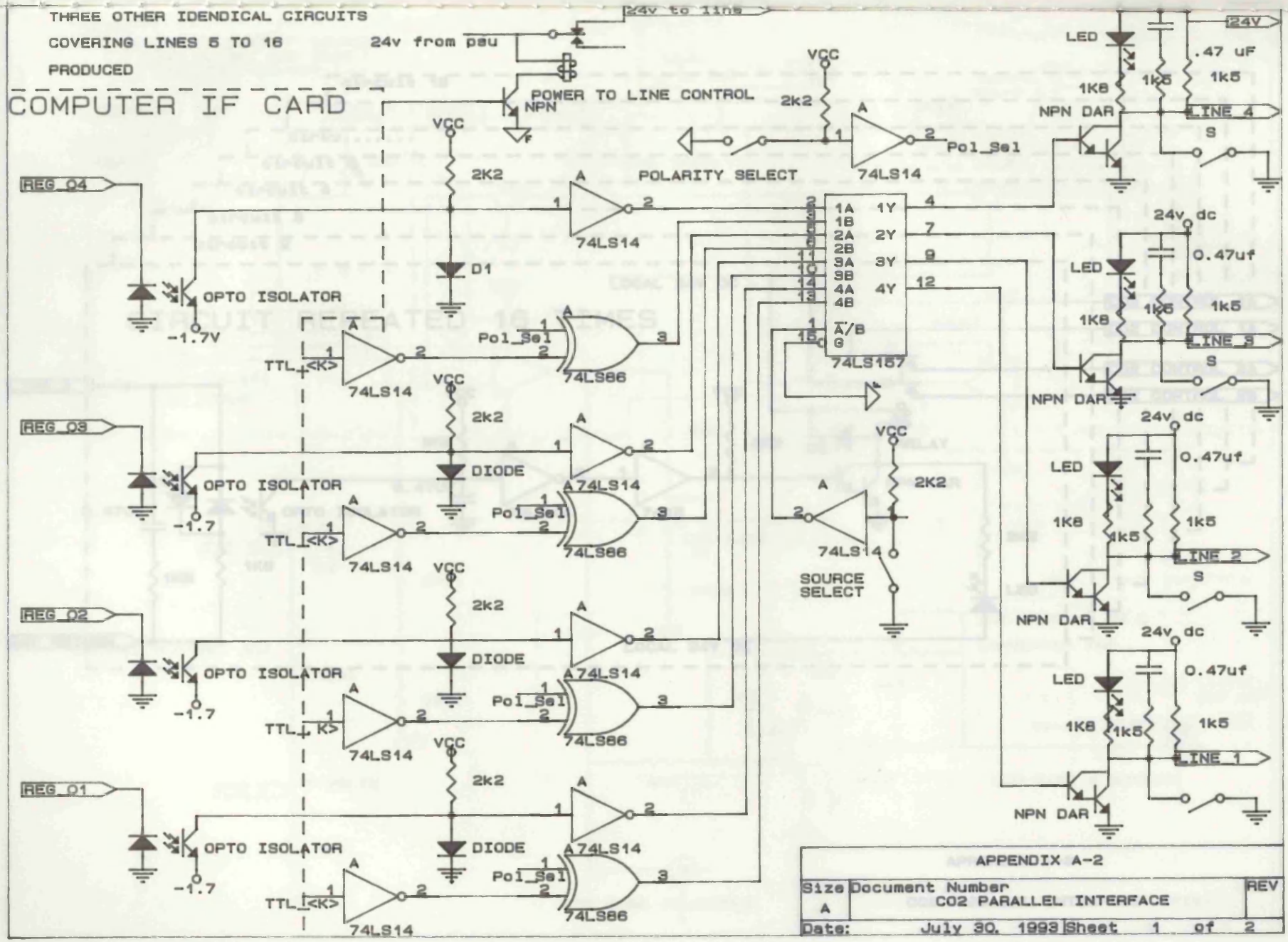
THREE OTHER IDENDICAL CIRCUITS
COVERING LINES 5 TO 16
PRODUCED
COMPUTER IF CARD
24v from psu
24v to lins
POWER TO LINE CONTROL
NPN
VCC
2K2
POLARITY SELECT
74LS14
Pol_Sel
74LS157
1A
1B
2A
2B
3A
3B
4A
4B
A/B
G
1Y
2Y
3Y
4Y
LED
1K8
1k5
.47 uF
NPN DAR
LINE 4
LINE 3
LINE 2
LINE 1
24v dc
0.47uf
S
REG_Q4
REG_Q3
REG_Q2
REG_Q1
OPTO ISOLATOR
-1.7V
-1.7
D1
DIODE
TTL_<K>
74LS86
SOURCE
SELECT
APPENDIX A-2
Size
A
Document Number
CO2 PARALLEL INTERFACE
REV
Date:
July 30, 1993
Sheet 1 of 2

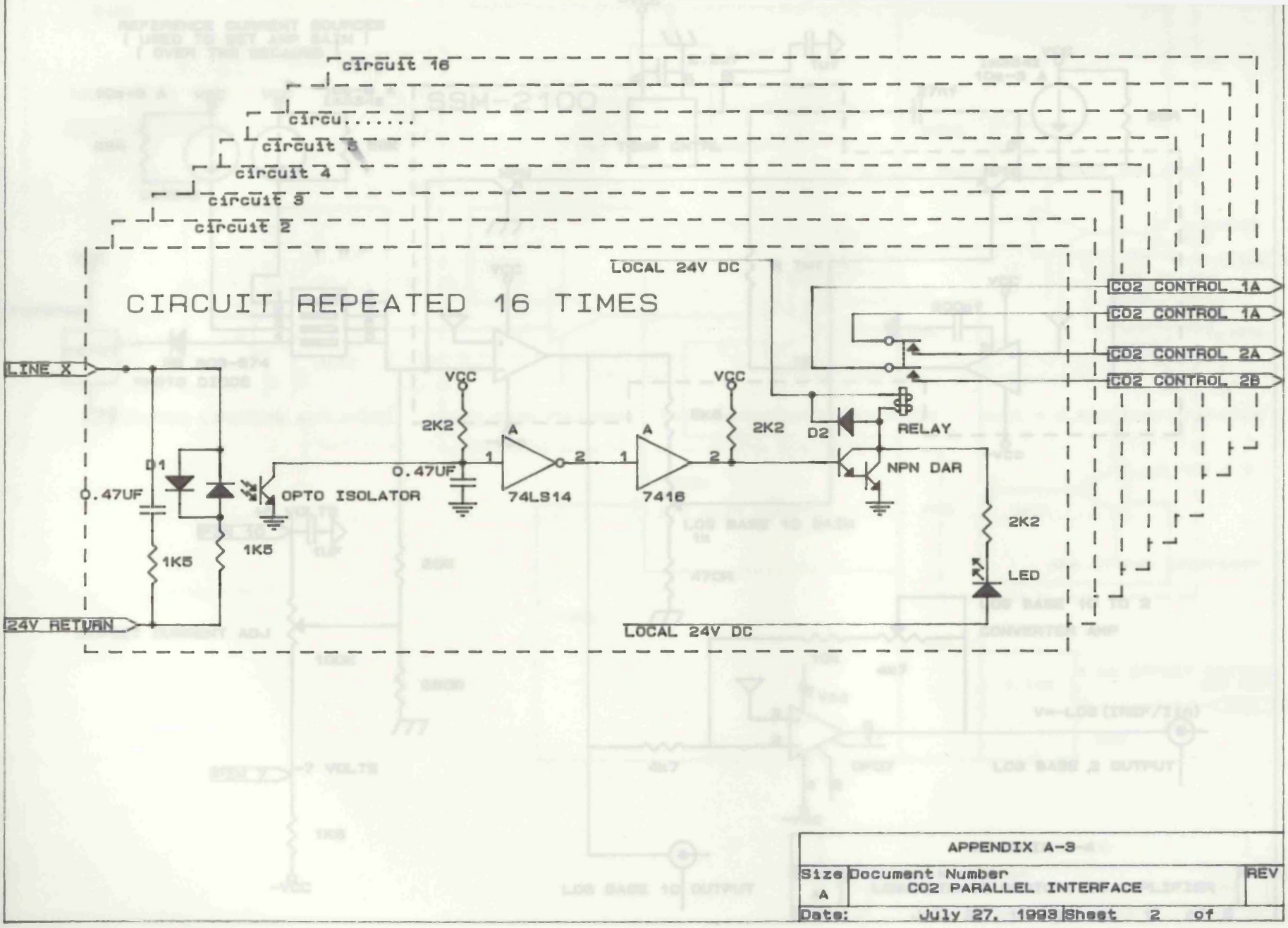

APPENDIX A-3		
Size A	Document Number CO2 PARALLEL INTERFACE	REV
Date: July 27, 1993	Sheet 2 of	

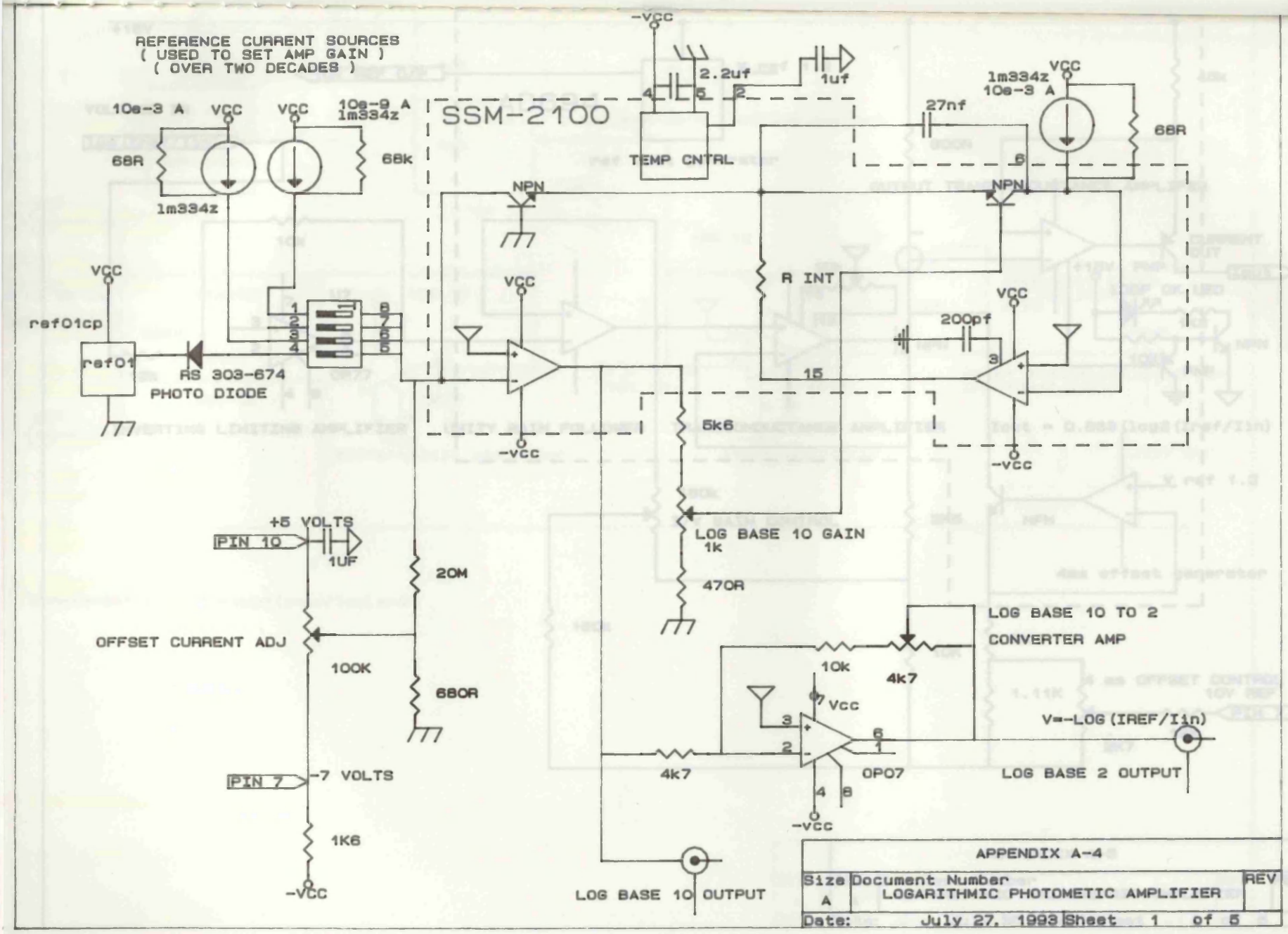
REFERENCE CURRENT SOURCES
(USED TO SET AMP GAIN)
(OVER TWO DECADES)
10e-3 A
VCC
VCC
10e-9 A
lm334z
68R
68k
lm334z
SSM-2100
-VCC
2.2uf
1uf
TEMP CNTRL
27nf
lm334z
10e-3 A
VCC
68R
NPN
NPN
VCC
R INT
VCC
200pf
ref01cp
ref01
RS 303-674
PHOTO DIODE
-VCC
5k6
-VCC
+5 VOLTS
PIN 10
1UF
20M
LOG BASE 10 GAIN
1k
470R
LOG BASE 10 TO 2
CONVERTER AMP
OFFSET CURRENT ADJ
100K
680R
10k
4k7
Vcc
V=-LOG(IREF/Iin)
PIN 7
-7 VOLTS
4k7
OP07
LOG BASE 2 OUTPUT
1K6
-VCC
-VCC
LOG BASE 10 OUTPUT
APPENDIX A-4
Size
A
Document Number
LOGARITHMIC PHOTOMETIC AMPLIFIER
REV
Date:
July 27, 1993
Sheet 1 of 5

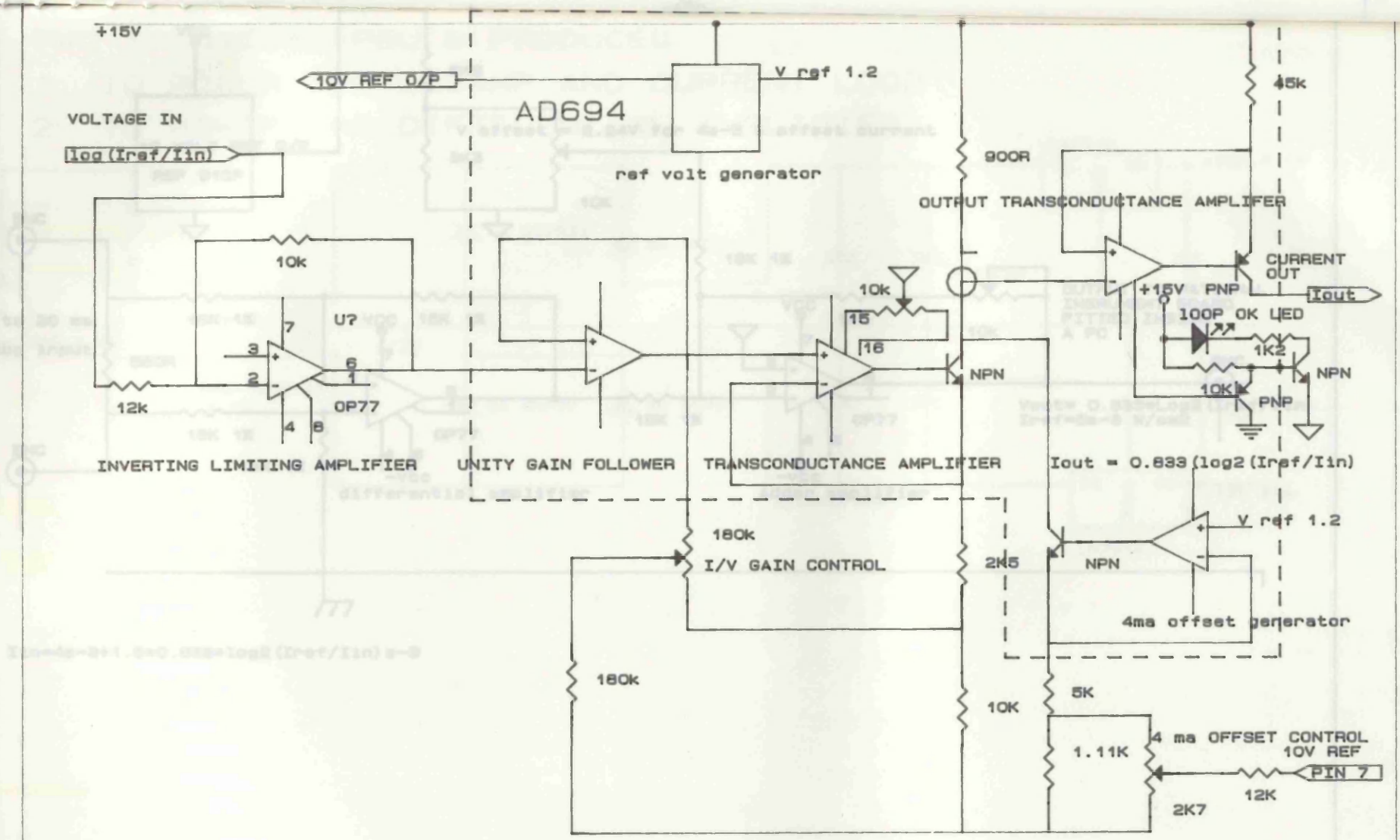

APPENDIX A-5		
Size A	Document Number LOGARITHMIC PHOTOMETRIC AMPLIFIER	REV
Date: July 30, 1993	Sheet 2 of 5	

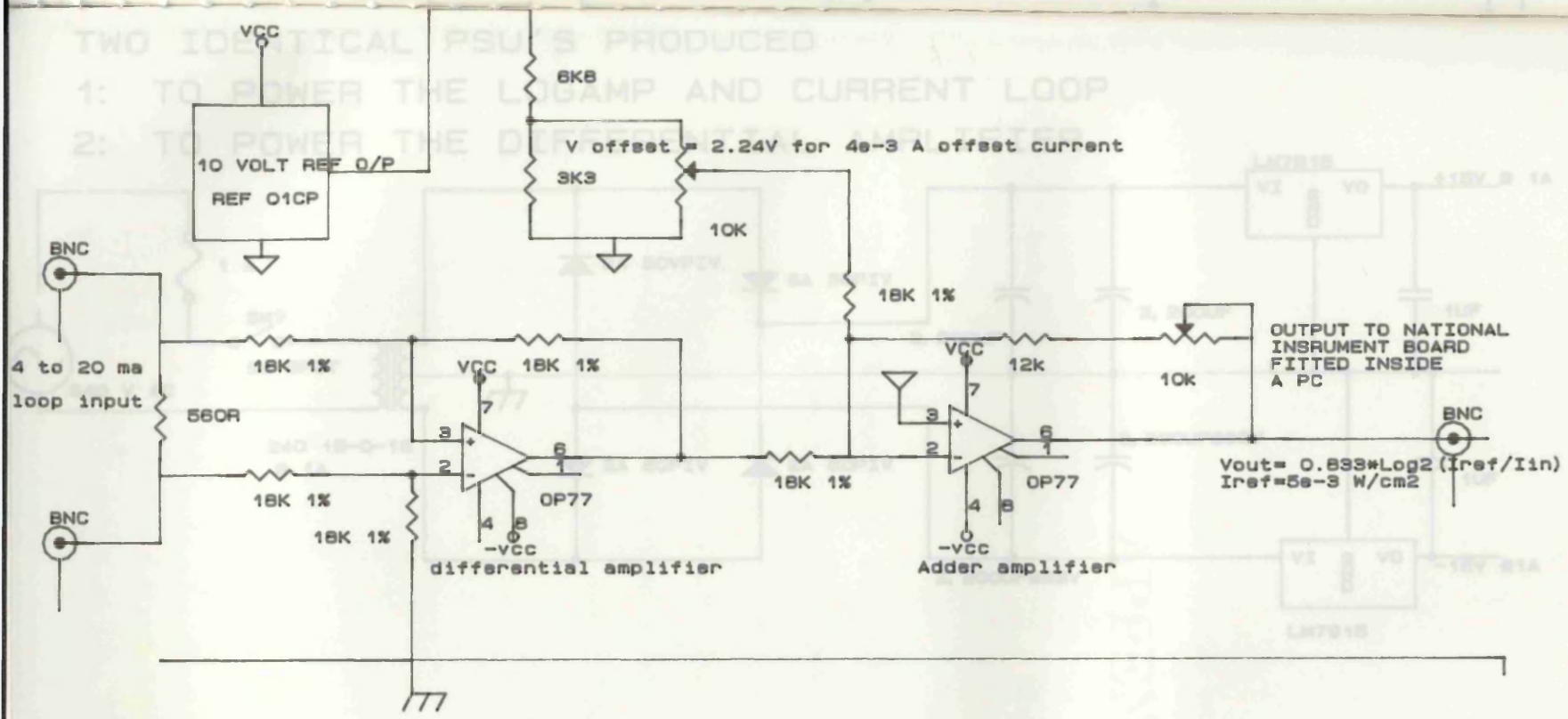

Iin=4e-3+1.6*0.833*log2(Iref/Iin)e-3

	APPENDIX A-6	
Size A	Document Number LOGARITHMIC PHOTOMETRIC AMPLIFIER	REV
Date: July 27, 1993	Sheet 1 of 5	

TWO IDENTICAL PSU'S PRODUCED

1: TO POWER THE LOGAMP AND CURRENT LOOP

2: TO POWER THE DIFFERENTIAL AMPLIFIER

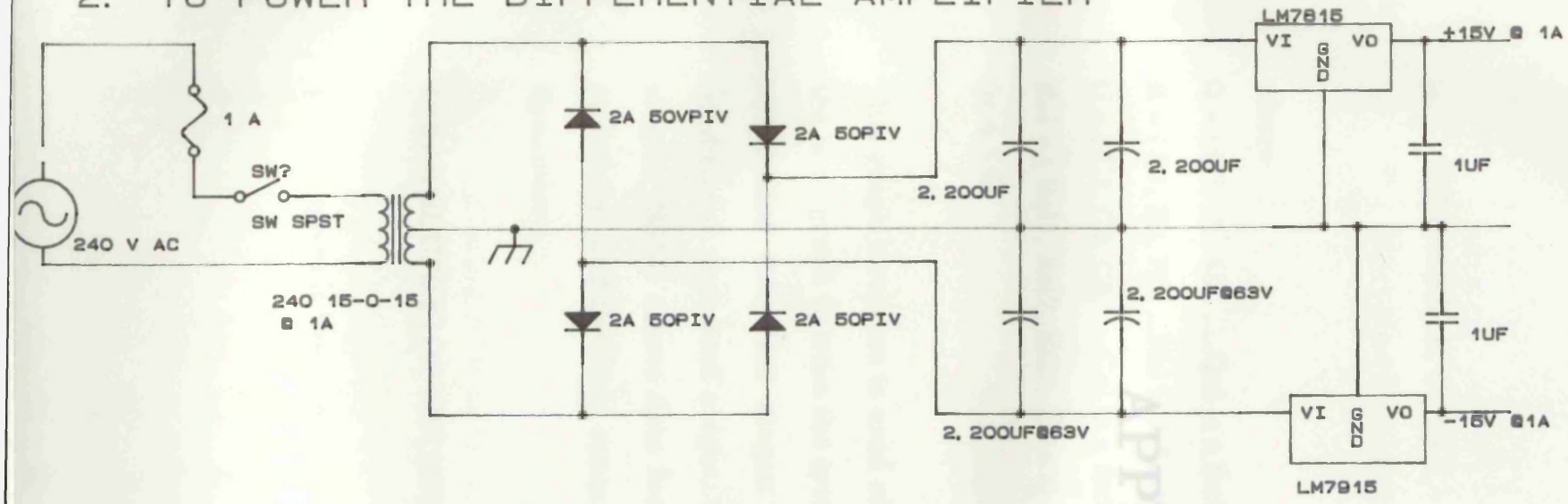

APPENDIX A-7		
Size A	Document Number LOGARITHMIC PHOTOMETRIC AMPLIFIER	REV
Date: July 27, 1993	Sheet 4 of 5	

APPENDIX B

SSBG

STATE SPACE BONDING GRAPH(SSBG)

A state space bonding graph is basically a structure of quadtuples comprising of query(Q), rules(R), conditions(C) and relations(Rel).

ie. SSBG = ß(Q, R, C, Rel);

where

Q = { Q1, Q2, Q3, ...Qn} is a finite set of queries.

R = { R1, R2, R3, ...Rn} is a finite set of rules.

C = { C1, C2, C3, ...Cn} is a finite set of conditions.

Rel = { Rel1, Rel2, Rel3, ...Reln} is a finite set of relational properties

(ie n > 0)

This graph structure is used after modelling the intelligent system using the bond graph to trace the system analysis of the input queries. SSBG is subdivided into four stages: the input or query state, the rule or conditional argument stages, the conditional stages and the relational stages. SSBG allows data fusion between the state space of the meta-knowledge and the state space of the process to be controlled (ie. process dynamics).

CONSTRUCTION OF THE SSBG:

i) A query is first input to the SSBG.

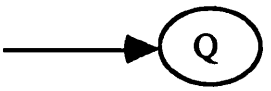

Fig B-1 Graph of ß(Query)

ii) The query then multiplexes in the rule kernel.

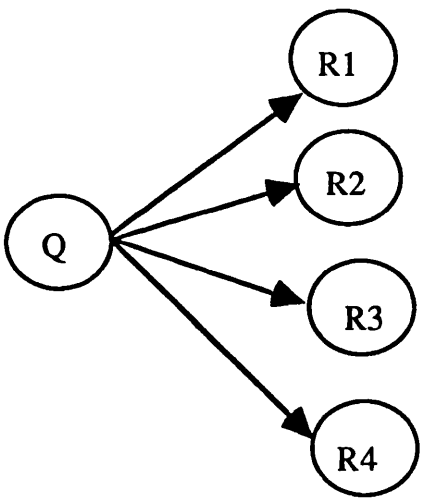

Fig B-2 Graph of ß(Query, Rule)

1. $Q: \forall Rules <- \{ \sum_{i=0}^{i=N} Rules\ i \}$

iii) Validated rules satisfying the query are then summed and mapped as input to the conditions kernel.

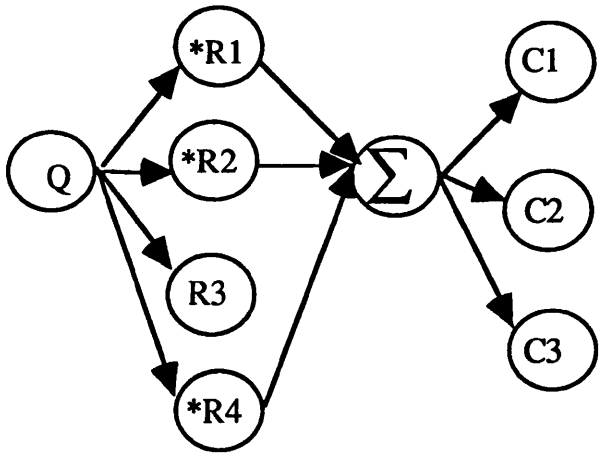

Fig B-3 Graph of ß(Query, Rules, Condition)

note: An asterisk(*) is tagged to the rules to provide a count for the total number of truth rules for the driving force strategy threshold and to denote which rules were fired.

1. $Q \rightarrow \{ \forall Rule : \exists (\|Rules\| \wedge Q) \}$

iv) Rules that satisfy the condition and relational attributes are validated.

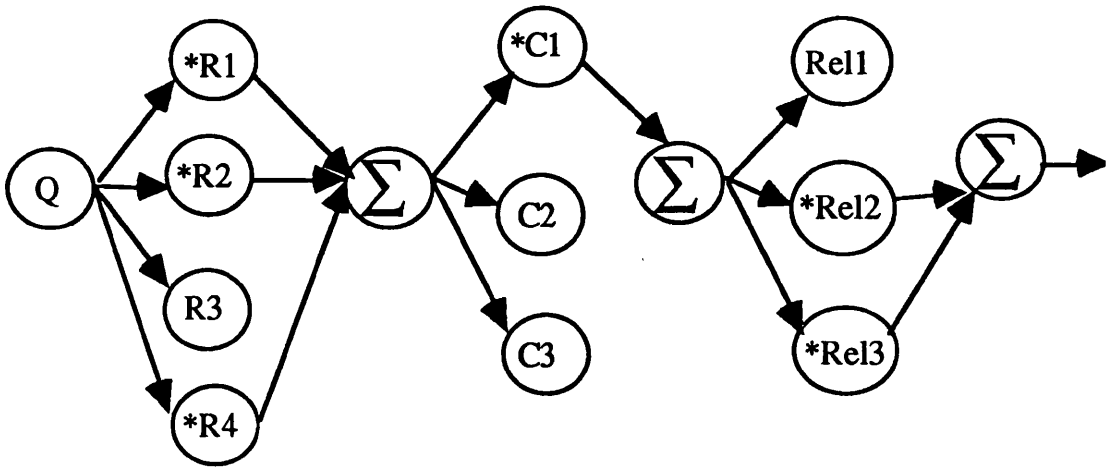

Fig B-4 Graph of ß(Query, Rules, Condition, Relation)

1. ∀ *Rules* (*conditions* , *relations*) ∧ *Query* (*conditions* , *relations*)
   -> ∃ (*Rules*(*Query* (*conditions* , *relations*))

APPENDIX C

Photographs of system and cut materials